



U.S. DRIVE Highlights of Technical Accomplishments

2014



March 2015



U.S. DRIVE

Highlights of Technical Accomplishments Overview

Through precompetitive collaboration and technical information exchange, U.S. DRIVE partners are accelerating the development and availability of clean, efficient automotive and energy technologies.

The U.S. DRIVE Partnership (*Driving Research for Vehicle efficiency and Energy sustainability*) is a voluntary government-industry partnership focused on precompetitive, advanced automotive and related infrastructure technology research and development (R&D). Partners are the United States Department of Energy (DOE); the United States Council for Automotive Research LLC (USCAR), a consortium composed of FCA US LLC (formerly Chrysler Group LLC), Ford Motor Company, and General Motors Company; Tesla Motors, Inc.; five energy companies, (BP America, Chevron Corporation, Phillips 66 Company, ExxonMobil Corporation, and Shell Oil Products US); two electric utilities, DTE Energy and Southern California Edison; and the Electric Power Research Institute.

The Partnership benefits from a history of successful collaboration across twelve technical teams, each focused on a key area of the U.S. DRIVE portfolio (see below). These teams convene the best and brightest scientists and engineers from U.S. DRIVE partner organizations to discuss key technical challenges, identify possible solutions, and evaluate progress toward goals and targets published in technology roadmaps. More recently, to complement its technical teams, U.S. DRIVE established two working groups: (1) cradle-to-grave analysis, identified as critical to better understanding the potential benefits of various technology pathways and alignment with the Partnership vision, mission, and goals; and (2) fuel properties for future engines, recognizing an important opportunity to evaluate how various fuel properties can increase the efficiency of advanced internal combustion engines. By providing a framework for frequent and regular interaction among technical experts in common areas of expertise, the Partnership accelerates technical progress, helps to avoid duplication of efforts, ensures that publicly-funded research delivers high-value results, and overcomes high-risk barriers to technology commercialization.

U.S. DRIVE technical teams selected the highlights in this document from many hundreds of DOE-funded projects conducted by some of the nation's top research organizations in the field. Each one-page summary represents what DOE and automotive, energy, and utility industry partners collectively consider to be significant progress in the development of advanced automotive and infrastructure technologies. The report is organized by technical team area, with highlights in three general categories:

Vehicles

- Advanced Combustion and Emission Control
- Electrical and Electronics
- Electrochemical Energy Storage
- Fuel Cells
- Materials
- Vehicle Systems Analysis

Crosscutting

- Codes and Standards
- Hydrogen Storage
- Grid Interaction

Fuels

- Fuel Pathway Integration
- Hydrogen Delivery
- Hydrogen Production

More information about U.S. DRIVE, including prior year accomplishments reports and technology roadmaps, is available on the DOE (www.vehicles.energy.gov/about/partnerships/usdrive.html) and USCAR (www.uscar.org) websites.

Advanced automotive and energy infrastructure technologies are entering the market in increasing numbers, and technologies that were only concepts less than a decade ago are now approaching initial commercial readiness. These advancements are the result of partners working together to achieve a common goal. With continued progress resulting from the joint efforts of government, industry, and academic experts, the U.S. DRIVE Partnership is helping to increase the competitiveness of American industry and secure U.S. leadership in an increasingly competitive global market to enable a clean and sustainable transportation energy future.

Table of Contents

VEHICLES	1
<i>Advanced Combustion and Emission Control</i>	<i>1</i>
Low-Temperature Oxidation Catalyst Test Protocol.....	2
New Injector Nozzle Design Enables Low Load Operation of Gasoline Compression Ignition Engine	3
25% Fuel Economy Improvement in Light-Duty Advanced Technology Powertrain	4
Gasoline Direct-Injection Compression Ignition Shows Potential for 39% Fuel Economy Improvement	5
New Solver Accelerates Simulation of New Fuels in Engines.....	6
Reactivity Controlled Compression Ignition Simulations Show Potential for 25% Improvement in Fuel Economy.....	7
Innovative Metal Oxide Catalyst Oxidizes Carbon Monoxide Near 150°C Without Precious Metals.....	8
Novel Engine Lubrication Anti-Wear Additives Demonstrate Improved Fuel Economy	9
Low-Temperature Gasoline Combustion Achieves “Diesel Engine” Load-to-Boost Ratios	10
Unique Spray Measurements Enable Improved Models	11
<i>Electrical and Electronics</i>	<i>12</i>
Manufacturability of Affordable Non-Rare Earth Magnet Alloys Demonstrated	13
Motor Thermal Management Spurs New Motor Designs	14
Plastic Heat Exchanger Improves Heat Transfer Efficiency and Reduces Inverter Weight.....	15
All Silicon-Carbide Inverter Meets 2015 Performance Targets	16
New System Improves Materials Characterization.....	17
Next-Generation Wide Bandgap Packaging Improves Inverter Efficiency	18
<i>Electrochemical Energy Storage</i>	<i>19</i>
Increased Cell Energy Density and Specific Energy through Advanced Technology Electrode Structure	20
Cradle-to-Gate Automotive Lithium-Ion Battery Impacts Reduced by Recycling	21
Effects of Fast-Charging on Lithium-Ion Cells	22
New High Capacity “Layered-Layered-Spinel” Composite Cathode Materials for Lithium-Ion Batteries	23
Understanding Factors Affecting Power Capability of High-Energy Lithium-Rich Layered Cathode Materials.....	24
Multifunctional Separator Performance Confirmed for Large Format Lithium-Ion Batteries	25
New Cathode Technology Demonstrates Significant Progress Towards Electric Vehicle Goals.....	26
Computer Aided Battery Engineering Tool Released to the Public.....	27
The Materials Project is Released to Public	28
Computer Aided Engineering Tools Now Available for Battery Engineers.....	29
Novel In-Line Atomic Layer Deposition Electrode Coating System for Lithium-Ion Batteries	30
Large Format Lithium-Ion Battery with Water-Based Electrode Processing	31
Resolving the Voltage Fade Mechanisms in LMR-NMC Composite Electrodes	32
Advanced Battery Recycling Opportunities and Issues.....	33
Micro-Sized Silicon-Carbon Composite Anode with Excellent Battery Performance Optimized and Analyzed	34
Abuse Propagation in Multi-Cell Batteries Characterized.....	35
Silicon Lithium-Ion Batteries Prepared from Rice Husks.....	36

<i>Fuel Cells</i>	37
Fuel Cell Catalysts Survive Harsh Durability Testing	38
Fuel Cell Membrane Meets Low-Humidity Milestone	39
Nanoframe Catalyst Achieves More than 20 Times Mass Activity of Platinum on Carbon	40
System Contaminant Library to Aid Research Community	41
Rotating Disk Electrode Technique Best Practices and Testing Protocol	42
<i>Materials</i>	43
Demonstrated Laser-Assisted Dissimilar Material Joining	44
Weld Fatigue Life Improvement Feasibility Demonstrated	45
Advanced Oxidation Process Improved for Carbon Fiber	46
A Microstructure-Based Modeling Framework Developed to Design a Third-Generation Steel	47
Mechanistic-Based Ductility Prediction for Complex Magnesium Demonstrated	48
High-Shear Deformation Process Developed to Form Magnesium Alloys	49
Novel Technique Developed for Joining Dissimilar Metals	50
Validation of Carbon Fiber Composite Material Models for Automotive Crash Simulation	51
Exceptional Ductility/High-Strength Third-Generation Advanced High-Strength Steel Produced	52
<i>Vehicle Systems Analysis</i>	53
Impact of Advanced Technologies on Engine Operating Conditions and Vehicle Fuel Efficiency	54
EETT/VSATT 2014 Vehicle Benchmarking Collaboration	55
Auxiliary Load: On-Road Evaluation & Characterization	56
Leveraging Big Data to Estimate On-Road Fuel Economy	57
CROSSCUTTING	58
<i>Codes and Standards</i>	58
Bridging the Gap between Hydrogen Component Safety and Performance Testing Capability	59
<i>Hydrogen Storage</i>	60
Optimizing Hydrogen Storage Materials by Defining Requirements via Adsorption System Modeling	61
Neutron Diagnostic Methods Accelerate Hydrogen Storage Materials Development	62
Lower-Cost, High-Performance Carbon Fiber	63
<i>Grid Interaction</i>	64
Developing the SAE J2953 Interoperability Standard Test Procedures and Tools	65
Plug-in Electric Vehicle Charging Technology and Standards	66
Comprehensive Data Set Informs Future Plug-in Electric Vehicle Infrastructure Planning	67
FUELS	68
<i>Fuel Pathway Integration</i>	68
Hydrogen Dispensing Pressure Analysis	69
Marginal Abatement Cost of Carbon	70

<i>Hydrogen Delivery</i>	71
14% Reduction in Hydrogen Delivery Cost using Tube Trailer Consolidation	72
<i>Hydrogen Production</i>	73
Advanced Oxygen Evolution Catalysts for Proton Exchange Membrane Water Electrolysis	74
Low Precious Group Metal Loaded Catalysts/Electrodes for Hydrogen Production by Water Electrolysis ...	75

VEHICLES

Advanced Combustion and Emission Control

A decorative graphic consisting of two curved, overlapping lines. The upper line is a medium blue color and the lower line is a lighter, pale blue color. Both lines curve from left to right, tapering off at the ends.

Low-Temperature Oxidation Catalyst Test Protocol

A standardized and realistic aftertreatment catalyst testing protocol will enable comparisons of catalyst performance data and accelerate the pace of catalyst innovation.

ACEC Low Temperature Aftertreatment Group

Low-temperature exhaust conditions associated with advanced powertrain technologies are especially challenging for current aftertreatment catalysts to meet U.S. Environmental Protection Agency (EPA) and California emissions standards. With new catalyst research focused on addressing this challenge at various institutions across the nation, the U.S. DRIVE/Advanced Combustion and Emission Control Technical Team identified the need for consistent and realistic metrics for aftertreatment catalyst evaluation. To support this need, a team of researchers at Pacific Northwest National Laboratory, General Motors, Ford, Chrysler, and Oak Ridge National Laboratory developed an oxidation catalyst test protocol, or standardized catalyst test procedure, that is adaptable in various laboratories and sufficiently captures a catalyst technology's performance capability.

The purpose of the protocol is to accelerate the pace of catalyst innovation by maximizing the value and impact of reported data. It is also intended to facilitate a fair comparison between various technology options in a manner that has industry and community consensus by being accurate and realistic to the engine. The protocol is not meant to dictate how research is conducted, but rather a provide guideline allowing comparison of research results within the technical community.

The testing protocol defines a minimum set of hardware requirements and specifications for the following:

1. Concentrations of important species to be used during testing (i.e., hydrocarbon, carbon monoxide, carbon dioxide, hydrogen, nitrogen oxides, oxygen, and water) that simulate the

exhaust composition from different engines and combustion modes.

2. Procedures for degreening, aging, and poisoning of the catalyst.
3. Evaluation methods (e.g., temperature ranges, ramp rates) for reproducibly measuring the oxidation activity of the catalyst as a function of temperature.

Figure 1 shows the outline of the oxidation protocol. Catalysts are screened for conversion efficiency (including low temperature activity and overall efficiency) after degreening, thermal aging to simulate high mileage conditions, and poisoning with sulfur dioxide to assess sensitivity to sulfur poisoning.

**Aftertreatment Protocol for Catalyst Characterization and Performance Evaluation:
Low-Temperature Oxidation Catalyst Test Protocol**

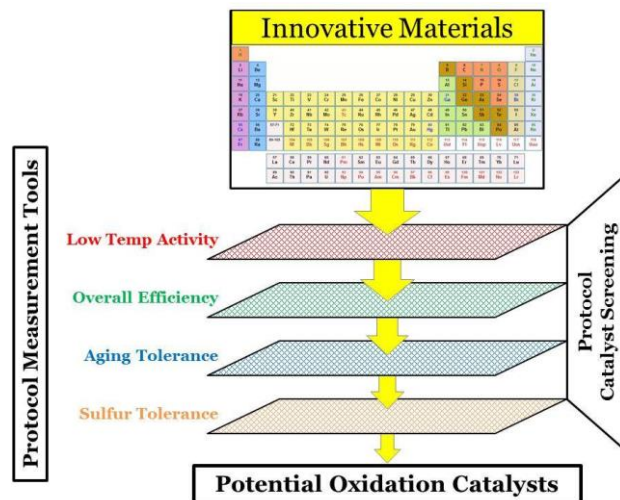


Figure 1. Oxidation catalyst test protocol for efficiently and reproducibly screening catalyst technologies for low-temperature activity, overall efficiency, and tolerance to thermal aging and chemical poisoning.

New Injector Nozzle Design Enables Low Load Operation of Gasoline Compression Ignition Engine

Using an enhanced fuel injection strategy and narrower angle nozzles, low load operation was extended to idle while maintaining excellent efficiency and combustion stability.

Argonne National Laboratory

Premixed compression ignition engine combustion concepts offer promise for increasing engine efficiency with low engine-out nitrogen oxide (NO_x) and soot emissions, but they have not demonstrated efficiency over the full engine load range with practical operating conditions.

Initial work with a multiple injection strategy on a 1.9L turbo-diesel engine platform allowed researchers to control gasoline compression ignition (GCI) combustion from 4 to 20 bar brake mean effective pressure (BMEP). Advanced computational fluid dynamics underlined the need for increased stratification and local fuel richness in the combustion chamber. As a result, condensing the multiple injection strategy into one well-timed single injection provided the conditions required for efficient low-load operation. Optimized injection timing allowed sufficient time in-cylinder for ignition but not too much time for the fuel to be over-dispersed in the combustion chamber and reduce its reactivity.

Recent computational fluid dynamics results showed reactivity enhancement with reduced injection pressure. A narrower injector nozzle umbrella angle of 120° and the lowest rail pressure possible were used to enhance reactivity for the minimum amount of fuel. Combining these factors allowed increased local fuel richness, resulting in stable operation of the multi-cylinder GCI engine using standard 87 octane gasoline. Low-load stability (see Figure 1) was achieved down to idle as indicated by a coefficient of variance (COV) of indicated mean effective pressure of less than 3% between 1-20 bar BMEP. At the idle point, researchers achieved less than 15 kPa standard deviation of indicated mean effective pressure (IMEP). Combustion noise levels were significantly

lower than equivalent diesel at idle, with ultra-low soot, NO_x, and carbon monoxide emissions. At high load, combustion noise mimicked diesel. Hydrocarbon emissions were elevated to the level of a spark-ignition gasoline engine rather than a diesel. For loads greater than 1 bar BMEP, exhaust temperatures were above 200°C, while at idle they dropped to roughly 150°C.

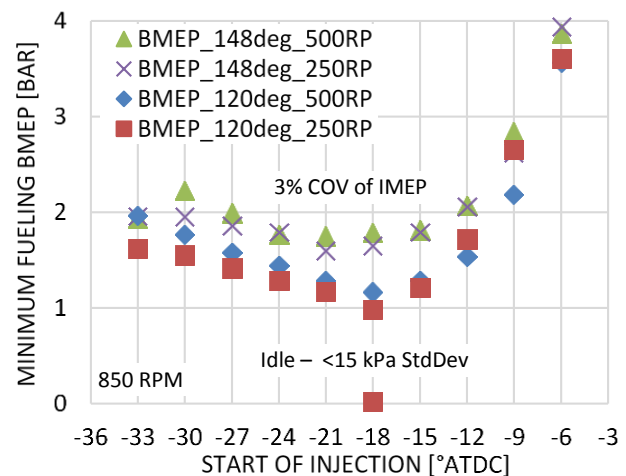


Figure 1. Combined effect of low injection pressure and narrower angle nozzles to enhance low load stability. ATDC = after top dead center. RPM = revolutions per minute.

Additional low load points, courtesy of the new nozzles, allowed 40 experimental operating conditions used as inputs for Autonomie simulations (2007 Cadillac BLS with six-speed manual transmission). This enabled more accurate interpolation points on U.S. Environmental Protection Agency drive cycles, showing a 29% fuel economy improvement for the combined cycle. These results show that GCI has potential to significantly improve fuel economy while using the most popular automotive fuel in the United States.

25% Fuel Economy Improvement in Light-Duty Advanced Technology Powertrain

Efficiency improvements using downsizing, boosting, high dilution with cooled exhaust gas recirculation, a novel ignition system, and dual-fuel.

Chrysler Group LLC, Argonne National Laboratory, Delphi, Bosch, and The Ohio State University

Chrysler and partners met U.S. Department of Energy project goals, achieving a fuel economy improvement of over 25% (relative to Chrysler's 4.0L V6 minivan) for combined city and highway cycles while also meeting the SULEV30 emission standard. The team developed a dual fuel advanced combustion concept to significantly improved engine efficiency.

The team designed, built, and tested a 2.4L I4 engine with high compression ratio (12:1), gasoline direct injection (DI), dual independent cam phasing, cooled exhaust gas recirculation (EGR), and two-stage turbo-charging (see Figure 1 – right). The high-charge motion port and chamber design, along with three spark plugs per cylinder, provided high dilution tolerance. Stoichio-metric fueling was used under all operating conditions, with EGR levels of up to 28% at loads above 8 bar brake mean effective pressure (BMEP). Port fuel injected E85 was blended in at higher loads to improve combustion phasing and avoid knock. Peak brake thermal efficiency (BTE) at 2000 rpm reached 38.5% with gasoline and 41% in dual-fuel mode (see Figure 1 – left). Two turbo-chargers were required: a small turbo for low-speed boost and a larger turbo for higher speeds. A pendulum-equipped crankshaft and nine-speed transmission enabled additional engine “down-speeding,” further reducing fuel consumption. Delphi's Ion sensing was used for combustion feedback control, and Bosch provided the DI fuel systems.

Chrysler worked with The Ohio State University (OSU) to develop an electrical load management control strategy that uses less fuel to maintain the same battery state of charge. A thermal system control feature was also developed with OSU that

used coolant bypass valves and a dual-mode coolant pump to more efficiently provide engine cooling and improve warm-up. Each feature showed a 1% fuel economy benefit.

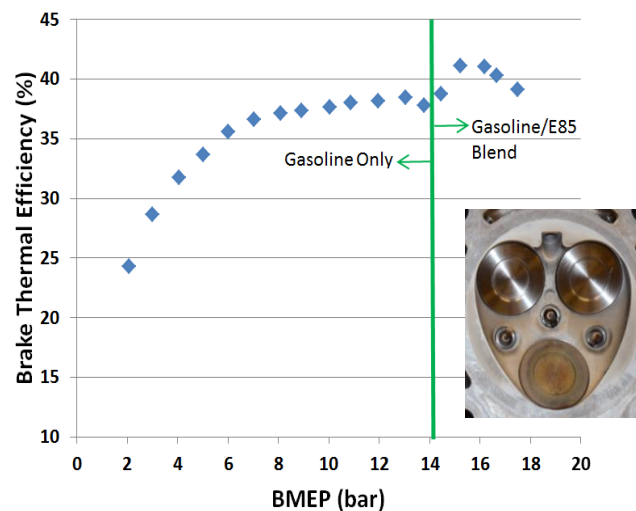


Figure 1. Peak BTE at 2000 rpm (left). The test engine (right).

Chrysler and Argonne National Laboratory (ANL) studied diesel micro pilot (DMP, dual-fuel with DI gasoline and diesel). Though not used in the demonstration vehicle due to combustion stability issues, it did yield notable achievements. ANL ran high-fidelity simulations, including a genetic algorithm optimization on key control parameters to maximize efficiency. Large eddy simulations of the fuel sprays were validated against x-ray radiography data from ANL's Advanced Photon Source. DMP and diesel-assisted spark ignition combustion modes were compared to standard spark ignition. Conventional diesel/gasoline achieved 42% BTE, while Fischer-Tropsch diesel/E85 gasoline achieved over 45% BTE.

Gasoline Direct-Injection Compression Ignition Shows Potential for 39% Fuel Economy Improvement

Gasoline direct-injection compression ignition low temperature combustion enabled a 39% fuel economy improvement on a warm, combined Federal Test Procedure cycle.

Delphi Automotive Systems, Hyundai America Technical Center Inc., and Wisconsin Engine Research Consultants

Delphi, Hyundai America Technical Center, Inc., and Wisconsin Engine Research Consultants, have demonstrated the potential of a low-temperature combustion approach, gasoline direct-injection compression ignition (GDCI), for improving fuel economy. The project, part of the U.S. Department of Energy’s (DOE’s) Advanced Technology Powertrains (ATP) program, culminated in the demonstration of a 39% combined city and highway fuel economy improvement with a warmed-up engine, relative to a 2009 port fuel injected (PFI) baseline vehicle with a 2.4L engine (see Figure 1). Thermodynamic benefits offered by low-temperature GDCI combustion (operating lean and at 15:1 compression ratio), as well as downsizing and engine downspeeding, contributed to the fuel economy gain.

Cycle	Run 1	Run 2	Run 3	Avg.
City - EPAIII (Warm, unadjusted E10 fuel)	38.19	38.47	38.44	38.37
Hwy (unadjusted E10 fuel)	57.04	57.86	59.54	58.15
CAFE method Combined FE (Warm, adjusted)	46.21	46.66	47.11	46.66
Percent Improvement over Baseline				
Combined FE comparison (Warm, adjusted)	38.0%	39.3%	40.7%	39.3%

Figure 1. Fuel economy performance improvement demonstrated for GDCI development vehicle over baseline.

The 1.8L GDCI engine, based on a Hyundai Theta L4, was developed specifically for the project and features several key enabling engine systems, including multi-hole central mount fuel injection, advanced valvetrain, thermal management, and engine controls. The engine’s twin stage boost system has a turbocharger and a supercharger as well as two intercoolers. Low-pressure loop cooled exhaust gas recirculation is used with lean operation, and exhaust rebreathing is used to increase charge temperatures and collapse the

pumping loop under light load conditions. The project included a development vehicle and full control system. All testing used 87 octane E10 gasoline (10% ethanol).

Although the project exceeded the DOE ATP target of a 25% fuel economy improvement and met combustion noise targets, it did not meet the emissions performance target (Tier 2, Bin 2). Preliminary emissions performance of the GDCI vehicle on city and highway cycles with a warmed-up engine are shown in Figure 2. Follow-on work is now focused on meeting Tier 3 emissions standards while maintaining or improving fuel economy.

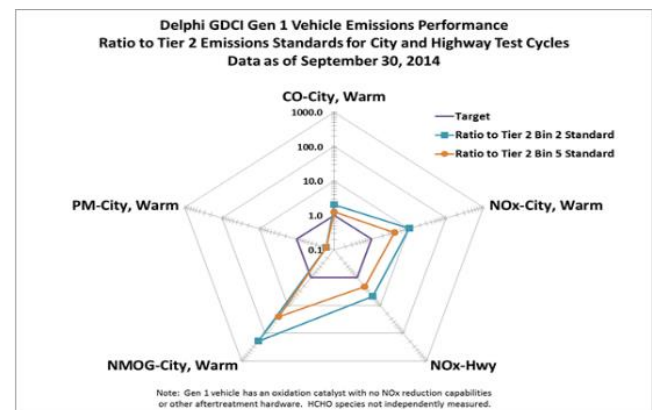


Figure 2. Relative performance of GDCI vehicle to Tier 2 Bin 2 and Tier 2 Bin 5 emissions standards. Target emissions performance for each pollutant is given by the purple line against each standard is then plotted as a ratio of that standard.

New Solver Accelerates Simulation of New Fuels in Engines

Rigorous chemical kinetics, fast chemistry solvers, and next-generation computing hardware aid development of advanced engines and investigations into new fuel performance.

Lawrence Livermore National Laboratory

The ability to handle detailed chemistry will be essential for developing advanced engines and investigations into new fuel performance. To meet this challenge, Lawrence Livermore National Laboratory (LLNL) is developing rigorous chemical kinetic models for new fuels, devising faster numerical solvers, and utilizing next-generation computer hardware.

Rigorous chemical kinetic models for new fuels are being developed, including gasoline, diesel fuel, and their mixtures with new fuel components. Recently, investigators identified and assembled a palette of 10 components, including n- and iso-alkanes, aromatics, naphthenes and olefins, to represent gasoline fuels and a corresponding comprehensive chemical kinetic mechanism. The comprehensive model has been successfully used to simulate the ignition behavior of selected fuels for advanced combustion engine gasolines, showing good agreement with experiments. This work is an important step toward simulations of gasoline fuel chemistry with sufficient fidelity to enable the integrated development of tomorrow's engines and fuels.

The software tools enabling use of detailed chemical kinetics in simulations include new methods for time integration and algorithms that take advantage of the newest massively parallel architectures. The new chemistry solvers employ advanced algorithms for large chemical systems to dramatically decrease the number of operations necessary to compute a solution. The solvers have been coupled to detailed engine simulations and are seven times faster than previous solution methods for large chemical mechanisms (see Figure 1). In addition, new algorithms were developed to compute the solution for many different chemical compositions

simultaneously using graphical processing units, drastically reducing the simulation time for the most intensive calculations performed by engine designers.

The new chemistry solvers are able to accelerate many reacting-flow simulations for both small and large-scale computing architectures. Commercializing these new capabilities in partnership with Convergent Science Inc., the producer of CONVERGE™ computational fluid dynamic software, ensures that they will be available to industrial users who advance engine design through simulation.

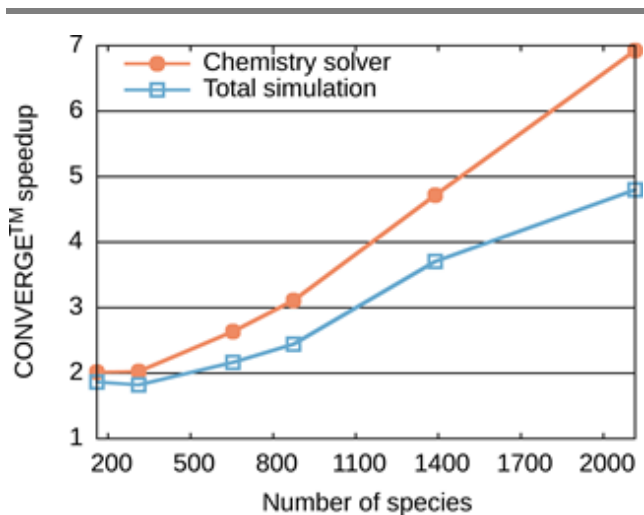


Figure 1. The LLNL solver accelerates the chemistry calculation by a factor of 7 in CONVERGE™ for fuel mechanism with 2,000 species (comparable in size to the gasoline surrogate used to study cetane-enhancers). Using a multizone model with 35 fluid cells per chemical reactor, the total simulation is accelerated by a factor of 4.8 for a homogenous-charge, compression-ignition.

Reactivity Controlled Compression Ignition Simulations Show Potential for 25% Improvement in Fuel Economy

Experimental results from a multi-cylinder engine were used as inputs to a vehicle simulation to model potential fuel economy improvements.

Oak Ridge National Laboratory

In-cylinder blending of gasoline and diesel to achieve reactivity controlled compression ignition (RCCI) combustion has been shown to reduce nitrogen oxide (NO_x) and particulate matter (PM) emissions while maintaining or improving brake thermal efficiency as compared to conventional diesel combustion (CDC). Investigators carried out multi-cylinder experiments on a light-duty diesel engine modified for gasoline port fuel injection (PFI) while maintaining the ability for direct injection of diesel fuel, thereby providing rapid control of overall fuel reactivity. The ability to tailor fuel reactivity to engine speed and load shows promise in allowing stable low-temperature combustion to be extended over more of the light-duty drive cycle load range. Differences in fuel properties and fuel reactivity have also been shown to enable load expansion with RCCI. Full coverage of a drive cycle may still require a multi-mode strategy in which the engine switches from RCCI to CDC when speed and load fall outside of the RCCI range, as determined by combustion noise and emissions constraints.

The team studied the potential for RCCI to improve drive cycle fuel economy by simulating the fuel economy and emissions for a multi-mode RCCI-enabled vehicle operating over federal U.S. city and highway drive cycles. The project explored experimental engine maps for multi-mode RCCI with three fuel combinations: E30 (30% ethanol/70% gasoline) and diesel fuel (ultra-low sulfur diesel [ULSD]), gasoline and ULSD, and gasoline and B20 (20% biodiesel/80% ULSD).

Autonomie simulations assumed a conventional mid-size passenger vehicle with a five-speed automatic transmission. The team compared modeled RCCI fuel economy results to a 2009 PFI

gasoline engine vehicle, the standard U.S. Department of Energy/U.S. DRIVE baseline. In all three RCCI fuel combination cases, the RCCI multi-mode strategy enabled at least a 25% improvement in modeled fuel economy compared to the baseline, and RCCI showed a 6-10% improvement compared to existing CDC (see Figure 1). Challenges remain, however. Modeling showed that nearly equal amounts of diesel and gasoline would need to be carried on-board, therefore requiring two fuel tanks. In addition, despite RCCI's lower engine-out NO_x, an increase in carbon monoxide (CO) and hydrocarbon emissions, together with lower engine exhaust temperatures associated with RCCI, will challenge aftertreatment systems. Follow-on research to reduce CO and hydrocarbon emissions with novel catalysts is underway.

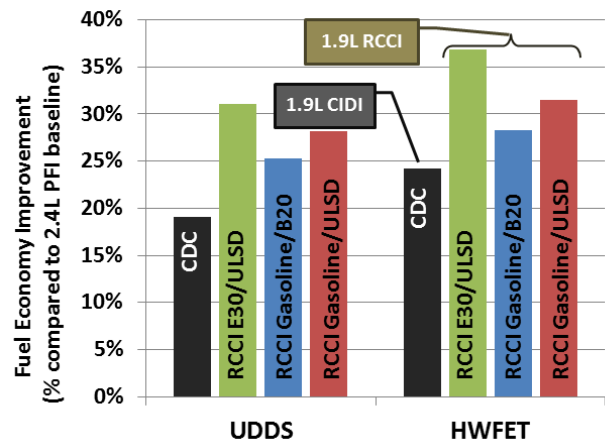


Figure 1. RCCI fuel economy simulations show potential for greater than 25% improvement over PFI baseline.

Innovative Metal Oxide Catalyst Oxidizes Carbon Monoxide Near 150°C Without Precious Metals

New precious metal-free catalyst oxidizes carbon monoxide without being inhibited by the presence of hydrocarbons.

Oak Ridge National Laboratory

Improvements in advanced combustion engine efficiency have the unintended consequence of challenging emission control systems. Greater fuel efficiency is leading to lower exhaust temperatures, where catalyst oxidation of carbon monoxide (CO) and other pollutants is more difficult. However, Oak Ridge National Laboratory (ORNL) has developed a new type of catalyst to enable improved low-temperature performance without using precious metal catalysts.

Platinum group metal (PGM) catalysts are the current standard for control of pollutants in automotive exhaust streams, but their high cost and susceptibility to inhibition at low temperatures are a hindrance. Inhibition occurs when one pollutant covers active catalyst sites and prevents other pollutant species from being oxidized. Of particular concern is the inhibition caused by interactions of CO and hydrocarbons (HC). Both CO and HC emissions are expected to increase for advanced combustion engines.

ORNL has developed a ternary mixed oxide catalyst composed of copper oxide, cobalt oxide, and ceria (dubbed CCC) as an alternative to PGM-based catalysts for low temperature CO oxidation (giving 90% conversion at 170°C). In powder form, the innovative CCC catalyst outperforms PGM catalysts for CO oxidation in simulated exhaust streams on a bench flow reactor. Surprisingly, the CCC catalyst shows no signs of inhibition by the model hydrocarbon, propene (C₃H₆), as shown in Figure 1.

This unique lack of inhibition exhibited by the low-cost CCC catalyst could be a key contribution enabling simultaneous low-temperature oxidation of CO and hydrocarbons. Inhibition has traditionally limited the ability of PGM catalysts. A

typical PGM-based catalyst must be heated to greater than 235°C to convert 50% of the C₃H₆ in the presence of CO; however, if CO is removed, this conversion can be achieved at significantly lower temperatures. Furthermore, the heat generated from the combustion of CO over the CCC catalyst would be beneficial with respect to activating the traditional catalyst formulations being used for hydrocarbons. These factors illustrate the great potential of this catalyst as a low-cost component in automotive exhaust streams of advanced combustion engines with low-temperature exhaust.

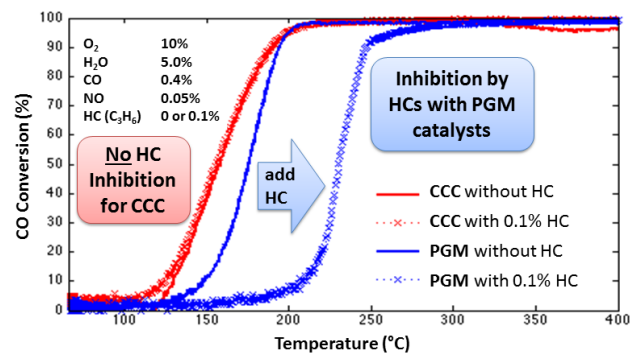


Figure 1. CO light-off curves of CuO_x-CoO_y-CeO₂ (CCC) and PGM-based catalysts in simulated exhaust conditions, which illustrates that the CO reactivity on CCC is unaffected by the presence of C₃H₆.

Novel Engine Lubrication Anti-Wear Additives Demonstrate Improved Fuel Economy

Prototype ionic liquid lubricant additives have improved friction and wear reduction characteristics, and have demonstrated 2% higher fuel efficiency compared to a commercial synthetic lubricant.

Oak Ridge National Laboratory, General Motors, Shell, and Lubrizol

Parasitic friction generally consumes 10-15% of the energy generated in an internal combustion engine. Lubricants are critical in mitigating the friction and wear of mechanical systems such as transportation vehicles. A potential path for reducing friction and increasing fuel economy is lowering oil viscosity to reduce hydrodynamic drag, but if too low, engine durability can be at risk due to inadequate wear protection.

Oak Ridge National Laboratory (ORNL), in two Cooperative Research and Development Agreements with General Motors and Shell, and in partnership with Lubrizol, has recently developed novel ionic liquids (ILs) as next-generation anti-wear lubricant additives to meet targets for lower viscosity and improved wear protection. These ILs also exhibit good oil miscibility, high thermal stability, non-corrosiveness, excellent wettability, and effective anti-wear and friction reduction characteristics. Last year, a prototype IL-enhanced low-viscosity (SAE 8) engine oil demonstrated 2% higher fuel efficiency with similar wear protection and aging performance compared to a commercial synthetic SAE 5W-30 engine oil in an industry-standard multi-cylinder engine dynamometer study.

This year, ORNL invented a new group of phosphonium-organophosphate ILs with symmetric cation structures [U.S. Patent Application 14/184,754] that has demonstrated better anti-wear performance than earlier compounds. Furthermore, the new ILs have shown synergistic effects when combined with conventional anti-wear additive ZDDP. As shown in Figure 1, the ZDDP+IL combinations outperformed either the ZDDP or the IL alone by ~30% in friction and 60-80% in wear. If backward compatible, the

low-friction and improved wear characteristics of these advanced lubricants could enable widespread deployment across the existing U.S. vehicle fleet, potentially saving billions gallons of fuel annually.

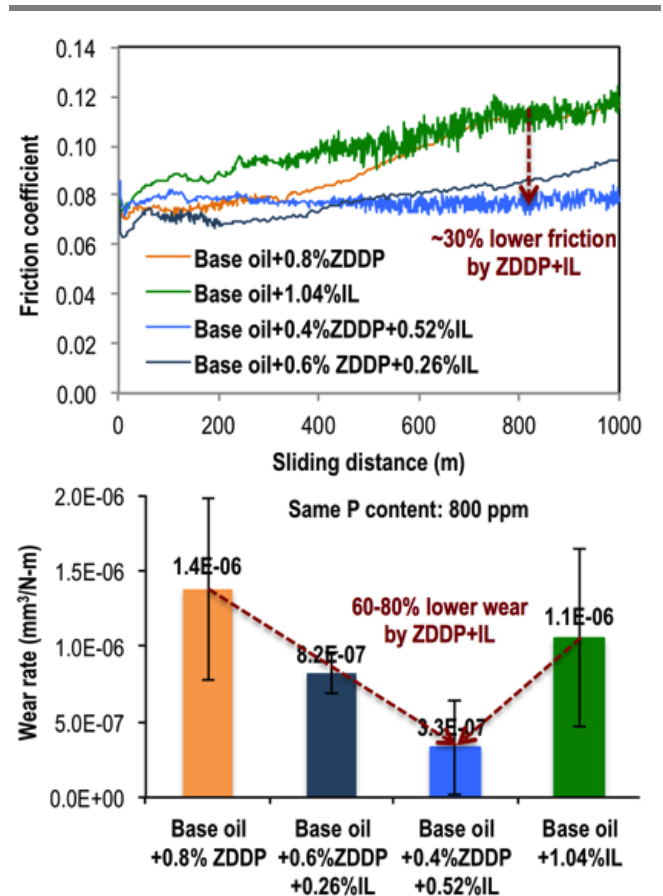


Figure 1. Synergistic effects of combining an ionic liquid and ZDDP (while maintaining allowable P content) reduce friction by 30% (top) and wear by 60-80% (bottom).

Low-Temperature Gasoline Combustion Achieves “Diesel Engine” Load-to-Boost Ratios

Boosted low-temperature gasoline combustion using direct-injection fueling overcomes a key technical barrier – achieving loads similar to diesel engines at similar boost pressures with efficiencies approaching 50%.

Sandia National Laboratories

Increasing internal combustion engine efficiency is critical for reducing petroleum consumption and carbon dioxide emissions. Low-temperature gasoline combustion (LTGC), based on the compression ignition of a premixed or partially premixed dilute charge, has strong potential for contributing to these goals since it can provide high efficiencies with low nitrogen oxide (NO_x) and particulate emissions. However, for conventional premixed LTGC (i.e., homogeneous charge compression ignition), high loads require relatively high boost pressures because of the high dilution levels needed to prevent knock.

With boosted operation, gasoline autoignition reactivity becomes sensitive to the local fuel-air mixture. Exploiting this phenomenon by using partial fuel stratification (PFS) causes the charge to autoignite sequentially, slowing the combustion process. This allows higher loads without knock, or for the same load, less timing retard, which gives higher efficiencies. Direct-injection (DI) fueling early in the intake stroke produces a level of stratification that works well with PFS.

As Figure 1 (top) shows, LTGC with early-DI, PFS can achieve a load of almost 20 bar indicated mean effective pressure, gross (IMEP_g) with only 2.0 bar of boost pressure for a compression ratio (CR) of 14:1, using standard certification gasoline. This is an increase of 17% over the maximum load with premixed fueling at this boost pressure, and it exceeds the maximum load of the production diesel version of this LTGC research engine. Moreover, the load-to-boost ratio is comparable to those of current production diesel engines, and achieving a ratio in this range overcomes a key technical barrier to LTGC with respect to turbocharger capabilities. Although LTGC commercialization faces other

challenges, these results from a single-cylinder research engine show great potential. Early-DI PFS also increases LTGC-engine efficiency to 48.4% for CR = 14:1, and raising the CR to 16:1 increases the maximum efficiency to 49.6% (see Figure 1, bottom), but with a modest reduction in the maximum load. All early-DI data points shown have no engine knock, undetectable soot, and $\text{NO}_x \leq 0.05$ g/kWh, reducing aftertreatment requirements.

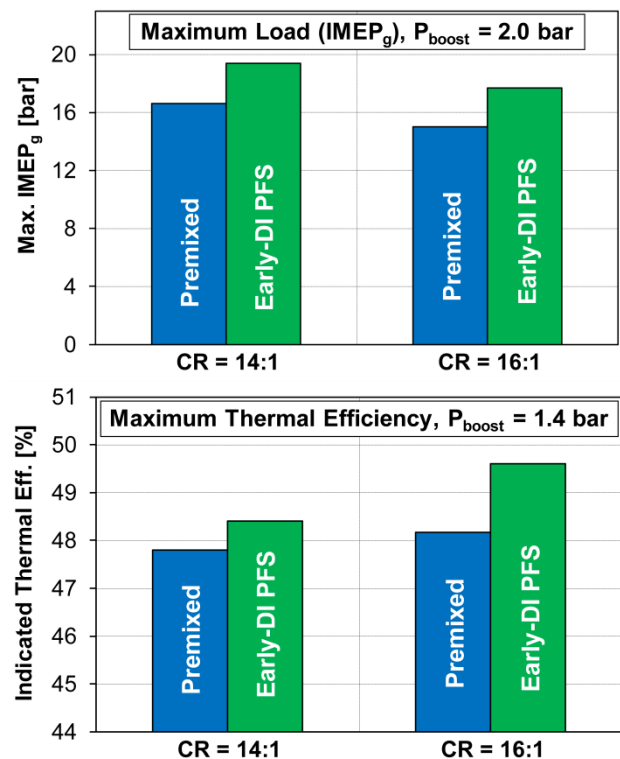


Figure 1. Maximum IMEP_g with an intake-boost pressure of 2.0 bar for premixed and early-DI PFS fueling at CR of 14:1 and 16:1, at 1200 rpm (top). Maximum gross indicated thermal efficiency with premixed and early-DI-PFS fueling, at 1200 rpm (bottom).

Unique Spray Measurements Enable Improved Models

A multi-laboratory collaboration contributing to the Engine Combustion Network provides a unique quantitative database and advanced modeling approaches to describe diesel fuel spray development.

Sandia National Laboratories and Argonne National Laboratory

Direct fuel injection technologies have enabled significant improvements in engine efficiency. However, current engine design and optimization efforts are hindered by uncertainties associated with fuel spray development. These uncertainties stem from the complexity of the high-pressure liquid flow passing through intricate nozzle geometries and from the two-phase mixing with gas outside of the nozzle—and ultimately affect the ensuing spray dispersion, mixing, and combustion. Available datasets have yet to quantify the liquid fuel dispersion in the near field where the spray is dense, and current spray models lack the capability to predict spray dispersion. Developing more capable spray modeling will streamline the optimization of future high-efficiency engines.

To address this barrier, Sandia National Laboratories and Argonne National Laboratory investigated how detailed internal nozzle geometry and needle movement couple to external spray development, including first-of-their-kind experiments for spray distribution. Measurements of the three-dimensional liquid volume fraction by x-ray radiography and tomography show the

developing mixing layer at the spray edge and the penetration of a pure liquid core of approximately 2 mm, as shown in Figure 1A. The existence of the liquid core is confirmed by observation of a partially transparent backlit spray using optical microscopy, as shown at Figure 1B. These measurements provide initial conditions supporting a massive dataset for the same spray developed through an international collaboration called the Engine Combustion Network (ECN). Models describing mixing and combustion datasets already available through the ECN can now be evaluated and improved using this unique dataset for spray mixing in the near-field.

The dataset also offers new understanding of the origin of dynamic variations in spray growth rate and a baseline for future spray modeling that links these variations to upstream disturbances within the injector. Advanced computational fluid dynamic simulations that begin inside the nozzle and extend outside into the near field of the spray are now being evaluated as part of the collaboration, as shown in Figure 1C.

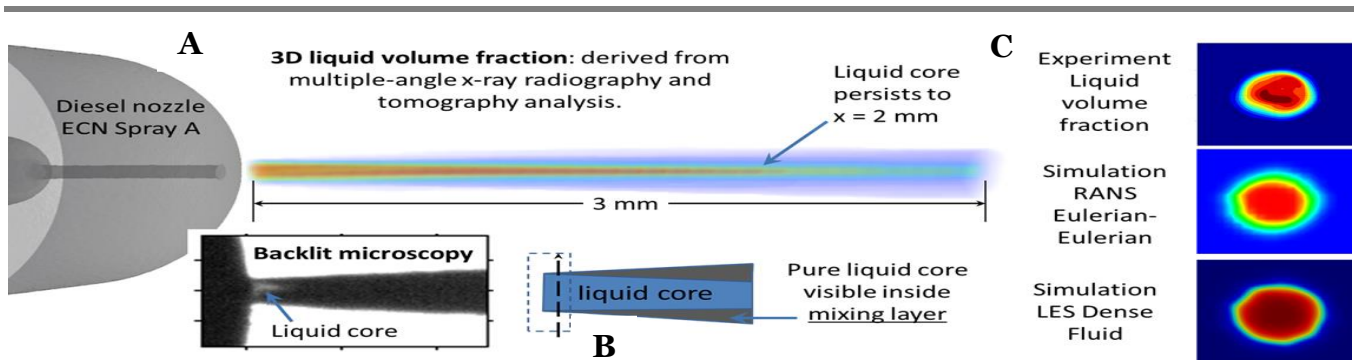


Figure 1. Experiments quantifying the growth and mixing of ECN spray compared to advanced spray simulations.

Electrical and Electronics



Manufacturability of Affordable Non-Rare Earth Magnet Alloys Demonstrated

Compression molding of gas atomized aluminum–nickel–cobalt identified as the preferred method for producing rare earth free magnets that will reduce the cost of electric traction drive motors.

Ames Laboratory

Ames Laboratory (Ames) led a group of researchers that has identified aluminum-nickel-cobalt (Alnico) magnets as the best near-term alternative to rare earth (RE) magnets in permanent magnet motors for electric drive systems. As part of the Beyond Rare Earth Magnets (BREM) research and development project, Ames developed a new means of processing Alnico that improves performance through compression molding of gas atomized magnet particles.

BREM researchers focused on refining Alnico alloys. Alnico 8 and 9 showed the most promise for improvement because of their higher starting coercivity (an important magnetic property), which is believed to be the result of the elongated iron-cobalt phase shape anisotropy. Using its in-house gas atomizer, Ames produced a uniform pre-alloy powder with a very spherical shape and a low-satellite particle content. In addition, this powder had excellent flowability and powder packing. Sintering and compression molding, with a binder, were investigated as potential methods to form the powder into bulk magnet shapes.

Investigators determined that compression molding of the gas atomized powder with a polypropylene carbonate binder (see Figure 1) is the preferred method for producing inexpensive bulk magnet shapes. The bulk magnets will require minimum amounts of post-processing, reducing final product cost.

From these successes, Ames has determined that an improved magnet composition (increased coercivity) can be produced for use in UQM Technologies Inc.'s non rare earth proof-of-design motor that the U.S. Department of Energy funded. This improved material will be a variation of Alnico 8.

Additionally, Ames successfully determined the key parameter that leads to increased coercivity: reduced spinodal spacing. Reduction in spinodal spacing is a direct function of the time spent at a specific magnetic annealing temperature. Atomistic modeling also suggested that decreased cobalt concentration in a nano-pattern matrix could boost coercivity, leading to re-design of Alnico 8 alloys to reduce cobalt by 40%, which also cuts product cost.

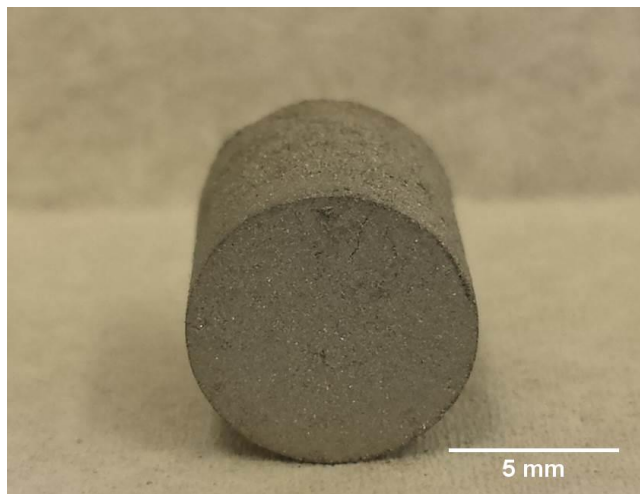


Figure 1. Compression molded Alnico 8 prototype magnet made from pre-alloyed gas atomized powder.

Motor Thermal Management Spurs New Motor Designs

New data for motor thermal management provides designers with critical information needed for modeling and designing motors.

National Renewable Energy Laboratory

Thermal management of motors directly improves power density and reliability; however, thermal management is a significant challenge because the heat transfer and fluid flow are complex. Improved accuracy of motor material thermal properties and convective heat transfer can improve simulation accuracy of motor performance by 20%. The National Renewable Energy Laboratory's (NREL's) motor thermal management expertise enabled more accurate measurements of thermal properties related to lamination stacks and automatic transmission fluid (ATF) cooling. This effort resulted in first-ever detailed motor component thermal data in the open literature, which will enable motor developers to improve motor models and designs.

NREL measured thermal conductivity and inter-lamination thermal contact resistance of multi-layer lamination stacks for a range of motor lamination materials. The through-stack thermal conductivity was between 3% and 9% of the bulk lamination material thermal conductivity. The thermal contact resistance between motor laminations (see Figure 1 top) reduces the through-stack thermal conductivity. The overall thermal conductivity depends on lamination surface profiles, contact pressure, bulk material thermal conductivity, and lamination thickness. The data quantify the difficulty in extracting heat axially through the lamination materials within the motor, which has significant impacts, especially on cooling rotors.

NREL also measured convective heat transfer coefficients with ATF jets (see Figure 1 bottom) impinging on surfaces representative of motor end-winding wire bundles. Over the tested flow rates, jet impingement on the wire surface resulted in a 10-34% increase in the average heat transfer coefficient

compared to available data for impingement on flat/smooth surfaces. The project also identified potential degradation in heat transfer, with increasing jet velocity, on the wire surfaces.

NREL's motor thermal management research improves understanding of motor cooling, enabling analysis that supports design of innovative electric motors with improved thermal performance. This capability, knowledge, and data are crucial for original equipment manufacturers and suppliers that require consistent characterization of ATF jets and motor thermal properties for new motor configuration design and development.

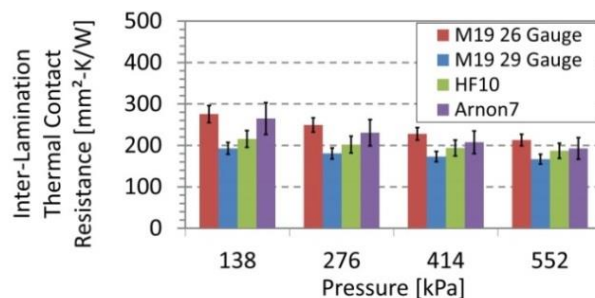


Figure 1. Results for inter-lamination thermal contact resistance (top). Picture of the test section for measurement of ATF jet heat transfer coefficient (bottom).

Plastic Heat Exchanger Improves Heat Transfer Efficiency and Reduces Inverter Weight

A plastic manifold incorporating jet impingement and surface enhancements increased the coefficient of performance by 17% at 100 kW electrical power and reduced the electric drive vehicle inverter weight by 19%.

National Renewable Energy Laboratory

A novel lightweight plastic heat exchanger prototype (see Figure 1), incorporating single-phase liquid jet impingement on microfinned surfaces on the module baseplate, was demonstrated in collaboration with UQM Technologies Inc. and Wolverine Tube Inc. At 100 kW electrical power, the new heat exchanger improved the coefficient of performance (COP) by 17%, the specific power by 36%, and the power density by 12% when compared to the channel-flow-based cold plate used in the commercial inverter (baseline UQM PowerPhase®). Performance improvements (see Table 1) were attributed to two main factors: a 17% decrease in thermal resistance and a 50% reduction in heat exchanger weight (6 kg to 3 kg). With the lower thermal resistance, the dissipation of heat generated by the power electronic devices increased by 20%. The total inverter weight was reduced from 16 kg to 13 kg (19% reduction).

At UQM Technologies Inc., scientists conducted full inverter-level experiments using dynamometers with water-ethylene glycol coolant (a 40-60% mixture) at 30°C and 10 L/min at 40 to 100 kW electrical power, dissipating 0.9 to 2.2 kW of heat. For the liquid jet impingement-based heat exchanger, the manifold is not part of the thermal pathway. Hence, using mass manufacturing techniques, the manifold can be made of lighter-weight, lower-cost thermal plastic (compared to manifold materials used in current manufacturing techniques). Compared to the channel-flow baseline, jet impingement yielded less variability in the junction temperatures of the power electronic devices (5-7°C lower). The jets provided high localized cooling underneath the devices where heat fluxes were the highest and heat transfer was most needed. The microfinned surfaces enhanced heat transfer by providing increased surface area upon which the jets

impinged, and created turbulence in the liquid coolant near the surface.

Metric	Improvement
Heat dissipation	20%
Weight	19%
COP	17%
Specific power	36%
Power density	12%

Table 1. Improvement over the baseline inverter.

Further efforts to promote adoption include advanced packaging design and integration to improve strategies to attach the power modules to the heat exchanger manifold, reducing risk of leaks. Methods to reduce costs must also be evaluated, and the sequence of applying the microfinned surface enhancements must be determined.

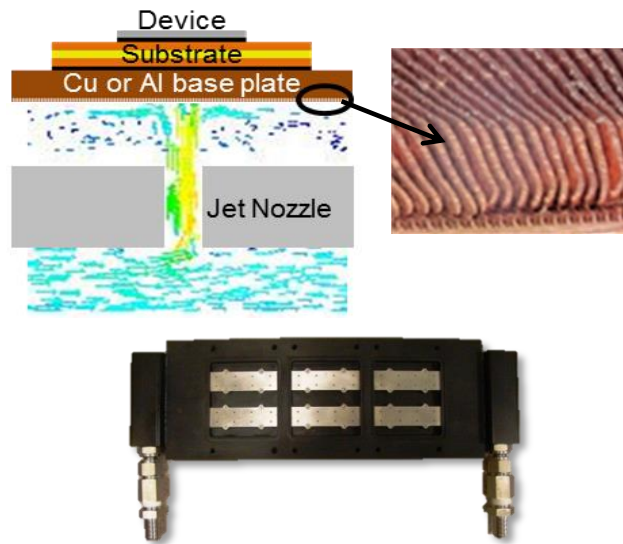


Figure 1. Cross-section of the jet impinging on the microfinned enhanced base plate of the power electronics module stack-up (top). The plastic manifold with the nozzle inserts (bottom).

All Silicon-Carbide Inverter Meets 2015 Performance Targets

Emerging wide bandgap semiconductors offer opportunities for higher power density, higher temperature, and higher frequency operation, as well as efficiency and reliability improvements.

Oak Ridge National Laboratory

Emerging wide bandgap (WBG) devices significantly improve power electronics. Their ability to operate at greater efficiencies over higher temperatures and operational frequencies reduce cooling requirements and minimize passive component requirements.

Oak Ridge National Laboratory developed a 10 kW, all-silicon carbide (SiC) inverter, shown in Figure 1, using 1,200 volt (V), 100 amp (A), SiC MOSFET modules. The direct bonded copper (DBC) design and layout were optimized for minimum parasitics and improved performance of the SiC devices.

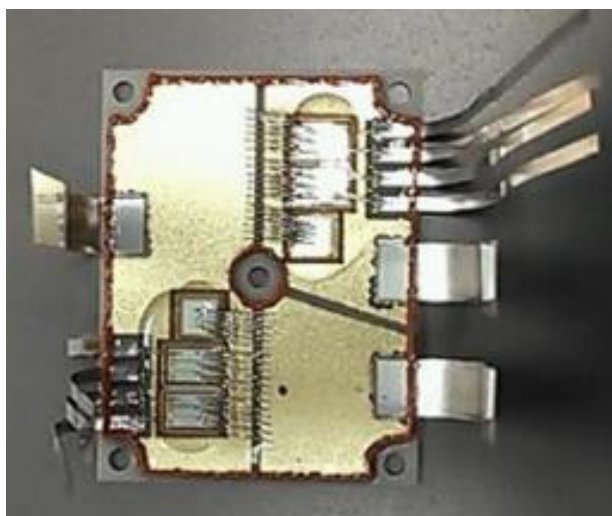


Figure 1. 1,200 V, 100 A SiC power module.

These modules were used to develop the inverter shown in Figure 2. The inverter prototype uses commercially-available gate drivers with galvanic isolation up to 3,000 V_{RMS} and integrated over current protection, undervoltage lockout, and temperature feedback features. The modules were mounted on top of a three-dimensional printed, additively manufactured heat sink with thermal grease as the heat transfer medium between the DBC and heat sink.



Figure 2. 10 kW SiC inverter prototype.

The inverter's total volume is ~1.5 L and its total weight is ~1.76 kg, not including connectors and housing. The total operating power density and the operating specific power based on the maximum tested conditions are ~13.3 kW/L and ~11.3 kW/kg, respectively (the U.S. Department of Energy's 2015 target is 12 kW/L).

Test results demonstrated successful inverter operation with an efficiency of 99% at 10 kW operating power (450 V, 5 kHz, 60°C coolant temperature, and flowrate of 1.6 gpm).

The additive manufacturing process contributed to several improvements. The specific power increased due to the reduced amount of material required by the innovative versus traditional metal processing techniques. New complex geometries internal to the heatsink were introduced for improving the heat transfer in specific areas for the semiconductor devices.

New System Improves Materials Characterization

Custom characterization system provides a deeper understanding of magnetization and loss mechanisms in electrical steel; provides information needed for high-fidelity electric motor modeling.

Oak Ridge National Laboratory

A newly-developed custom magnetic characterization tool observes localized properties in electrical steel. The measurement stage of the characterization system, shown in Figure 1, includes excitation coils that apply a magnetic field to a single sheet sample as the local magnetic field on the surface of the sample is measured.

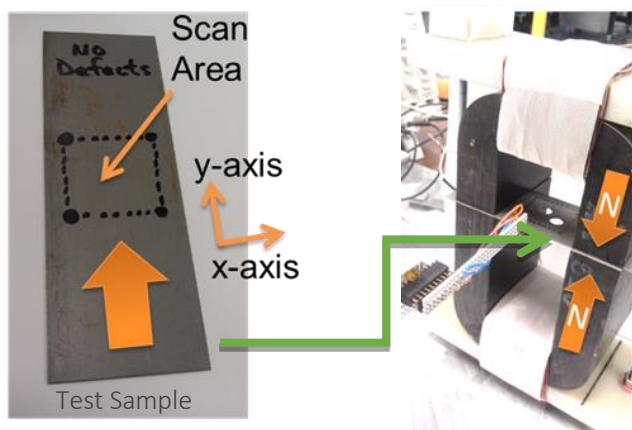


Figure 1. Measurement stage of the magnetic material test sample (left) and characterization system (right).

Conventional motor simulation techniques assume that material properties are homogeneous for all of the soft magnetic material. However, many factors impact magnetic properties, including residual stress from stamping or laser cutting. Additionally, stamped or laser cut edges are near the air gap, which is a critical location for the magnetic circuit and operation of the motor.

Characterizing the impact of residual stress on magnetic properties has revealed significant degradations near areas that have sustained mechanical deformation. Figure 2 shows the resulting magnetic field, with a flux density of 1.4 Tesla, after a brief application of laser pulses in five different areas of the sample. Although the disturbed areas are barely visible on the physical

sample, five distinct areas are visible in the plot of the scanning results, where the magnetic properties are significantly impacted.

Other test results indicate that stamped edges can have magnetic fields up to five times higher at the deformation zone for a given flux density. Substantial negative impact on magnetic properties is incurred on the order of millimeters from the site of deformation. These degradations significantly impact motor performance and losses; results indicate that improved modeling of magnetic properties can improve simulation accuracy for torque and power by up to 20%.

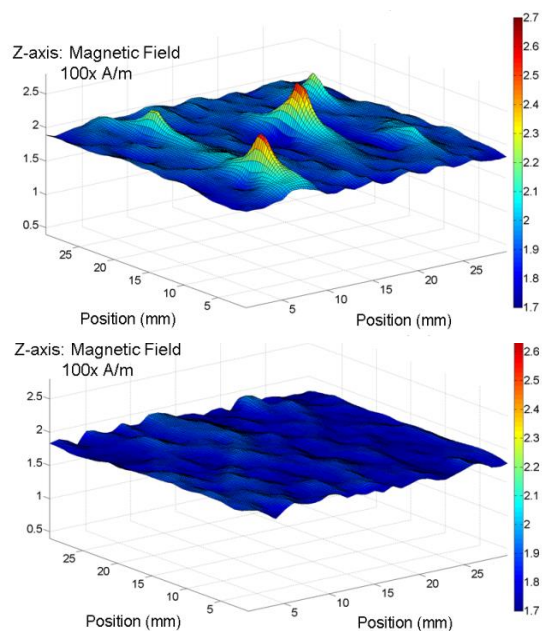


Figure 2. Magnetic field results before disturbances (top). After a brief application of five laser pulses (bottom).

Next-Generation Wide Bandgap Packaging Improves Inverter Efficiency

Advanced, three-dimensional planar-interconnected silicon carbide power module features innovative packaging and offers comprehensive improvements in performance, efficiency, density, and cost.

Oak Ridge National Laboratory

Oak Ridge National Laboratory (ORNL) is developing wide bandgap (WBG) automotive power electronics technologies with advanced packaging technology development to help achieve U.S. DRIVE targets.

The ORNL Packaging Laboratory fabricated an all-silicon carbide (SiC) 100 amp (A)/1,200 volt (V) single phase-leg power module using an innovative, planar-bond-all (PBA) packaging technology, shown in Figure 1. This innovative approach employs area bonding instead of wire bonding to build multiple layer/multiple component stacks in a two-step process. The module uses the latest industrial SiC power devices and a three-dimensional (3D) planar interconnection with double-sided direct cooling (both forced air and liquid).

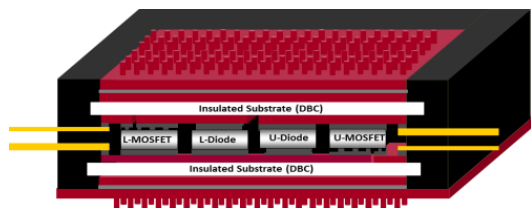
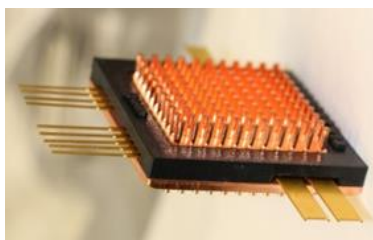


Figure 1. ORNL PBA-SiC power module with 3D planar interconnection and double-sided heat sinks.

Figure 2 shows the PBA-SiC power module prototype integrated with an innovative coolant manifold. Combining the superior attributes of SiC devices with advancements in packaging, the PBA-SiC module reduces electric parasitic parameters by

70% and specific thermal resistivity by more than 45%, compared to the Toyota Camry module shown in Figure 3. These improvements are represented by a four-times larger allowed current density of the SiC device in the module for the same temperature increase. The packaging improvements also allow system operation at high efficiency (50% power loss), resulting in five-times higher frequency. This is significant for achieving efficiency, power density, and cost targets for power electronic systems in electric drive vehicles.

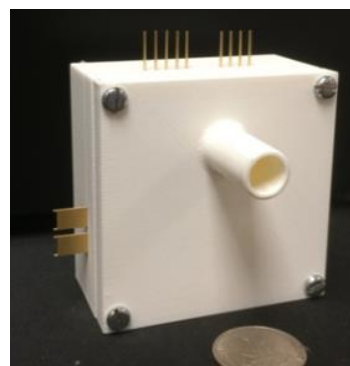


Figure 2. Double-sided cooling integrates the PBA power module into a coolant manifold.

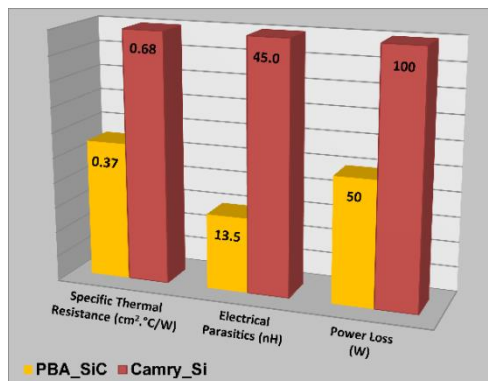


Figure 3. Technical relative performance comparison between ORNL PBA-SiC (yellow) and Toyota Camry Si (red) modules.

Electrochemical Energy Storage



Increased Cell Energy Density and Specific Energy through Advanced Technology Electrode Structure

Innovative silicon nanowire anode enables next-generation lithium-ion cells with more than 30% more energy per unit of weight and volume than current cells.

Amprius

Automakers produce batteries for electric vehicles by packaging state-of-the-art lithium-ion cells into battery packs. Amprius has developed next-generation cells with over 30% more energy per unit of weight and volume than those used in electric drive vehicle batteries today (see Figure 1). Amprius' advanced technology anode could thus enable higher-energy battery packs, which could correspondingly extend driving range and accelerate electrification.

Manufacturers have limited room to increase the energy of today's lithium-ion cells using standard active materials. Those active materials – an anode made from graphite paired with a cathode made from one of several commercially-available material combinations – are used at energy capacities close to their fundamental limits and the cells' packaging has already been optimized. An advanced anode or cathode approach is thus needed to boost cell and battery performance. Amprius developed a higher-energy anode material and structure combination, replacing graphite anodes with silicon, which offers nearly 10 times higher capacity per unit weight. However, conventional approaches with silicon have not produced cells with the long cycle life required for electric vehicles. The approaches have not addressed silicon's propensity to swell – by up to four times its volume – when charged with lithium ions.

Amprius aims to address silicon's cycle life (see Figure 2) challenge by building anodes using a new and unique structure, nanowires, rather than the conventional structure, particles. Amprius' porous and patent-protected nanowires permit silicon to expand and contract internally and repeatedly without breaking. Because the nanowires are attached to the current collector, Amprius does not

rely on particle-to-particle contact and is able to achieve not only high energy and cycle life, but also high power (fast charge and discharge).

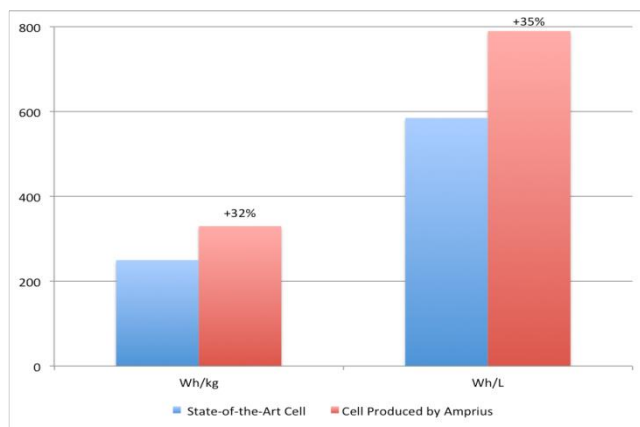


Figure 1. The pouch cells Amprius delivered to Idaho National Laboratory averaged 330 Wh/kg and 790 Wh/L, and had >30% more energy than in a State-of-the-Art pouch cell.

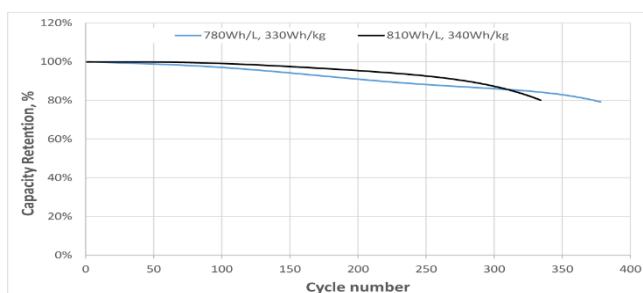


Figure 2. The >2.5 Ah silicon-based cells Amprius built and tested internally achieved >330 Wh/kg, >780 Wh/L, and >300 C/2 cycles at 100% depth of discharge.

Cradle-to-Gate Automotive Lithium-Ion Battery Impacts Reduced by Recycling

The relatively small contribution of lithium-ion batteries to electric vehicle life-cycle energy consumption and greenhouse gas emissions can be reduced through recycling, as can the local impacts of cathode metal mining.

Argonne National Laboratory

Argonne National Laboratory (ANL) carries out life-cycle analyses of automotive lithium-ion batteries (LIB) to identify critical energy or environmental impacts in their supply chain and potential mitigation measures for these impacts. Furthermore, ANL investigates possible integration of materials recovered from pyrometallurgical, physical, and hydrometallurgical recycling processes into batteries to reduce life-cycle energy consumption, greenhouse gas (GHG) emissions, and sulfur (SO_x) emissions.

Figure 1 illustrates the cradle-to-gate energy consumption of producing LIBs with different cathode materials. Materials production drives energy consumption; assembly is a minor contributor. Batteries with cobalt- and nickel-containing cathode materials have the greatest energy consumption on a per-mass-of-battery basis. On a per-battery basis, the battery containing a lithium- and manganese-rich nickel manganese cobalt oxide (LMR-NMC) cathode and graphite anode has approximately the same cradle-to-gate energy consumption as a battery with a lithium manganese oxide (LMO) cathode. LMR-NMC is about three times as energy intensive to produce as LMO, but about 41% less of it is needed in the battery (when both batteries use graphite as the anode material) because its capacity is 250 mAh/g, 2.5 times greater than that of LMO.

Recycling shows great potential to reduce LIB energy consumption and environmental impacts. For example, if recycled lithium cobalt oxide (LCO) were incorporated into automotive batteries that would have used virgin LCO prepared hydrothermally, the cathode material contribution to overall battery GHG intensity would decline from 57% to 25% and overall battery GHG intensity would decline by 43%.

LIBs generally contribute less than 5% of electric vehicle life-cycle emissions. In the case of LIBs with cobalt- or nickel-containing cathode materials, however, ore smelting at the beginning of the supply chain elevates SO_x emissions. Recovering cathode material through recycling is an important strategy to reduce these impacts. Recycling also reduces material scarcity concerns, which, among commonly used cathode materials, are greatest for cobalt.

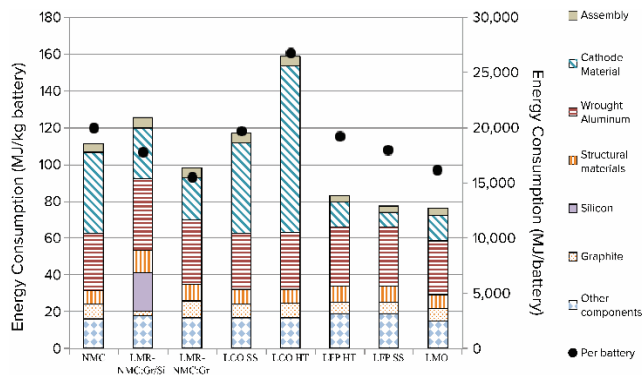


Figure 1. Energy intensity of battery electric vehicle production with 28 kWh batteries from cradle-to-gate with different cathode materials.
 NMC = $\text{LiNi}_{0.4}\text{Co}_{0.2}\text{Mn}_{0.4}\text{O}_2$.
 LMR-NMC = $0.5\text{Li}_2\text{MnO}_3 \cdot 0.5\text{LiNi}_{0.44}\text{Co}_{0.25}\text{Mn}_{0.31}\text{O}_2$.
 LCO = LiCoO_2 .
 LFP = LiFePO_4 .
 LMO = LiMn_2O_4 .
 Gr = graphite.
 Si = silicon.
 HT = hydrothermal.
 SS = solid state.

Effects of Fast-Charging on Lithium-Ion Cells

Testing and post-test diagnostics of the effect of fast-charging on commercial cells resulted in changes in electrical performance and damage to cell components that were directly proportional to charge rate and inversely proportional to amount of charge returned, respectively.

Argonne National Laboratory

With further vehicle electrification, consumers may desire battery charging to take about the same amount of time that refueling an internal-combustion engine-powered vehicle currently does. This “fueling” does not have to be a full charge, but can be a partial charge. The Fast-Charge Test, in the U.S. Advanced Battery Consortium (USABC) Electric Vehicle Manual,¹ was designed to measure the impact of charging a battery from 40-80% state of charge (SOC) at successively higher rates, starting from about twice the overnight rate. The high charge rates used may introduce new degradation modes, causing the performance of the battery to decline faster than expected, and thus an initial investigation into these possible modes was undertaken.

Commercially-available, 18650-sized, lithium-ion cells were charged at rates in the range of 0.7- to 6-C. The charge returned (the amount the cell was charged) was either 100% or 40% and the discharge rate was C/1 (100% returned) or C/3 (40%). Figure 1 shows the impact of charge rate on cell resistance. The increase in resistance versus time was non-linear in all cases. Additionally, the rate of resistance tended to accelerate with increasing time.

The physical factors that contributed to the results in Figure 1 were identified by post-test examination. As shown in Figures 2a and 2b, the amount of charge returned also had an effect. As shown in the figures, there was more delamination with less charge returned. The extensive delamination seen in Figure 2b may be the cause of rapid resistance increase. As delamination increased, the contact between the copper foil and anode decreased. Most likely, the more extensive damage was caused by

the 40%-charge-return cells getting hotter due to a shorter total cycle time; that is, there was not as much “low-rate” discharge time in each cycle during which the cell could cool down.

These results imply that fast-charging can introduce its own failure mode. The fast-charge test of the USABC manual might accordingly be evaluated to also take into considering the amount of charging done; and, more importantly, battery pack designs must be capable of adequate heat rejection during fast-charge.

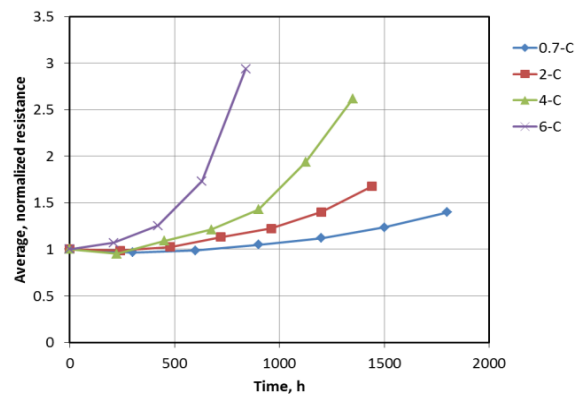


Figure 1. Average, normalized resistance versus time and charge rate. The cells were charged from 0 to 100% SOC at the rates given in the legend.

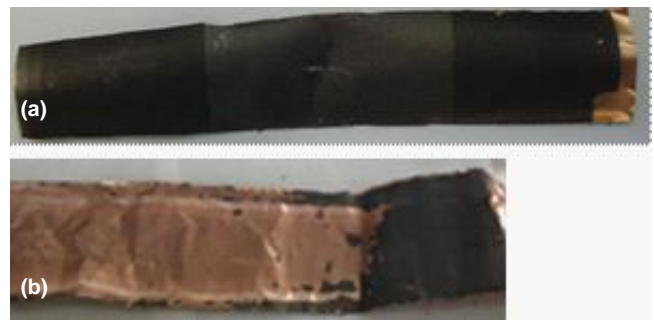


Figure 2. Delamination of anode as a result of changing the charge returned, a=100%; b=40%. The charge rate in both was 4C.

¹ USABC Electric Vehicle Battery Test Procedures Manual, Rev. 2, January 1996.

New High Capacity “Layered-Layered-Spinel” Composite Cathode Materials for Lithium-Ion Batteries

Advances have been made in increasing stability of “layered-layered” composite cathodes by integrating a spinel component, highlighting the importance of optimizing electrode composition and structural control.

Argonne National Laboratory

“Layered-layered” composite lithium- and manganese-rich nickel manganese cobalt oxide structures, so named because they are comprised of two layered components in complex structural arrangements, are attractive cathode candidates for meeting the goals for advanced, high energy density lithium (Li)-ion batteries. Despite their high capacity, damaging structural changes occur on cycling to high potentials that result in voltage fade, thereby limiting their appeal for electric vehicle applications. Recent advances to stabilize “layered-layered” electrodes have been made by introducing a structurally-compatible spinel component into their structures.

A high-resolution transmission electron microscopy (HRTEM) image of a $0.25\text{Li}_2\text{MnO}_3 \cdot 0.75\text{LiMn}_{0.375}\text{Ni}_{0.375}\text{Co}_{0.25}\text{O}_2$ electrode, targeted to contain 15% spinel, is shown in Figure 1a, and is consistent with the simulated HRTEM image of material with integrated layered and spinel components (see Figure 1b).

Electrochemical cycling data of “layered-layered-spinel” electrodes (targeting a 15% spinel content), derived from lithium deficient $0.25\text{Li}_2\text{MnO}_3 \cdot 0.75\text{LiMn}_y\text{Ni}_y\text{Co}_{1-2y}\text{O}_2$ compositions with various values of y, are shown in Figure 1c. The cells were first activated at 4.6 volt (V) and subsequently cycled between 4.45 V and 2.0 V. Lowering the cobalt content (i.e., increasing y) improved both the capacity and cycling stability of this system. In particular, a “layered-layered-spinel” electrode with a targeted 15% spinel content, derived from a lithium deficient $0.25\text{Li}_2\text{MnO}_3 \cdot 0.75\text{LiMn}_{0.375}\text{Ni}_{0.375}\text{Co}_{0.25}\text{O}_2$ composition, exhibited the greatest cycling stability, while providing approximately 190 mAh/g (see Figure 1c – blue line). The dQ/dV plots (see Figure

1d) over 20 cycles demonstrate that the selected cycling protocol and this particular composition exhibits minimal voltage activity below 3.5 V, relative to highly rich “layered-layered” electrodes that suffer from voltage decay that drifts towards 3 V on repeated cycling.

Synthesis studies of “layered-layered-spinel” cathode compositions have been initiated at Argonne National Laboratory’s Materials Engineering Research Facility to validate the electrochemical performance of laboratory cathodes and to scale up the production of the most promising materials.

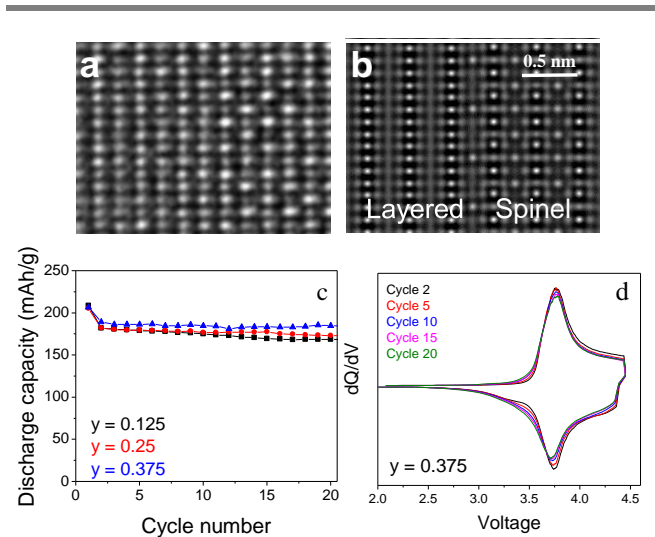


Figure 1. (a) HRTEM image of a composite electrode with integrated layered and spinel components. (b) Simulated HRTEM image of a composite “layered-spinel” structure. (c) Cycling stability of Li cells containing Li-deficient $0.25\text{Li}_2\text{MnO}_3 \cdot 0.75\text{LiMn}_y\text{Ni}_y\text{Co}_{1-2y}\text{O}_2$ cathodes with a targeted 15% spinel content. (d) dQ/dV stability over 20 cycles for the $y=0.375$ composition in (c).

Understanding Factors Affecting Power Capability of High-Energy Lithium-Rich Layered Cathode Materials

Synchrotron-based advanced time-resolved x-ray absorption spectroscopy is used to find the individual contribution of transition metals to the power capability of lithium-rich layered cathode materials.

Brookhaven National Laboratory

For powering electric vehicles using high-energy lithium- and manganese-rich nickel manganese cobalt oxide (LMR-NMC), a number of important issues need to be addressed, including their relatively poor power capability. Experimental results distinguishing the kinetic property of each component in the composite material would be helpful in understanding the fundamentals of the power properties. For the elemental factor, the charge transfer rate of each individual transition metal (TM) element (nickel [Ni], cobalt [Co], and manganese [Mn]) is important, especially for Mn, which has at least two different structural environments (LiMO_2 and Li_2MnO_3).

Brookhaven National Laboratory applied a combination of X-ray diffraction (XRD) and X-ray absorption spectroscopy (XAS) to elucidate the contribution from each component and element to the capacity. Then a novel time-resolved XAS technique was applied to study the reaction kinetics regarding different components and elements as a function of time.

The results show that Mn sites have slower reaction kinetics compared to Ni and Co, both before and after activation of the Li_2MnO_3 component. This is the first direct experimental observation that differentiates the reaction kinetics at different TM sites in these cathode materials (which have multiple reaction sites).

Figure 1 plots the comparative Fourier transformed magnitude of the Ni, Co, Mn K-edge EXAFS spectra during constant voltage charge at 5 volt (V) using color scale. For Ni, the first coordination peaks (Ni-O) show dramatic changes in both position and intensity within the first 100 seconds, which indicates that the charge compensation occurs at the Ni sites. The peak intensities decreased first (from 0 seconds to ~60 seconds) due to the Jahn-

Teller distortion caused by the oxidation of Ni^{2+} to Ni^{3+} , then turned around to increase with further oxidation of Ni^{3+} to Ni^{4+} . The EXAFS features remain unchanged after 160 seconds, indicating the oxidation of Ni^{2+} to Ni^{4+} was almost completed within the first three minutes. For Co and Mn, the first coordination shell peak (Co-O and Mn-O) intensities show a continuous decrease. No obvious Co-O peak intensity changes can be observed after 200 seconds at 5 V charge, while Mn-O peak intensities continued to decrease for the entire observation time scale (900 second), indicating much slower delithiation kinetics around Mn sites.

These results show that Mn sites have slower reaction kinetics both before and after initial "activation" of Li_2MnO_3 , compared to Ni and Co, providing better understanding of the role of these factors in the balance of energy to power in various Li-rich layered materials for different applications. Finally, this result corroborates test data showing that LMR-NMC materials with higher Mn content have, in general, lower power capability.

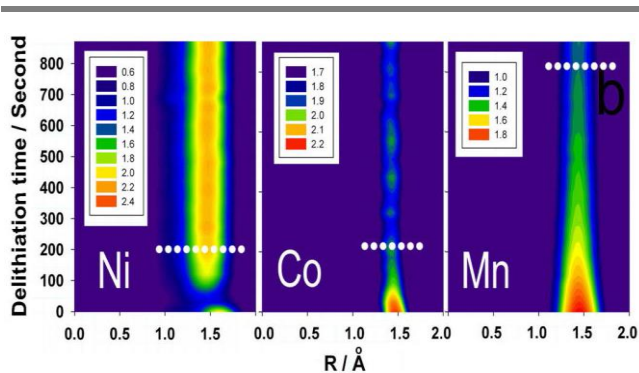


Figure 1. EXAFS spectra of $\text{Li}_{1.2}\text{Ni}_{0.15}\text{Co}_{0.1}\text{Mn}_{0.55}\text{O}_2$ during constant voltage charging at 5 V. Ni, Co, Mn reacted simultaneously using time-resolved XAS technique. Projection view of corresponding Ni-O, Co-O, Mn-O peak magnitudes of the Fourier transformed K-edge spectra as functions of charging time.

Multifunctional Separator Performance Confirmed for Large Format Lithium-Ion Batteries

Inorganic-filled separators demonstrate improved thermal stability, lower resistance, and longer cell cycle life.

ENTEK Membranes LLC and United States Advanced Battery Consortium

ENTEK has addressed the problem of separator integrity at temperatures well above the melting point of polyethylene by producing composite silica-filled membranes with ultra-high molecular weight polyethylene. These composite separators demonstrated very low shrinkage at high temperatures (<5% at 200°C). In addition, the silica filler provides several other benefits (higher porosity, faster wetting with electrolyte, and a better interface with battery electrode), which led to unanticipated improvements in battery performance.

The goal of the third, and final, phase of this project was optimizing material selection and processing to make higher strength, defect-free separator materials, and to supply samples to battery makers who would test these separators in large format batteries. ENTEK produced separator films by extrusion followed by biaxial orientation, using spray dried and jet milled silica materials selected to improve filler dispersion and reduce defects in the film. The polymer-to-filler ratio was optimized and the fabrication process was modified to increase the film mechanical strength without compromising its high temperature stability. A doubling of the separator puncture strength was demonstrated.

Improved cell performance (cycle life, calendar life, and power capability) was demonstrated in both cylindrical 18650 cells and in prismatic cells for hybrid electric vehicles (HEVs). The enhanced low-temperature power capability (see Figure 1), as well as improved cycle life and high-temperature calendar life (see Figure 2), may enable cost reductions for lithium-ion batteries in hybrid and electric vehicle applications, through a decrease in the oversizing of battery systems needed to

compensate for power performance loss at low temperatures and for capacity loss over the battery lifetime.

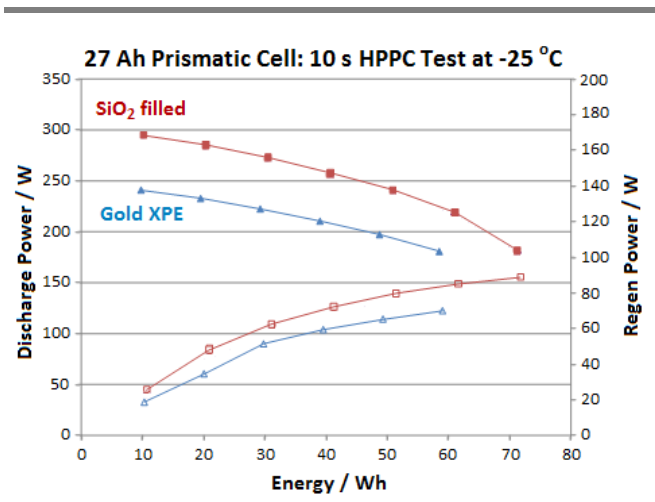


Figure 1. HEV cells with a silica-filled separator demonstrate improved low-temperature power capability over cells.

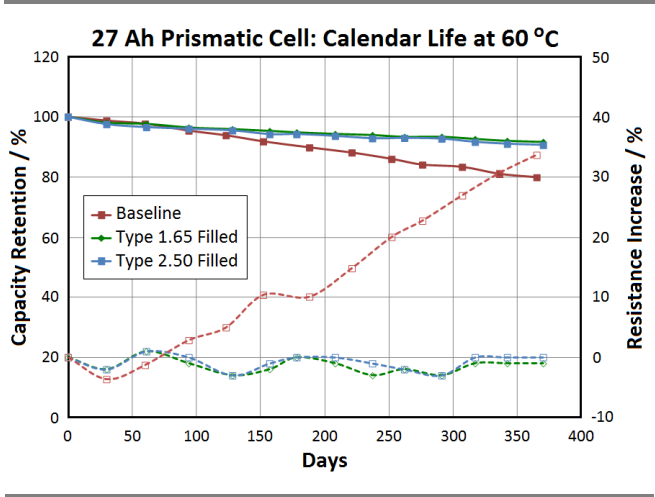


Figure 2. HEV cells with a silica-filled separator show improved capacity retention and no increase of resistance at 60°C and 4.1 volt over one year.

New Cathode Technology Demonstrates Significant Progress Towards Electric Vehicle Goals

Applied to large cells, this technology is able to significantly improve on the state-of-the-art energy density, while demonstrating cycling durability, approaching United States Advanced Battery Consortium goals.

Envia Systems and United States Advanced Battery Consortium

The lithium-ion battery pack that powers many pure electric vehicles today costs nearly 50% of the car's cost. Battery costs can be dramatically reduced by using electrode materials that store more energy. Optimizing these electrode materials is the key to unlocking the electric vehicle market.

The program's objective was to develop and integrate proprietary high-capacity cathodes with commercial graphitic anodes and high voltage electrolytes into high capacity pouch cells to meet the United States Advanced Battery Consortium's (USABC) long-term goals for electric vehicles. Envia has met a majority of USABC's stringent power and energy requirements for electric vehicle batteries while lowering costs. Gravimetric (214 Wh/kg) and volumetric energy and power requirements have been demonstrated at the cell level. Envia has also exceeded the cycle life requirement of 1,000 dynamic stress testing (DST) cycles. Figure 1 shows >1,000 DST cycles before the specific energy reaches 80% of the beginning of life target.

With respect to calendar life, improvements have been made but more progress is required. The current cathode development has demonstrated a predicted six years to 20% capacity loss (see Figure 2). Power fade is greater and needs further investigation. Abuse test results also showed that the cells were comparable to conventional cell technologies, indicating that the new cathode did not negatively alter the battery chemistry's reactivity.

Envia's second USABC program, which began in June 2014, will leverage the learning from the first program and integrate its high capacity cathode with high capacity silicon-based anodes to achieve even more aggressive cell performance targets

(most notably higher energy and power density) and a 15-year calendar life.

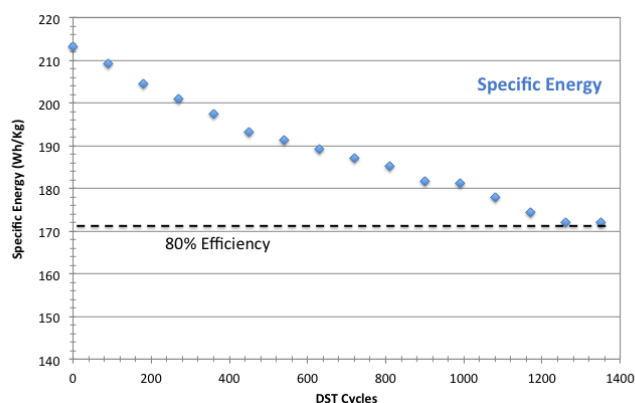


Figure 1. DST cycle life versus specific energy for 20 Ah pouch cells.

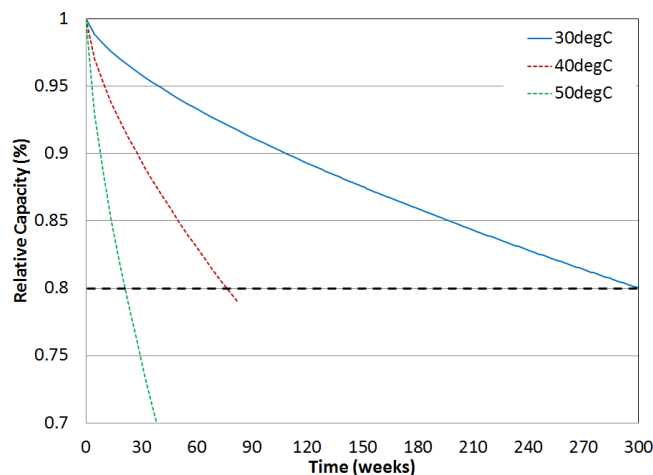


Figure 2. Capacity-based calendar life projection for 20 Ah pouch cell.

Computer Aided Battery Engineering Tool Released to the Public

Computer Aided Engineering for Electric Drive Batteries tools will assist and accelerate design processes for high-performance lithium-ion battery packs for electric drive vehicles.

General Motors Company, ANSYS, Inc., and ESim LLC

As part of the U.S. Department of Energy’s (DOE’s) Computer Aided Engineering for Electric Drive Batteries (CAEBAT) activity initiated three years ago, General Motors Company (GM), ANSYS Inc., and ESim LLC have collaborated to develop a flexible and efficient battery modeling and design capability based on the ANSYS multi-physics simulation platform. With support from the National Renewable Energy Laboratory (NREL), the team implemented NREL’s multi-scale multi-domain battery modeling approach in the ANSYS/Fluent CAE platform. Working with the team, ANSYS leveraged and enhanced its commercial products to provide component-level (Fluent) and system-level (Simplorer) capabilities. The first versions of these tools are now commercially available.

The software tools aim to support cell developers, pack integrators, and vehicle manufacturers with a practical balance between model fidelity and computational cost. The models capture the relevant physics, including electrochemical, thermal, and fluid response, focusing on the intra-cell and inter-cell non-uniformities that critically impact battery performance, life, and thermal response. Figure 1 shows the conceptual view of the battery design tool architecture, which is the basis for ANSYS software development. As part of a follow-on project to the CAEBAT activity, NREL developed a “User Defined Function” (UDF) within ANSYS’ Fluent platform to integrate a new computationally efficient, physics-based electrochemical model. This UDF functionality allows users to implement their own models to improve the baseline software capabilities, and in this case, NREL’s new model improves computation speed by more than 100 times compared to the previous version of the tool.

GM engineers used the data from comprehensive testing on a 24-cell liquid-cooled prototype module to validate the modeling tools (see Figure 2).

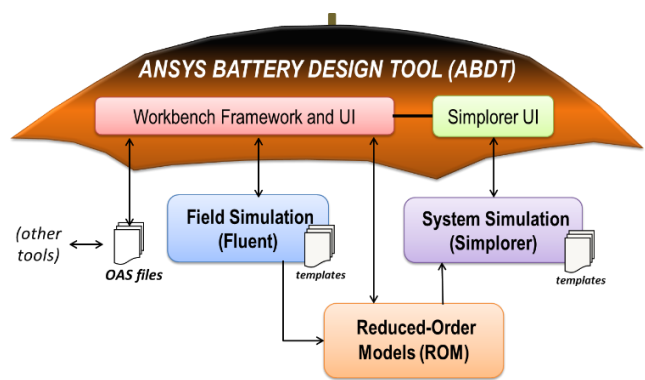


Figure 1. Conceptual view of the ANSYS Battery Design Tool.

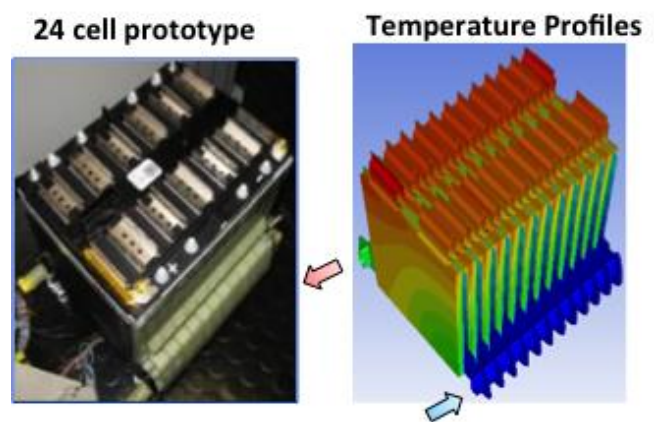


Figure 2. Validation of the ANSYS electrochemical-thermal models in Fluent -15 with GM’s comprehensive experiments for a 24-cell module.

The Materials Project is Released to Public

The Materials Project was created to harness the power of supercomputing to predict materials properties through first-principles methods. As one example within the lithium-ion battery space, detailed insights regarding the instability of “Li-excess” cathode materials were obtained.

Lawrence Berkeley National Laboratory

The Materials Project is a publicly available database (www.materialsproject.org) of calculated properties of materials. By scaling state-of-the-art techniques for computing electronic structure across supercomputing centers, the Project has generated data on almost 60,000 systems and allows users to screen a vast chemical-structural space for new materials with target properties. The site already includes over 9,000 registered users from around the world, of whom approximately 15% are from industry (large and established companies as well as startups). Of particular use to the electrochemistry field is the “Battery App,” which today contains data on over 2,000 lithium (Li) intercalation electrode materials and over 16,000 Li conversion electrode materials. To date, users have employed this App to generate almost 8,000 search queries by exploring potential new anode and cathode materials. Past use of data has uncovered several novel Li-ion battery cathode materials and extensions of the Project are being used to screen for multivalent intercalation compounds as part the DOE Joint Center for Energy Storage Research.

Similar first principles methodologies as that powering the Materials Project were recently used at Lawrence Berkeley National Laboratory (LBNL) to uncover the chemical and structural instability of Li_2MnO_3 – a critical component in the family of high-capacity “Li-excess” materials that have been attracting attention as high-energy cathode materials for Li-ion batteries. The findings support an unusual charging mechanism for Li_2MnO_3 – mainly focused on the anion (oxygen) specie, which couples to a structural and chemical instability of the material (see Figure 1). The extraction of > 1 Li/formula unit, even locally, results in a strong driving force for manganese migration into the Li

layer, which is accompanied by a structural degradation of the material. These insights are now being used to explore target chemical variations of the material aimed at increasing its stability.

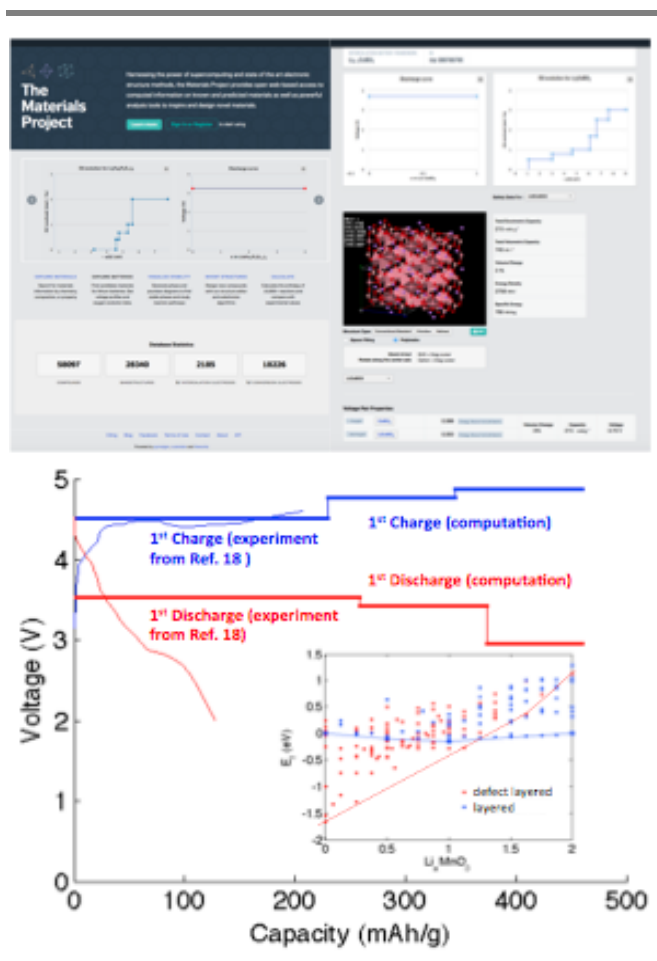


Figure 1. Materials Project site that freely provides first principles calculated properties for thousands of active materials. An example of the data for each material (top left). Results for Li_2MnO_3 showing how the charge mechanism is mainly explained by oxygen oxidation (top right). The predicted structural and chemical instability qualitatively in agreement with experimental results (bottom) [Lee and Persson, Adv Energy Mat. 2014, 4, 1400498].

Computer Aided Engineering Tools Now Available for Battery Engineers

The Computer Aided Engineering for Electric Drive Batteries activity has delivered three competitive commercial software tools for electrochemical-thermal simulation and design of batteries that will assist and accelerate design processes for high-performance lithium-ion battery packs for electric drive vehicles.

National Renewable Energy Laboratory and Collaborators

The U.S. Department of Energy's Vehicle Technologies Office launched the Computer Aided Engineering for Electric Drive Batteries (CAEBAT) project in 2010 with the objective of supporting development of simulation tools that could aid battery engineers and researchers in designing better batteries faster. The National Renewable Energy Laboratory (NREL) coordinated the CAEBAT activity by issuing a competitive request for proposals to industry for developing multi-physics, multi-dimensional computer aided engineering tools for batteries. Three teams (General Motors, CD-adapco, and EC Power) were selected to develop CAEBAT tools through 50-50 cost-sharing subcontracts over three years. NREL continued enhancing its multi-scale multi-domain (MSMD) battery-modeling framework for supporting CAEBAT subcontractors. Oak Ridge National Laboratory (ORNL) is developing an open software architecture (OSA) to facilitate interfacing between CAEBAT tools.

The three CAEBAT project subcontractor teams have commercially released three competitive electrochemical-thermal software suites for battery simulation and design. General Motors and its partners, ANSYS and ESim, have developed a flexible and efficient three-dimensional battery modeling capability based on the industry-leading Fluent multi-physics simulation platform (see Figure 1). NREL supported this team to implement its MSMD framework in the Fluent platform. CD-adapco and its partners, Battery Design, JCI, and A123Systems, have collaborated to develop electrochemical-thermal module for the Star-CCM+ multi-physics simulation platform. EC Power and its partners JCI, Ford, and Penn State University, developed thermal electrochemical design tools in AutoLion™. ORNL's OSA interfaces between the

CD-adapco, EC Power, and ANSYS CAEBAT tools. NREL developed a computationally efficient, physics-based electrochemical model and generated an application programming interface that allows industry users to access NREL's latest, state-of-the-art battery models.

These software tools were validated with comprehensive battery test data sets. More than 50 end-users (material and cell developers, pack integrators, vehicle manufacturers, and others) have used these tools to consider battery design for better performance, life, and thermal response characteristics.

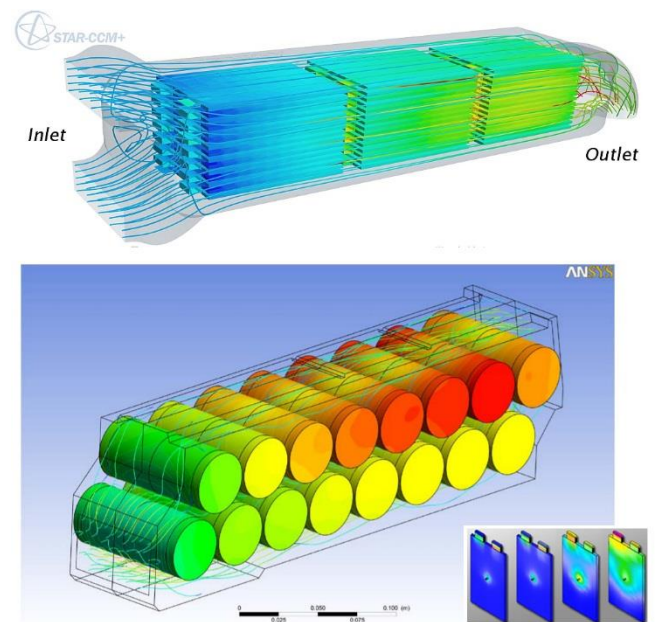


Figure 1. Example simulation results with CAEBAT tools from ANSYS, CD-adapco, and EC Power.

Novel In-Line Atomic Layer Deposition Electrode Coating System for Lithium-Ion Batteries

New reactor design demonstrates the potential for integrating an atomic layer deposition coating technology with state-of-the-art roll-to-roll lithium-ion battery electrode manufacturing.

National Renewable Energy Laboratory and University of Colorado at Boulder

National Renewable Energy Laboratory (NREL), in partnership with the University of Colorado at Boulder (CU), has shown in earlier work that extremely thin, conformal coatings of aluminum oxide deposited with the atomic layer deposition (ALD) technique on electrodes are capable of improving cycle life, abuse tolerance, and safety of lithium-ion (Li-ion) cells. Based on this early work, interest in the potential benefit of ALD coatings has driven research by a wide variety of entities, including companies such as LG Chem and Envia.

Despite the potential benefits provided for Li-ion cells modified with ALD protective coatings, questions remain about the practical ability to integrate ALD coating technology with state-of-the-art roll-to-roll Li-ion electrode manufacturing. Presently, ALD coating technologies involve the sequential and separate exposure of a sample surface to gas phase precursors that react to form a film in a single reaction chamber. This chamber must be extensively purged using inert gases between reactant precursor exposure steps, leading to excessively long processing times. This batch or semi-batch process is not compatible with high-speed in-line electrode manufacturing processes; therefore, it would not be cost-competitive.

To address the issue, the NREL-CU team has conceived and designed a novel in-line ALD reactor for the roll-to-roll process (see Figure 1). The new in-line ALD reactor allows a flexible, coated electrode foil to pass through different reaction zones to, in effect, achieve separation of reactant exposure steps in space and time, limiting the need for extensive purging, and thereby accelerating processing times.

In 2014, the NREL-CU team developed and demonstrated this in-line, roll-to-roll ALD coating process for the manufacture of next-generation coatings for Li-ion battery electrodes. The team successfully deposited coatings on a variety of flexible substrates, representing aluminum or copper foils, under manufacturing-relevant conditions, demonstrating that this improved coating technology is amenable to high-volume manufacturing and has the potential to contribute to the development of advanced Li-ion batteries with improved life and safety.

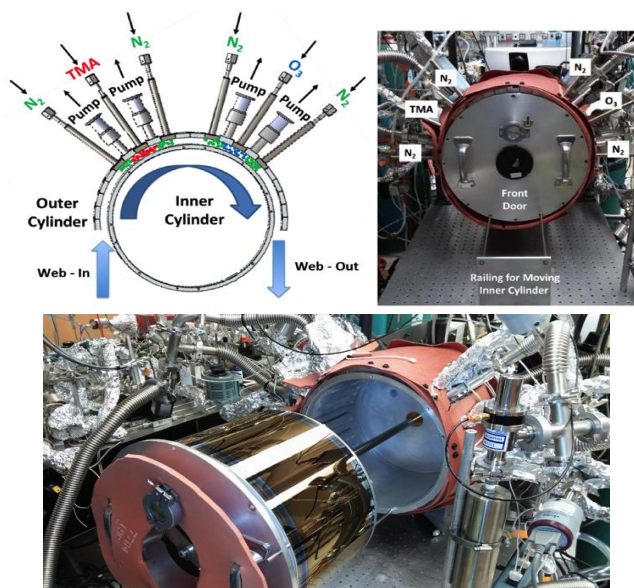


Figure 1. A simple schematic of the in-line ALD process designed for flexible roll-to-roll coating, as well as the completed reactor and ALD alumina-coated film.

Large Format Lithium-Ion Battery with Water-Based Electrode Processing

Excellent performance achieved while reducing the manufacturing cost of lithium-ion batteries and increasing the associated manufacturing sustainability.

Oak Ridge National Laboratory

The U.S. Department of Energy (DOE) target is to reduce lithium-ion battery (LIB) cost for electric vehicles (EVs) from the current cost of ~\$300/kWh to \$125/kWh by 2020. To meet this goal, substantial progress is required in cost reduction of both materials and associated processing because they comprise over 80% of the total costs of EV batteries. An organic solvent, N-methyl-2-pyrrolidone (NMP), that is frequently used as the solvent in conventional electrode manufacture is expensive, of environmental concern, flammable, and requires costly solvent recovery in the manufacturing process. Oak Ridge National Laboratory (ORNL) is developing aqueous processing for LIB manufacturing, in which the expensive NMP (>\$1.25/L) is replaced with deionized water (\$0.015/L), which enables significant cost reduction in the raw materials and processing and eliminates NMP treatment and recovery processes. In addition, the process can also reduce carbon dioxide emission in LIB manufacturing and is more environmentally benign. This novel processing route is estimated to have a measurable impact on full battery pack cost.

Currently, over 70% of all commercial graphite anodes are manufactured through aqueous processing. However, aqueous processing remains challenging for the diverse array of LIB cathodes. ORNL has been tackling the challenge by optimizing water soluble binder and mixing sequences, developing stable and uniform slurries, designing electrode formulas, improving electrode coatings, and optimizing drying procedures.

Good progress has been demonstrated in half- and full-coin cells in past years. In 2014, ORNL further demonstrated the excellent performance of composite cathodes from aqueous processing in

large format pouch cells. An example of this work is shown in Figure 1, which shows cycling data for a 3 Ah pouch cell with $\text{LiNi}_{0.5}\text{Mn}_{0.3}\text{Co}_{0.2}\text{O}_2$ (NMC 532) cathode from aqueous processing and A12 graphite anode. The pouch cell exhibits useful rate performance. The capacity retention in cycling begins to approach that of the pouch cells with NMC 532 cathodes from conventional NMP-based processing, which indicates the aqueous processed electrode can have the potential to deliver useful electrode performance.

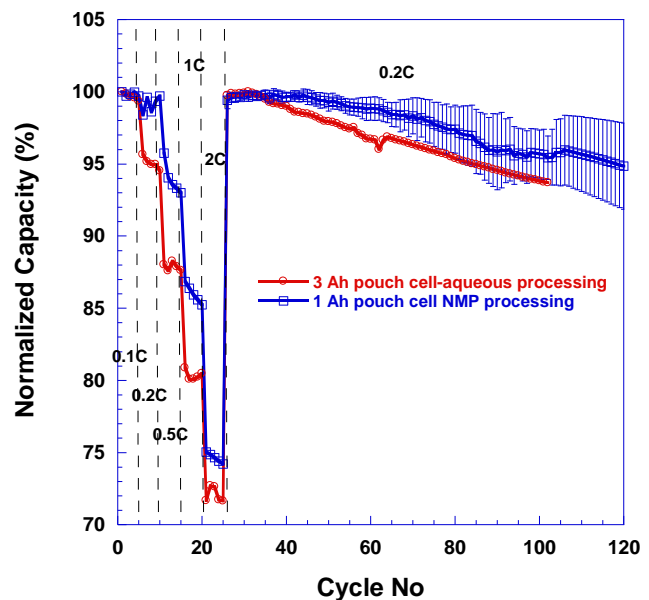


Figure 1. Battery performance comparison from a 3 Ah pouch cell with NMC532 cathode through aqueous processing and a 1 Ah pouch cell with the same electrode produced using NMP-based processing.

Resolving the Voltage Fade Mechanisms in LMR-NMC Composite Electrodes

Key mechanistic features and atomic migration pathways for layered-to-spinel conversion in high-energy cathode electrodes are devised to obtain insights into the voltage fade phenomena.

Oak Ridge National Laboratory

High-voltage lithium- and manganese-rich nickel manganese cobalt oxide (LMR-NMC) are potential cathode candidates for high-energy-density lithium (Li)-ion batteries. However, voltage fade (see Figure 1) during cycling is one of the major issues impeding their usage.

Layered-to-spinel (LS) structural rearrangement in LMR-NMC oxides has been identified as one of the principal reasons for this voltage fade phenomena. The mechanism of this process needs to be confirmed so that the oxide's composition and structure can be manipulated to suppress the voltage fade. By employing high-energy neutron beams, this work unravels the unique cation migration paths and key mechanisms for LS transformation in LMR-NMC oxides.

Oak Ridge National Laboratory (ORNL) has performed neutron diffraction experiments on LMR-NMC oxides at different states of charge (3.5 volt (V), 4.1 V, and 4.5 V) to obtain insights into the atomic occupancies in different crystallographic sites to uncover the root cause of voltage fade. Neutron diffraction analysis provides evidence that LMR-NMC transforms to a spinel phase via an intermediate structure with tetrahedral cation occupancies (see Figure 1) that blocks the Li diffusion pathways, and serves as a “building block” for the creation of a spinel-like framework. The key cation migration paths for LS transformations are: (i) diffusion of Li atoms from octahedral to tetrahedral sites of the Li layer [$\text{Li}_{\text{Li:oct}} \rightarrow \text{Li}_{\text{Li:tet}}$] which is followed by the dispersal of the lithium ions from the adjacent octahedral site of the metal layer to the tetrahedral sites of the Li layer [$\text{Li}_{\text{TM:oct}} \rightarrow \text{Li}_{\text{Li:tet}}$]; and (ii) migration of manganese (Mn) from the octahedral sites of the transition-metal (TM) layer to the “permanent” octahedral site of the Li layer via the tetrahedral site of the Li layer

[$\text{Mn}_{\text{TM:oct}} \rightarrow \text{Mn}_{\text{Li:tet}} \rightarrow \text{Mn}_{\text{Li:oct}}$]]. Complementing the results from neutron studies (see Figure 1 lower panel) shows the corresponding x-ray tomographic reconstruction of individual aggregated LMR-NMC cathode particles derived from their corresponding Mn, cobalt (Co) and nickel (Ni) K XANES edges to obtain a three-dimensional (3D) picture of TM segregation upon cycling and probe the changes in their internal morphologies as well as porosities under continuous high voltage cycling.

These findings suggests that the key to suppressing or eliminating the voltage fade behavior should be directed towards minimizing the TM and/or Li migration using methods such as revisiting compositional phase space or dopant substitution that would stabilize the lattice against excess delithiation.

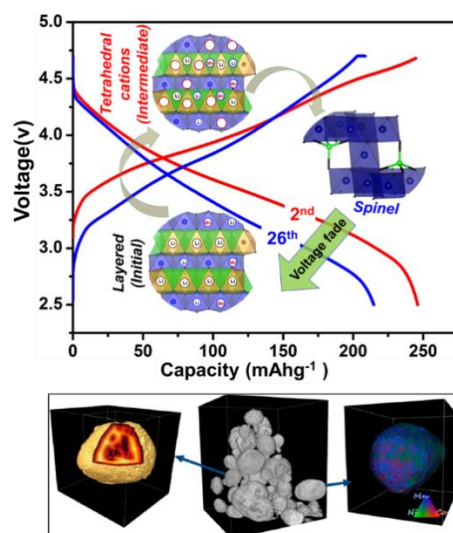


Figure 1. Voltage and capacity curves from a LMR-NMC high-energy cathode showing voltage fade phenomena after 26 cycles and LS transformation mechanism deduced from neutron diffraction. Insets show initial layered structure transforms to spinel (top). Tomographic reconstruction of LMR-NMC cathode particles showing internal voids (left) and a 3D rendering of the corresponding Mn, Ni and Co from XANES (bottom).

Advanced Battery Recycling Opportunities and Issues

Lithium-ion batteries manufactured from recycled material demonstrate efficiencies, potential cost reduction opportunity, and a technical basis for a future recycling service industry for electric vehicle batteries.

OnTo Technology LLC

This work demonstrates the first use of recycled electric vehicle (EV) cathode material in EV-grade batteries. Advanced battery recycling demonstrates: (1) robust, long lifetimes for recycled nickel manganese cobalt oxide (NCM) cathodes; (2) re-utilization of lithium and other critical materials; and (3) an efficient, green solution with cost reduction potential for EVs and other advanced battery applications.

EV battery cathode materials are commonly composed of $\text{LiNi}_{1/3}\text{Co}_{1/3}\text{Mn}_{1/3}\text{O}_2$ (NCM111) and other formulations such as 433, 424, and 523. Their merits include cost of \$160-\$200/kWh, volumetric energy density of 300 Wh/L, and specific energy of 150 Wh/kg. The cathode material represents 20-40% of the cell cost and is thus a good target for the use of lower-cost recycled materials. As part of the supporting infrastructure for EVs, advanced battery recycling can produce lower cost, manufacturing grade material, and can positively affect the overall material life cycle.

Considering the NCM battery end of life, the existing metal refining technologies, based on cobalt economics, are financially challenging for recycling, resulting in advanced battery total life cycle cost reduction opportunities. Based upon conservative estimates for current battery recycling costs, the potential for total life cycle cost reduction on a materials-only basis could be significant.

In this project, 50% capacity-faded NCM batteries were recycled through a pre-pilot line. The cathode material was separated and characterized in test cells to confirm low capacity (~45 mAh/g). The recycled NCM (RNCM) (see Figure 1) was produced with soft-chemical, low cost processes designed to recover high performance cathode material. RNCM characteristics matched rate capability and capacity

of standards (165 mAh/g). Material transfer limitations contributed to the 90% yield. In cooperation with Xalt Energy, RNCM was manufactured into six, 2.2 Ah, full cells along with standard NCM controls for comparison. These were tested in parallel for life and rate capability, as shown in Figure 2.



Figure 1. Test cells manufactured from RNCM (RNMC in the photo).

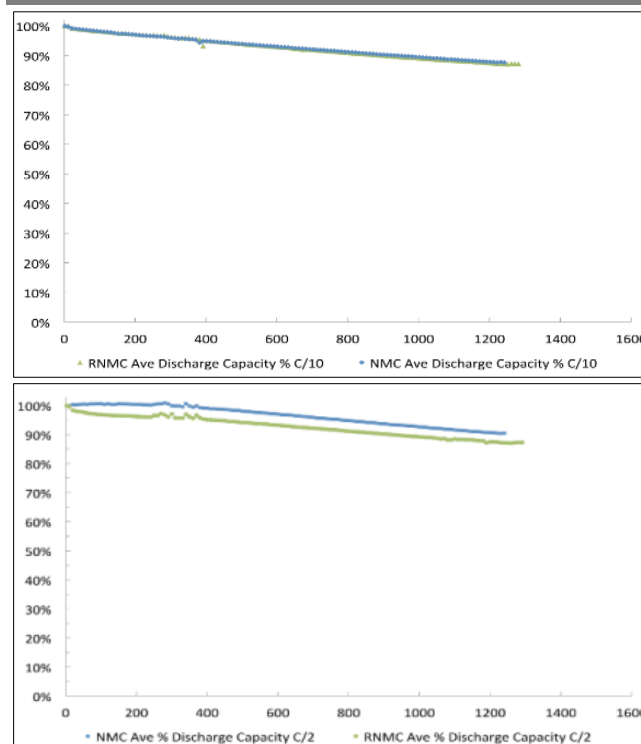


Figure 2. Performance is shown as average percent discharge capacity versus cycle number for discharge rates of C/10 (top) and C/2 (bottom).

Micro-Sized Silicon-Carbon Composite Anode with Excellent Battery Performance Optimized and Analyzed

High lithium-ion capacity, stability, and efficiency have been achieved in a micron-sized silicon-carbon composite anode, and these properties have been fundamentally linked to material parameters.

Pennsylvania State University

Silicon is one of the most promising anode materials for lithium-ion batteries but suffers from low efficiency and fast capacity fading due to its large volume change and the attendant issues of particle fracture and unstable solid-electrolyte interphase growth. Many materials designed to combat this have either had limited success or are nanoparticles with very poor volumetric capacity, preventing practical use. Research at Pennsylvania State University has developed novel micron-sized nanoporous silicon-carbon (Si-C) composites with interconnected, nanosized Si and C building blocks that significantly address these issues. The materials' fine-tuned structures allow for high density (0.78 g/cm³), high gravimetric and volumetric capacities (initial capacities up to 1843 mAh/g and 1437 mAh/cm³) two to five times that of graphite anodes, stability (up to 1662 mAh/g after 200 cycles), and coulombic efficiency as lithium-ion anodes in half cells (see Figure 1).

Two straightforward methods have been applied to prepare Si-C composites. The first uses top-down etching: a Si/SiO₂ composite is prepared and the SiO₂ is etched away. The second uses bottom-up direct synthesis and self-assembly: a Si/salt template composite is formed in situ via reduction and the templates are removed by washing with water. Both methods generate nanoporous Si, which is then coated with carbon to fill the pore via decomposition of precursor gas. These simple processes are promising for practical use and also allow material properties to be tuned by simply altering the heat treatment and carbonization temperatures. This process was used to build fundamental links between properties and performance. Battery performance was found to be inextricably linked to both surface oxides and carbon quality, with larger Si building block size

leading to a smaller native oxide content, and higher carbon coating temperature leading to more reduction of surface oxides by carbon precursor and formation of better-quality carbon. A size of 15 nm was shown to be optimal for Si building blocks, combining fracture mitigation due to small size with relatively low oxide content.

Both syntheses also allow easy doping and other modifications, such as adding a boron-containing precursor to the initial step. Boron-doped Si-C had improved conductivity, giving it a much better rate capability at a high current of 6.4 A/g, with twice the capacity than the un-doped one.

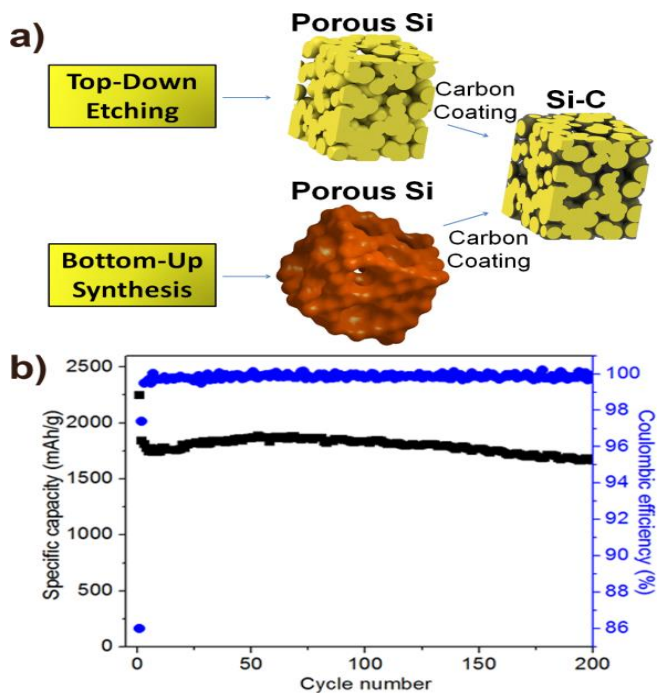


Figure 1. (a) Schematic representation of micro-sized Si-C composite synthesis methods. (b) Representative cycling performance and coulombic efficiency of the micro-sized Si-C composite anode prepared by the first method.

Abuse Propagation in Multi-Cell Batteries Characterized

Understanding how battery chemistry, cell type, design, and configuration impact the likelihood of a single-point failure to propagate through an entire battery system – in order to further improve safety.

Sandia National Laboratories

Lithium-ion batteries are currently used across multiple scales, from Ah-sized batteries for portable electronics, to kWh-sized batteries for vehicles, to cargo container-sized Megawatt-hour batteries for utility storage. However, these large-scale lithium-ion batteries are not without their design challenges with respect to abuse tolerance. Among other potential considerations are failure modes that initiate at the cell level, leading to a thermal runaway condition that can propagate through the entire battery system and even spread to the rest of a product or surrounding area. Sandia National Laboratories is working to better understand how battery chemistry, cell type, design, and configuration may impact the ability of a single-point failure to propagate from cell-to-cell through an entire battery system.

Initial work is focused on investigating the effect of series (S) and parallel (P) electrical configurations on single-point failure propagation. Batteries in 10S1P and 1S10P (series/parallel string configuration) were built in a close packed geometry using commercially-available laptop computer cylindrical cells. Failure was initiated by an axial nail penetration through the bottom of the center cell (Cell 6 in Figure 1). For the 10S1P configuration, no thermal runaway propagation was observed for the induced single cell failure. However, for the 1S10P configuration, failure propagating through the entire battery was observed over the course of five minutes after the initial induced single cell failure (see Figure 1). This result may be impacted by the high current that is drawn by the initial induced-failure cell from each cell connected to it in parallel and by the greater cell-to-cell heat transfer in the parallel configuration.

Similar experiments were performed on 1S5P and 5S1P stacked pouch cells to determine the effect of cell type on failure propagation. With a similar nail penetration trigger, thermal runaway propagation in these specific cell sizes and strings was observed for both series and parallel configurations. For these cell string configurations, higher heat transfer through the larger contact surface area between cells may provide a more significant contribution to the thermal runaway propagation, as opposed to the possibly greater role of the electrical configuration and short circuit current contributions in the 10S1P and 1S10P laptop cell configuration observations.

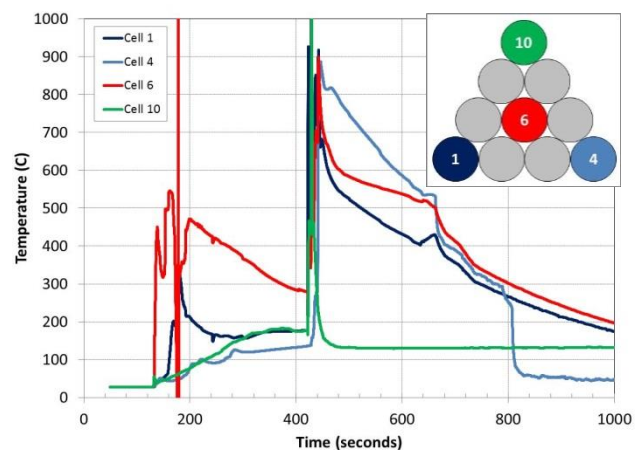


Figure 1. Cell temperature as a function of time for Cells 1, 4, 6, and 10 showing failure propagation of a 1S10P battery of off the shelf commercially available cylindrical cells that was exposed to nail penetration bottom center of pack.

Silicon Lithium-Ion Batteries Prepared from Rice Husks

Rice husks, which are agricultural waste products, were recycled to prepare low-cost, porous silicon nanostructures for high-performance lithium-ion battery anodes.

Stanford University

Silicon (Si) anodes can store 10 times more capacity by weight than graphite anodes (3,000 versus 300 mAh/g), but they also have major drawbacks: the cycle life is limited due to large volume changes during cycling. Much effort has been devoted to designing Si nanostructure-based anodes with long cycle life, as detailed in previous reports and publications. Although nanostructured Si anodes have been successful in extending the cycle life, they introduced at least two challenges: high cost and low mass loading.

Stanford University developed a method to synthesize Si porous structures for lithium (Li)-ion battery anodes directly from rice husks, which are an agricultural waste product (see Figure 1). Rice husks were first converted to pure silica by burning in air and then reduced to silicon by magnesium. The synthesis process results in a five weight percentage yield of Si according to the weight of the initial rice husks. Considering the abundance (1.2×10^8 tons/year) and low price ($\sim \$18/\text{ton}$) of the rice husks, this raw material may dramatically reduce the costs of nanostructured Si, which may pave the way for large-scale application of Si anodes in vehicles.

This method results in a porous Si structure composed of interconnected nanoparticles, which were physically connected with each other in the synthesis, resulting in retention of good contact during cycling. The densely packed structure also allows for high mass loading levels. In addition, the gap between the nanoparticles provides sufficient space for volume expansion during lithiation, resulting in useful cycling capability. The final porous Si nanostructures were made into slurry-type electrodes and tested in half cells versus Li metal. The initial discharge capacity is ~ 4100 mAh/g at the slow rate of C/50. After this, the rate

is increased to C/2, and a stable capacity of about 1750 mAh/g is exhibited over 300 cycles.

Even at relatively high mass loading $0.6 \text{ mg}/\text{cm}^2$, the late-cycle capacity of this porous structure is about 1700 mAh/g, after early-cycle irreversible losses diminish. Thus, investigators demonstrated an anode with a capacity above $1 \text{ mAh}/\text{cm}^2$ and cycle life above 100 cycles (see Figure 2).



Figure 1. Photographs of rice panicle, porous silicon structures from rice husks, and lithium ion batteries with silicon anodes.

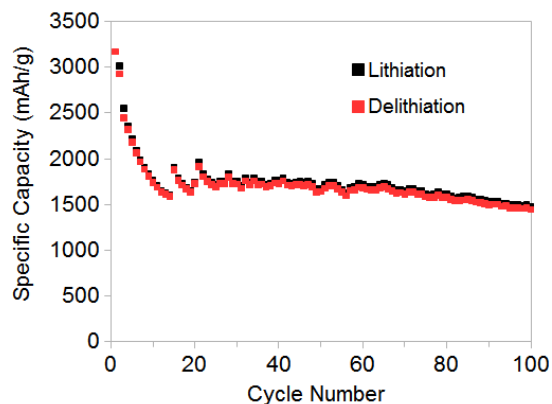


Figure 2. Charge discharge cycling data for the first 100 galvanostatic cycles. The rate was C/20 for the first cycle, C/2 for subsequent cycles.

Fuel Cells



Fuel Cell Catalysts Survive Harsh Durability Testing

Incorporating refractory metal interlayers has enabled anode-protection catalysts to withstand harsh gas switching and load cycling tests.

3M Company

Transient fuel cell operating conditions, including startup/shutdown and fuel starvation events, can cause degradation of fuel cell catalysts and other cell components. A project led by 3M has produced oxygen evolution reaction (OER) catalysts that can protect both the anode and cathode during transient operation. An unprotected cell can experience corrosion via oxidation of catalysts and supports during transient events, but adding OER catalyst enables oxidation of water instead, protecting the cell components.

Testing of anode OER catalysts in fuel cell stacks revealed an unexpected degradation mode: gas switching events, in which hydrogen and air mix on the anode (likely to occur during startup and shutdown), can destroy the OER catalyst. Loss of OER catalyst leaves the cell unprotected from fuel starvation events, which can cause the cell to reverse and the anode to be corroded. In 2014, 3M successfully addressed this issue by adding a refractory metal interlayer between the anode catalyst and the OER catalyst. When physically separated from the platinum-based anode, the OER catalyst experiences less exposure to heat and destructive free radical species that are produced in the catalytic oxidation of hydrogen. Incorporating an interlayer between the anode catalyst and the OER catalyst has enabled the OER catalyst to survive multiple cycles of gas switching, as well as load cycling, and continue to protect the anode during cell reversal events.

An additional, unexpected benefit of the interlayers is that they can increase the activity of the OER catalyst, allowing it to protect the anode from even harsher cell reversal events (see Figure 1). Anodes with interlayers containing hafnium or a mixture of

hafnium and zirconium have been the most successful of those tested so far, demonstrating a capability to protect the anode from cell reversal events lasting ten hours or more, even after being subjected to 200 cycles of gas switching and load cycling.

While the ability of interlayers to protect the OER catalyst has been demonstrated, further work is needed to clarify the mechanism by which gas switching degrades the OER catalyst and by which the interlayer protects the OER catalyst. Further work is also needed to determine whether other materials may be even more effective as interlayers.

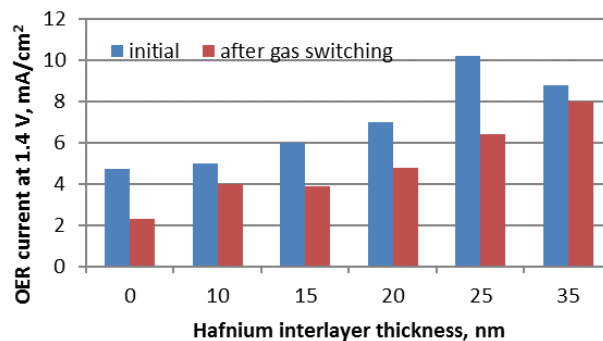


Figure 1. Adding a hafnium interlayer between the anode catalyst and the OER catalyst makes the OER catalyst more effective and protects it from degradation caused by gas switching.

Fuel Cell Membrane Meets Low-Humidity Milestone

A durable fuel cell membrane based on a multi-acid side chain ionomer and a nanofiber support has enabled fuel cell voltage 10% higher than a state-of-the-art membrane.

3M Company

A fuel cell membrane research and development project led by 3M has produced a new membrane that enables durable high performance fuel cell operation under real world operating conditions. The electrolyte membrane is a critical component of a fuel cell, serving to keep hydrogen and air on separate sides of the fuel cell while allowing ionic current to flow through. A good membrane must be able to provide high ionic conductivity and must remain reliable and durable under a wide range of temperature and humidity conditions. The 3M project combines a novel multi-acid side chain ionomer with an electrospun nanofiber support to produce a new membrane that enables excellent fuel cell performance under challenging (hot and dry) conditions, while also being durable enough to meet mechanical and chemical degradation targets. By enabling operation under dry conditions, the new membrane could reduce humidification requirements or allow the humidifier to be eliminated altogether, decreasing system cost and improving reliability.

By incorporating two or more acid sites into each ionomer side chain, multi-acid side chain ionomers such as perfluoro imide acid (PFIA, see Figure 1) can provide the high density of superacid sites required for good conductivity, while maintaining the crystalline ionomer backbone required for good mechanical properties. Conventional ionomers, which include only one acid site per side chain, quickly lose conductivity as temperature increases and humidity goes down, causing fuel cell performance to suffer. During fuel cell testing at 95°C and 50% relative humidity, a PFIA membrane was demonstrated to have ionic resistance 25% lower than a state-of-the-art conventional membrane. This reduction in resistance enabled the cell to reach nearly 0.6 volt (V) at 1.5 A/cm², a

performance level that greatly exceeds the 0.5 V project milestone and is 10% higher than measured performance with a state-of-the-art conventional membrane.

Changes in humidity and hydration during operation can cause fuel cell membranes to shrink and swell, and repeated cycles can create cracks and holes that cause the membrane to fail. The nanofiber support used in the 3M membrane provides mechanical strength, decreasing the amount of swelling and enabling the membrane to surpass the target of 20,000 humidity cycles. The membrane is also chemically stable, surpassing the target of 500 hours stability during a chemically destructive open circuit voltage hold test.

Further work in this project involves adding even more acid sites to each side chain in an effort to enable further reduction in humidification requirements.

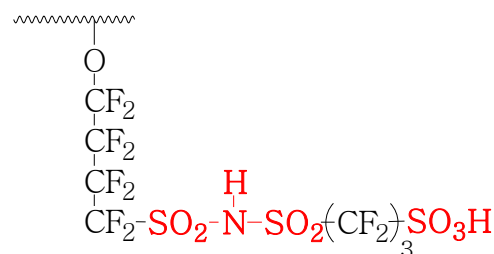


Figure 1. PFIA. Each side chain contains two super acid groups: one imide and one sulfonic acid.

Nanoframe Catalyst Achieves More than 20 Times Mass Activity of Platinum on Carbon

New, highly active durable catalyst could substantially lower fuel cell cost by reducing platinum content.

Argonne National Laboratory and Lawrence Berkeley National Laboratory

The cost of platinum-(Pt) based cathode catalysts is one of the main contributors to fuel cell system cost. Argonne National Laboratory (ANL) and Lawrence Berkeley National Laboratory (LBNL) have discovered a nanoframe catalyst that could substantially decrease the amount of Pt needed, thus reducing cost. The new nanoframe catalyst has over 20 times higher activity per gram of Pt than state-of-the-art platinum on carbon (Pt/C) and exceeds the U.S. Department of Energy's mass activity target (see Figure 1). In addition, the Pt skin provides high durability demonstrated in voltage cycling experiments. The Pt₃Ni nanoframe catalyst activity was unchanged after 10,000 potential cycles from 0.2 to 1.0 Volt (V).

The nanoframe catalyst's increased activity is due to its controlled size and surface structure and the three-dimensional (3D) accessibility of oxygen atoms to the Pt.

A molecular modeling representation and a transmission electron microscopy (TEM) image of the nanoframe are shown in Figure 2 left and right, respectively. The open structure of the Pt₃Ni nanoframes addresses some of the major design criteria for advanced nanoscale electrocatalysts, namely, high surface-to-volume ratio, 3D surface molecular accessibility, and optimal precious metal utilization. The approach used to obtain the nanostructure from a solid bimetallic polyhedra can be readily applied to other multimetallic electrocatalysts.

The starting material is crystalline PtNi₃ polyhedra. These polyhedra have Pt-rich edges and nickel (Ni)-rich faces and interior. Selective dissolution of the Ni effectively removes the faces, leaving a hollow particle with the Pt-rich edges behind that has

three-dimensional molecular accessibility. Both the interior and exterior catalytic surfaces of this open framework structure are composed of the nano-segregated Pt-skin structure that exhibits enhanced oxygen reduction reaction activity.

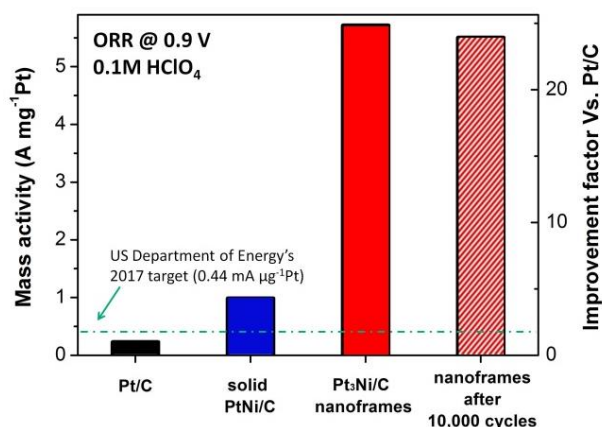


Figure 1. Comparison of nanoframe mass activity with conventional Pt/C before and after cycling.

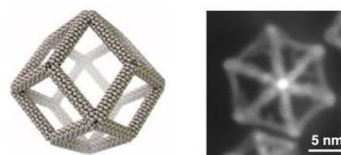


Figure 2. Model nanoframe structure (left). Micrograph of nanoframe (right).

System Contaminant Library to Aid Research Community

Structural plastics, adhesives, seals, and lubricants can all contaminate fuel cell stacks. For the first time, an extensive study will alert developers to which materials cause contamination.

National Renewable Energy Laboratory

Within a fuel cell system, numerous materials are used as structural plastics, adhesives, seals, and lubricants. Many of these materials contact the humidified hydrogen and air streams that enter into a fuel cell stack and therefore may possibly contaminate the stack. As developers seek to reduce system weight and reduce cost, structural plastics and the seals that facilitate them are generating greater interest. For developers to move quickly and confidently toward low cost material selection, a comprehensive database on possible contamination effects is needed.

The National Renewable Energy Laboratory (NREL), in collaboration with General Motors and the University of South Carolina, has assembled such a database by first identifying the fundamental classes of contaminants and then testing them to determine the severity of each class and the impact of operating conditions. Contamination models are then derived from understanding contamination mechanisms. Fundamental classes of contaminants include epoxy, silicone, urethane, and numerous polymers, especially fluoropolymers, polybutylene terephthalate (PBT), polyphthalamide (PPA), polyamide (PA), and others.

For structural plastics, the investigators defined a “leaching index” based on immersing the plastics in water at elevated temperature for six weeks. The leaching index is based on the combination of total organic carbon found in the leachant solution and on the electrical conductivity of the solution. As shown in Figure 1, an increased leaching index appears to show a trend with increased voltage losses. Investigators also defined metrics for voltage loss in a cell due to contamination, as well as the voltage loss that would remain with passive recovery following a period of contamination.

Parameters such as temperature and concentration were varied for both the leaching experiments and the fuel cell experiments. In fuel cell tests, the team also studied and reported the effects of platinum loading and relative humidity on cell potential.

Data from this project are available on the NREL website:

<http://www.nrel.gov/hydrogen/contaminants.html>.

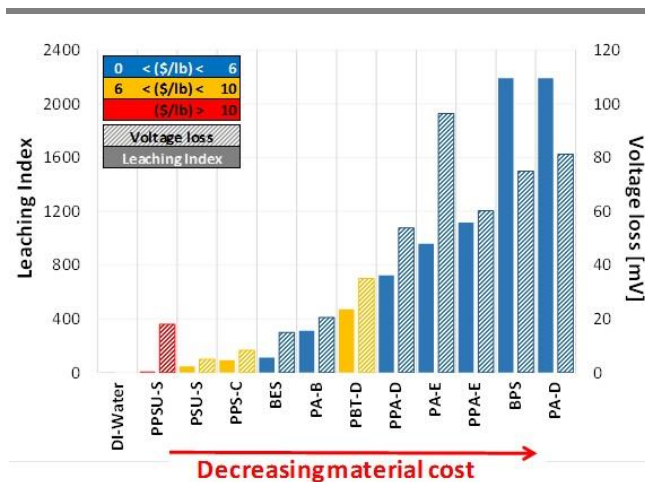


Figure 1. Data showing that the leaching index scales with voltage loss experienced in an operating fuel cell.

- DI = deionized.
- PPSU = polyphenylsulfone.
- PSU = polysulfone.
- PPS = polyphenylene sulfide.
- BES = Bakelite epoxy-based material.
- PA = polyamide.
- PBT = polybutylene terephthalate.
- PPA = polyphthalamide.
- BPS = Bakelite phenolic-based material.
- S = Solvay.
- C = Chevron Phillips.
- B = BASF.
- D = DuPont.
- E = EMS.

Rotating Disk Electrode Technique Best Practices and Testing Protocol

Standardized testing protocol and best practices will enable procedure consistency and minimize results variability from different laboratories, allowing the research community to accurately benchmark novel catalyst performance and durability and expedite ultra-low-platinum group metal catalyst development.

National Renewable Energy Laboratory and Argonne National Laboratory

The rotating disk electrode (RDE) technique is widely used to study the activity and stability of polymer electrolyte membrane fuel cell electrocatalysts. The use of RDE in acidic liquid electrolyte eliminates the need to fabricate membrane-electrode assemblies (MEAs) as the first step in the catalyst evaluation process and eliminates the influence of other cell components on initial catalyst performance and durability assessment. However, discrepancies in activity values reported between research groups and improvements in the technique that have not been uniformly adopted introduce issues of inaccurate and unreliable catalyst screening and benchmarking. For example, activity values reported over the last decade for the same catalyst tested in different laboratories have varied by as much as 200%.

The National Renewable Energy Laboratory (NREL) and Argonne National Laboratory (ANL) established standardized RDE test protocols and best practices to allow for more precise and reproducible data and reliable comparisons to be made by catalyst and fuel cell developers when evaluating novel synthesized catalysts in small quantities. The team developed a standard electrode preparation method that includes an approach towards ink dispersion and employs a spin coating method to deposit and dry thin catalyst films on the electrode. Investigators addressed electrolyte impurity issues by proposing standardized cell cleaning and evaluating perchloric acid electrolyte sources. They proposed a standardized testing protocol and acquired three carbon-supported platinum (Pt/C) electrocatalysts from three different suppliers (Johnson Matthey, Umicore, and TKK) as well as polycrystalline Pt for protocol validation. Subsequently, using identical

standardized protocols and the standardized electrode preparation method of spin coating, the three electrocatalyst materials were evaluated at NREL and in two ANL laboratories. A comparison of the oxygen reduction reaction mass activity between laboratories for the three catalysts indicates acceptable reproducibility, as shown in Figure 1.

Standardization of the RDE technique will allow for accurate first gate screening of newly-developed catalysts in comparison to baseline Pt/C, rendering RDE a reliable tool for the scientific community, especially those who lack the expertise and resources for more elaborate MEA fabrication and testing.

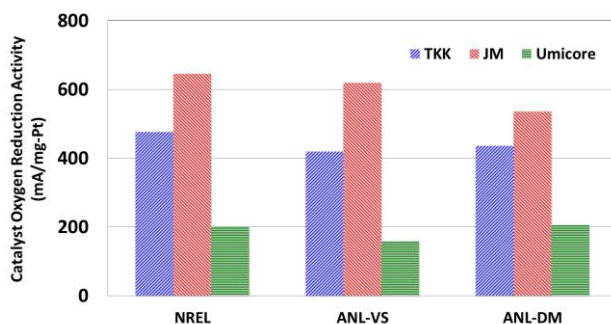


Figure 1. Comparison of oxygen reduction activity between three laboratories of three Pt/C electrocatalysts.

Materials



Demonstrated Laser-Assisted Dissimilar Material Joining

New laser texturing technology improves joining of carbon fiber polymer composites and aluminum components.

Oak Ridge National Laboratory, 3M, Cosma, and Plasan Carbon Composites, Inc.

Oak Ridge National Laboratory (ORNL); 3M Company (3M); Cosma, Inc., (Cosma); and Plasan Carbon Composites, Inc. (Plasan) have partnered to demonstrate a breakthrough laser technology to prepare carbon fiber polymer composites (CFPC) and aluminum (Al) components for adhesive bonding. The innovations include the texturing of both the Al and CFPC surfaces and engineering “rough” surfaces on Al and CFPC prior to an adhesive bonding operation. 3M formulated the adhesives, Plasan provided the composite and Cosma provided the Al.

To date, joining CFPC and Al 5000-, 6000-, or 7000-series components is done by simply overwrapping the CFPC composite over the Al or using specially-formulated adhesives coupled with extensive surface preparation techniques. These processes are empirical, employing several steps, such as labor-intensive surface preparation methods that are incompatible with the degree of automation required in automotive applications.

Using a laser structuring technique prior to the adhesive bonding operation, ORNL replaced the untreated smooth adhesive/composite interface of the Al and CFPC with a rough fiber reinforced interface, which was expected to increase the bond strength of the CFPC/adhesive interface. Additionally, laser surface treatment of the substrate surface can be optimized to minimize the surface preparation cleaning processes, increasing industrial acceptance for high volume applications. From the mechanical testing data, the lap shear strength increased up to eight times with respect to the solvent-cleaned-only samples. When compared to the abraded and cleaned baseline (manufacturer-recommended preparation method, see Figure 1), the improvement in strength was 46% (see Figure

2). “Abraded and cleaned” are those joints prepared in accordance with adhesive manufacturer standard surface preparation techniques.

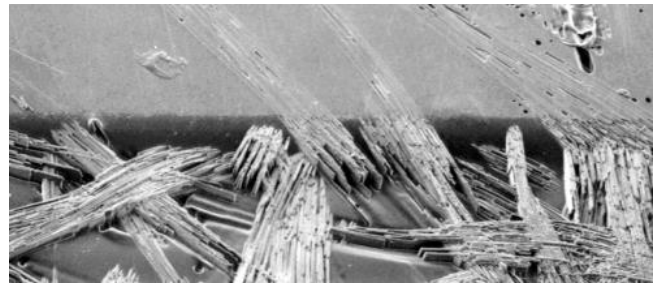


Figure 1. Composite surface showing unablated regions (top) and ablated regions (bottom).

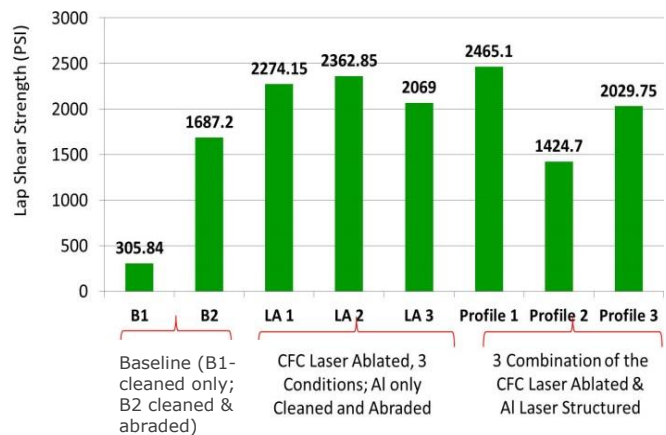


Figure 2. Lap shear strength for carbon fiber composite – Al dissimilar material joints for three different surface preparation conditions: baseline; carbon fiber composite laser structured without cleaning and cleaned Al; and carbon fiber composite and Al both laser structured without cleaning. The best result was an increase in lab shear strength to 2465.1 PSI.

Weld Fatigue Life Improvement Feasibility Demonstrated

Substantial improvement in weld fatigue life for advanced high-strength steels offers promise for cost-effective, practical solutions for the auto industry.

Oak Ridge National Laboratory and ArcelorMittal

Under a cooperative research and development agreement, Oak Ridge National Laboratory (ORNL) and ArcelorMittal USA are working together to develop the technical basis and demonstrate the viability of innovative technologies that can substantially improve the weld fatigue strength and durability of auto body structures. Durability is one of the primary metrics related to designing and engineering automotive body structures. The fatigue performance of welded joints is critical to the durability of the body structure because weld locations in general can serve as damage initiators.

The lack of an inherent weld fatigue strength advantage for advanced high-strength steels compared with conventional steels is a major barrier for vehicle weight reduction through down-gauging, as down-gauging leads to increases in stresses, which may reduce durability under the same dynamic road loading conditions. Improving fatigue life is critical to achieving optimum lightweight vehicle weight. In this project, innovative weld residual stress mitigation techniques were identified and investigated to substantially improve the weld fatigue performance and durability.

ORNL developed a thermomechanical weld stress control approach and clearly demonstrated its feasibility to significantly improve the weld fatigue life in a specially-designed lap joint weld fatigue test, mimicking the weld configuration common in auto-body components. In a laboratory set-up experiment, the approach shows considerable improvements in weld fatigue lives at low stress levels that are more prevalent for the durability of auto-body structure components (i.e., low stress, high-cycle). As shown in Figure 1, at 2,000 lb. load level, investigators achieved over an order of

magnitude increase (approximately) in cycle to failure. In fact, the weld coupons with the residual stress management technique did not fail at 10⁷ cycles (i.e., labeled as run-out). The observed improvement at low-stress levels is consistent with the principles of residual stress effect on fatigue life and the effectiveness of residual stress modification. ORNL is working on implementation techniques to adopt this approach in the auto-body production welding environment. Technologies developed in this project are expected to provide cost-effective, practical solutions to the auto industry.

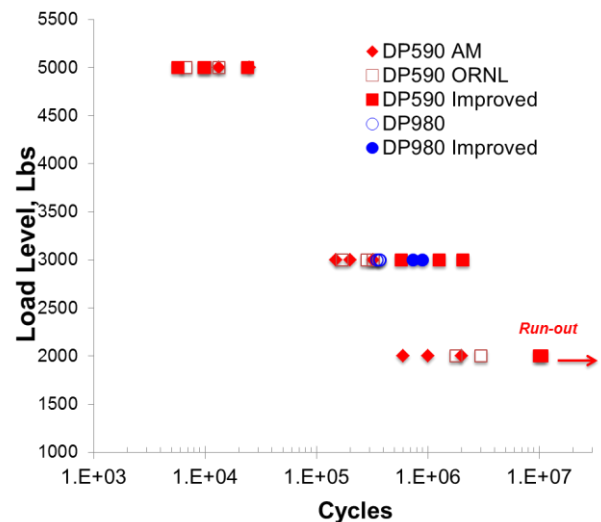


Figure 1. At 2,000 lb. load level, over an order of magnitude increase in cycle to failure has been achieved. In fact, the weld coupons with the residual stress management technique did not fail at 1×10⁷ cycles.

Advanced Oxidation Process Improved for Carbon Fiber

Plasma-based oxidation process demonstrated at a one ton/year level.

Oak Ridge National Laboratory and RMX Technologies, Inc.

The cost of producing carbon fiber (CF) is one of the largest obstacles to incorporating it in future automotive systems. According to a cost study, 51% of CF production cost is attributable to the precursor cost, 43% is attributable to the conversion of the precursor into CF and activating the surface for resin compatibility, and the remaining 6% is for spooling and handling. Significant effort is being expended on developing lower-cost, higher-rate production technologies. Conversion work includes development of a higher-speed, lower-cost oxidative stabilization process. This project addresses elimination of the bottleneck in CF production.

Oak Ridge National Laboratory (ORNL) and RMX Technologies (RMX) have partnered to develop and scale up a plasma-based oxidation process to the one ton/year level. This one ton/year plasma oxidation oven (see Figure 1), was made fully operational in fiscal year 2014 and has already demonstrated the ability to fully oxidize multiple small 24k tows in 30 minutes and single large tows three times faster than conventional conversion processes. Unit energy consumption results from these tests project at least a 30-50% unit energy savings (kWh/kg of CF) over conventional oxidation. Mechanical properties of this oxidized polyacrylonitrile fiber (OPF) match properties of conventional OPF. Work continues to refine the process and optimize equipment to achieve carbonized fiber mechanical properties equal to conventional results and even faster oxidation time.

In the last year, ORNL and RMX completed construction and made operational the one ton/year plasma oxidation oven and conducted trials to resolve most engineering issues. They processed two tows of commodity-grade, 24k precursor fiber in the large reactor in 30 minutes,

reducing the oxidation time from the 80-120 minutes for conventional process. All properties exceeded U.S. Department of Energy (DOE) thresholds of 250 ksi tensile strength, 25 Msi tensile modulus, and 1% strain to failure. Additionally, RMX established an industrial partnership with a major CF manufacturer to further commercialize the plasma oxidation technology. In a competitively-awarded, cost shared project with DOE, RMX will continue this work to scale the technology to 500 ton/year and demonstrate it in an industry partner's conventional conversion line.



Figure 1. The one ton/year plasma oxidation oven.

A Microstructure-Based Modeling Framework Developed to Design a Third-Generation Steel

Investigators established an integrated experimental and simulation framework to achieve third-generation advanced high-strength steel properties.

Pacific Northwest National Laboratory and Colorado School of Mines

Advanced high-strength steel (AHSS) is an important class of materials for reducing vehicle weight to improve fuel efficiency. These steels have evolved with new alloying and processing strategies to tailor microstructures containing various mixtures of ferrite, martensite, bainite, and retained austenite. Pacific Northwest National Laboratory and the Colorado School of Mines are working together in a study of third-generation (3G) AHSS concepts to identify low-alloy steels with ultra-high-strength and sufficient formability for automotive lightweighting. The project has two purposes: 1) Develop fundamental understandings of the microstructural level deformation mechanisms in multi-phase AHSS and their influences on the macro-properties; and 2) Develop 3GAHSS with improved performance using an integrated experimental and simulation framework.

The team adopted the quenching and partitioning (Q&P) process as a potential way to generate 3GAHSS properties. The first heat Q&P samples were produced based on different chemistry and heat-treating parameters and then investigated experimentally. The team then used in-situ high energy X-ray diffraction to estimate the properties of the various phases and the austenite stability, which served as input for the computational work.

Investigators generated microstructure-based finite element models for the selected Q&P steels, then performed systematic investigations on the effects of various material parameters on tensile properties to identify possible directions for property improvement. Investigators then conducted computational materials design, based on the results to suggest a new set of individual phase properties that will achieve improved bulk properties (see Figure 1).

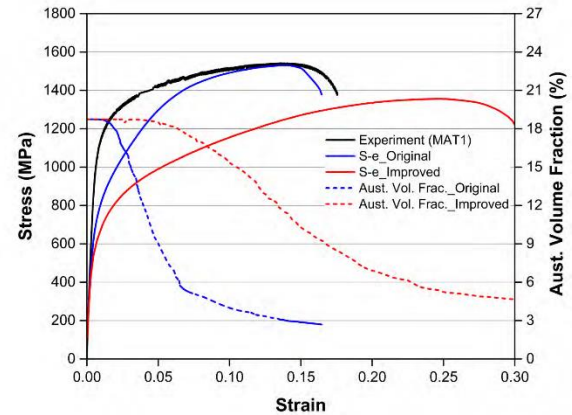


Figure 1. Illustration of performance improvement achieved with computational materials design.

The second and third heat samples were subsequently produced at Colorado School of Mines, based on the findings of the integrated framework. The properties achieved in some of those samples showed enhanced performance and met the U.S. Department of Energy's 3GAHSS requirement of excellent strength (greater than 1,500 MPa) with good ductility (greater than 20%) (see Figure 2).

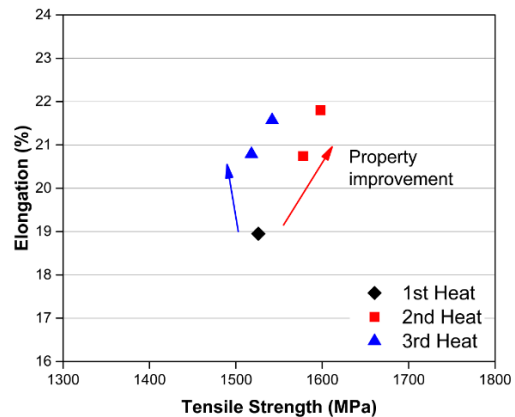


Figure 2. Property improvement of Q&P steels in tensile strength versus total elongation plots.

Mechanistic-Based Ductility Prediction for Complex Magnesium Demonstrated

An integrated experimental and multi-physics modeling approach can predict cast magnesium ductility with better than 90% accuracy.

Pacific Northwest National Laboratory, Ford Motor Co., and University of Michigan

Magnesium (Mg) castings are of interest for vehicle light-weighting because Mg and its alloys are the lightest metallic structural material. However, limited ductility hinders wider use in vehicle applications. Microstructure features (e.g., properties and distributions of porosity, brittle eutectic phases, and grain size) can significantly influence the ductility of Mg castings, and they vary from alloy to alloy, with different casting processes, and in different locations on a single casting. This project seeks to develop a mechanistic-based ductility-prediction capability to provide a modeling framework applicable to future alloy design and casting process development and optimizations.

Ford Motor Company cast plates and bars in different conditions and characterized them through metallographic preparation. Tensile testing was conducted on as-cast samples and samples cut from the plates. To assess the impact of different microstructural features on the tensile behavior, the samples were systematically heat-treated to reduce shrinkage-induced micro-porosity and micro-structure level heterogeneity (see Figure 1).

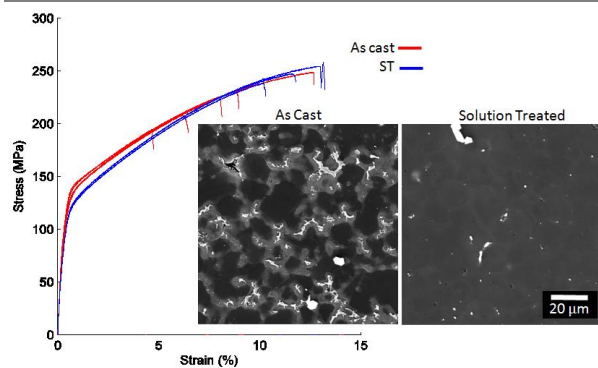


Figure 1. Comparison between as-cast and solution-treated samples.

A synthetic microstructure based model was then used to predict the matrix properties, including the

initial yield, hardening parameter, and ductility limit, by considering the volume fraction and morphology of the eutectic beta phase (see Figure 2).

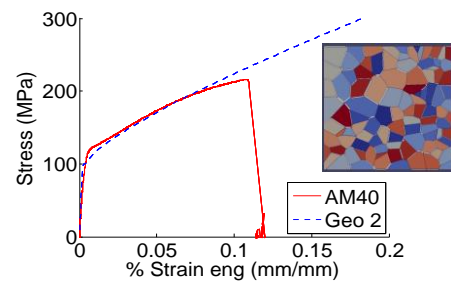


Figure 2. Comparison of predicted (dashed) and measured (solid) intrinsic properties for AM40.

Finally, the ductility of the tensile samples was predicted by explicitly mapping the pores measured from x-ray tomography into a three-dimensional finite element model with the matrix properties predicted by the intrinsic model. Figure 3 shows the excellent correlation between the measured and predicted final failure modes and the ductility of four AM50 samples reported in the literature.

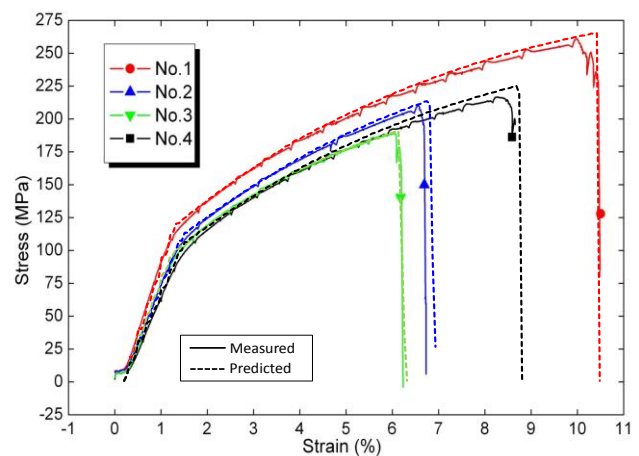


Figure 3. Comparison of predicted and measured failure modes for sample No. 2 and overlay of predicted (dashed) and measured (solid) ductility for four AM50 samples.

High-Shear Deformation Process Developed to Form Magnesium Alloys

Low-cost high-strength magnesium alloy, without the addition of rare-earth elements, and complimenting manufacturing process, will help make the technology viable to the automotive industry.

Pacific Northwest National Laboratory and Magna Cosma International

Pacific Northwest National Laboratory and Magna Cosma International have been collaborating on technologies relevant to the automotive industry that support the U.S. Department of Energy’s mission of improving process and product efficiencies, and at the same time reducing automobile weight. The use of high-performance magnesium (Mg) alloys is often limited due to the addition of costly rare-earth (RE) elements and the slow rate of processing techniques used to form these alloys. Current work aims to address these challenges and improve processing efficiency.

Phase I developed high-energy absorbing microstructures using Mg alloys with RE additions as model systems. The project obtained the necessary combination of grain size, texture, precipitate size, and distribution, and alloying additions to make the desired Mg alloy. Experiments demonstrated that Mg alloys can successfully replace currently-used aluminum alloys and can reduce the weight of the component by 20% without any compromise in the existing properties.

Phase II focused on replicating the desired microstructure from Phase I without using RE elements. Alloys were down-selected based on cost and relevance to the automotive industry, in consultation with Magna Cosma International. Studies determined that a shear-enhanced method successfully deformed the precipitates in these test compositions and yielded the best properties in the final Mg alloys.

Phase III used inverse process modeling to develop a cost-effective approach to produce the alloy with the desired energy absorbing properties. The technique, called “Shear Assisted Indirect Extrusion,” uses a rotating, axially-fed ram to

plasticize a small region of billet material near the extrusion orifice (see Figure 1). This results in significantly lower extrusion pressure compared to existing indirect extrusion approaches for Mg alloys. Because this process uses friction to locally heat only the material that is being extruded, it is possible that external heating of the billets may not be needed.

This provides significant opportunities to reduce the cost of the end product without compromising properties and to tailor the microstructure to desired properties. This novel technique now is being developed further to support parts pertinent to the automotive industry.

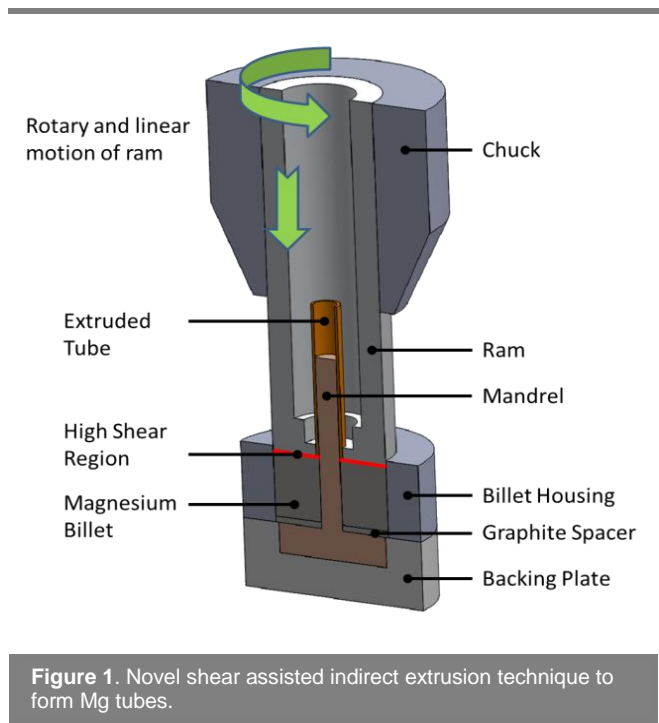


Figure 1. Novel shear assisted indirect extrusion technique to form Mg tubes.

Novel Technique Developed for Joining Dissimilar Metals

Demonstrated ability to join dissimilar metals as an enabler for increasing the use of magnesium as a lightweighting material.

U.S. Automotive Materials Partnership LLC

The U.S. Automotive Materials Partnership has extended prior achievements of its “Magnesium Front-End Research and Development” project in the engineering, fabrication, and evaluation of large-scale, magnesium (Mg)-intensive, vehicle front-end substructures to include capabilities for incorporating dissimilar metals, including galvanized steel and aluminum (Al). Greater integration of Mg alloys into substructure assemblies could advance the vehicle weight reduction goal of the U.S. DRIVE’s Materials Technical Team to improve vehicle efficiency.

Of the principal technical challenges identified in the project, foremost are: 1.) Development and implementation of technologies required to produce robust joints of dissimilar metals (e.g., steel and Al) with Mg; and 2.) Durability (strength, fatigue resistance, and corrosion resistance) of such joints once formed in actual demonstration structures.

The project team developed three joining technologies for dissimilar metals: 1.) Self-piercing rivets (SPR) for Mg to Al, 2.) Friction stir linear lap welding for Al to Mg, and 3.) Adaptable insert welding for steel to Mg. Development of SPR joints, where Mg is the “top” member, is complete, and the remaining SPR effort is focused on corrosion performance. Friction stir linear welding of Al to Mg was shown to be feasible but critically dependent on process controls to thwart the extensive formation of brittle intermetallic compounds and associated joints. Adaptable insert welding is a novel joining approach developed in this project for joining steel to Mg, or potentially other dissimilar materials wherein at least one member material is capable of being resistance spot welded.

Figure 1 illustrates the joint between a “captured” high-strength low-alloy (HSLA) steel panel with an applied insulating surface layer, and an AM60 B Mg die casting. The technology requires that the “captured” member has a clearance hole, through which the insert contacts the base metal and is subsequently secured by resistance spot welding. Such welding has been demonstrated successfully for Mg alloys, and the example shown below in cross section indicates the original position of the Mg-Mg interface and resultant weld nugget formed. The Mg insert piece deforms during formation of the weld nugget and hence “adapts” to the dimension of the clearance hole, resulting in a strongly clamped joint, in this case having lap-shear strengths matching or exceeding those of other typical dissimilar metal joining techniques. Corrosion-resisting coatings are employed for the captured metal piece permitting a degree of galvanic isolation. Final assemblies are amenable to standard electrocoat finishing.

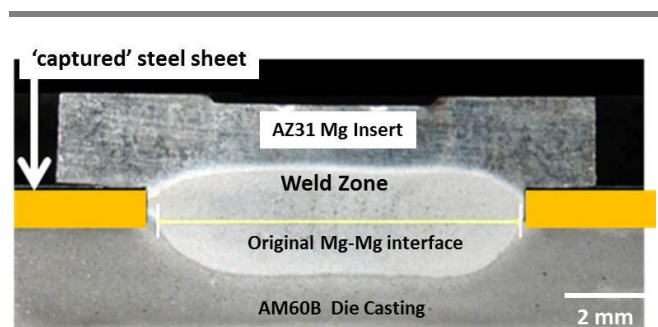


Figure 1. Cross-sectional view of an “adaptable insert” joint affixing a coated HSLA EG steel panel to an AM60B Mg die casting using an AZ31 Mg insert.

Validation of Carbon Fiber Composite Material Models for Automotive Crash Simulation

Materials selected and characterized and test component design completed for validation of carbon fiber material models to enable high-volume use of lightweight carbon fiber composites in structural crash and energy management applications.

U.S. Automotive Materials Partnership LLC

The four-year project, “Validation of Crash Material Models for Automotive Carbon-Fiber Composite Structures Via Crash Testing,” has completed its second year of extensive analytical modeling and physical testing to validate commercial constitutive models implemented in crash codes (e.g., ABAQUS, LS-DYNA, PAM-CRASH and RADIOSS), as well as two newer crash models developed by academic partners: a meso-scale representative unit cell (RUC) model¹ (University of Michigan [UM]) and a micro-plane RUC model² (Northwestern University [NWU]). The project team includes the U.S. Automotive Materials Partnership, original equipment manufacturers, and academia representing computer aided engineering (CAE), materials testing, and crash testing functions, as well as automotive design/engineering suppliers, composite manufacturers, material suppliers, and test laboratories.

The project goal is to validate material models for reliably designing structural automotive carbon fiber composites for crash applications. The team chose a front bumper beam and crush-can (FBCC) subassembly application to validate the material models, developing a composite FBCC that can be shown to absorb impact energy equivalent to a baseline steel FBCC under various crash-loading modes and comparing its actual performance to simulations.

The team developed and analyzed several innovative design and material concepts for the carbon fiber FBCC and selected a thermoset epoxy-based material system for which a material property database was developed. This database will be used

in design/CAE and modeling of FBCC performance using selected material models from UM, NWU, and the four commercial codes. The FBCC design (see Figure 1) uses a C-channel bumper with internal carbon SMC ribs and two-piece conical crush cans. Wayne State University established target crash energy and peak loads for the carbon fiber. All crash test fixtures applicable to both carbon fiber and the baseline steel testing were fabricated. To address the secondary objectives of volume production, all demonstration components will be compression molded from epoxy prepreg and joined by adhesive bonding with mechanical peel stoppers. Several thermoplastic carbon fiber laminates were also procured for further evaluation via material modeling.

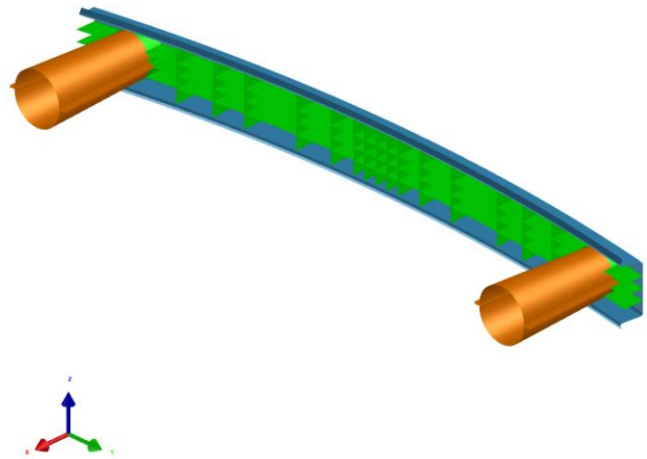


Figure 1. Initial designs for the thermoset FBCC made from two compression-molded conical hat sections joined at the flanges, and the bumper beam, a compression molded thermoset carbon fiber C-channel with carbon SMC ribs.

¹ Song S, Waas AM, et al., *Composites Science and Technology*, 67, pp 3059-3070, 2007.

²Caner, F.C., et al., *Journal of Engineering Materials and Technology*, 133, pp 1-12, 2011.

Exceptional Ductility/High-Strength Third-Generation Advanced High-Strength Steel Produced

New advanced high-strength steel will improve the accuracy of material models and facilitate model inclusion in integrated computational materials engineering framework.

U.S. Automotive Materials Partnership LLC, AK Steel, and Colorado School of Mines

The U.S. Automotive Materials Partnership LLC (USAMP) used integrated computational materials engineering (ICME) to produce third-generation advanced high-strength steel (3GAHSS) coupons with mechanical properties similar to U.S. Department of Energy (DOE) targets for exceptional ductility, high-strength steel. This accomplishment is significant as it represents successful scale-up from small, laboratory-size melts using lab equipment to larger-size melts using production-like equipment, and because the 3GAHSS mechanical properties will facilitate model development and improve ICME model predictive accuracy.

The overall project goal is to demonstrate ICME applicability for the development and deployment of 3GAHSS for immediate weight reduction in passenger vehicles. DOE targets for this work include both an exceptional ductility, high-strength steel and an exceptional strength, high-ductility steel (see Figure 1).

At the project's initiation, there were no commercially-available 3GAHSS steels, so the project selected a QP980 steel to provide baseline data; QP980 steel has mechanical properties on the cusp of the 3GAHSS envelope. Steels with

representative material microstructures and mechanical properties are essential to model development and accuracy. This necessitated creating interim 3GAHSS heats with mechanical properties within the 3GAHSS envelope.

The Colorado School of Mines (CSM) evaluated published data and provided a 3GAHSS recipe for a transformation-induced plasticity steel. AK Steel, working in collaboration with CSM and the Auto/Steel Partnership Steel Expert Team, cast and cold-rolled the steel per the defined recipe. As shown in Figure 1, the mechanical properties of the steel (Medium Mn 1) fell within the 3GAHSS envelope, with mechanical properties approaching that of DOE's target for the exceptional ductility, high-strength 3GAHSS.

In just the first year of this four-year project, the team has shown that it is feasible to produce steel with mechanical properties within the once-hypothetical 3GAHSS space. Advances in material modeling based on this 3GAHSS alloy are expected to yield more accurate ICME models that will enable automakers to weight-optimize component designs using tailor-made and virtually designed 3GAHSS alloys.

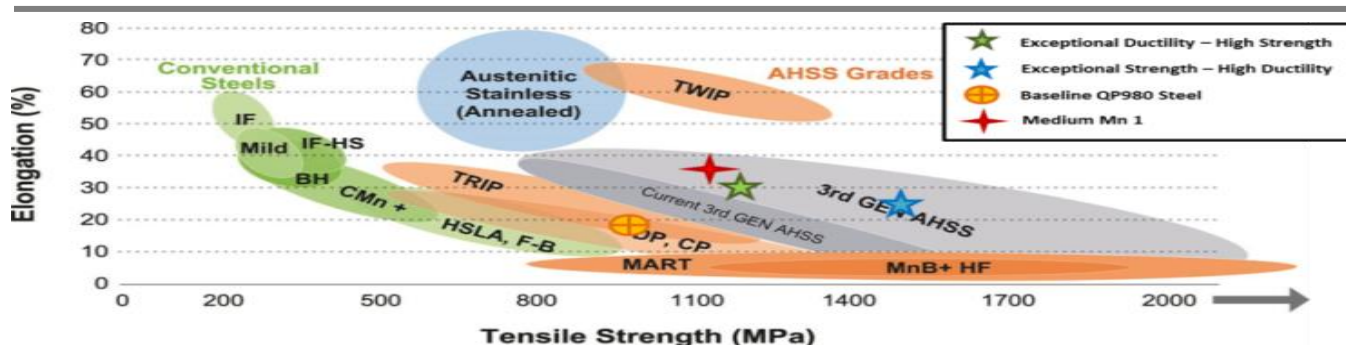


Figure 1. 3GAHSS mechanical properties.

Vehicle Systems Analysis



Impact of Advanced Technologies on Engine Operating Conditions and Vehicle Fuel Efficiency

High-fidelity simulation models help to identify opportunities for and impacts of advanced technologies on engine and vehicle operation.

Argonne National Laboratory

As a result of more stringent environmental regulations and increased customer expectations, automotive manufacturers are considering a wide range of technologies to improve vehicle fuel economy, including advanced engines and transmissions.

To assess the impact of advanced technologies on engine operating conditions and energy consumption, Argonne National Laboratory leveraged hi-fidelity engine simulation models from the automotive engineering firm IAV and dedicated transmission gear ratio design methods using the Autonomie modeling and simulation platform to evaluate the potential operation of future engine technologies. Project investigators developed 17 engine simulation models representing near- and long-term advances in engine technology, including combinations of variable valve lift, cylinder deactivation, direct injection, and friction reduction. Different levels of engine down-sizing and turbo-boosting were also considered. See Figure 1 for a sample comparison of the engine operating points for two different technology packages.

Key accomplishments of this work include:

- An improved understanding of the impact of advanced transmissions, hybridization, and light-weighting on advanced engine operating conditions, relative to current U.S. DRIVE targets.
- Quantification of the energy impact of a wide range of powertrain technologies on standard drive cycles for a representative compact car in the year 2020 to inform future R&D.

Simulation results demonstrated that advances in transmissions, compounded by start-stop systems (i.e., mild hybridization) and turbo-boosting would

result in significant engine down-speeding. Therefore, engine technology development targets may need to be recalibrated for part load operation in order to accurately reflect likely engine operation in future powertrains.

Future work will focus on ensuring that advanced technology benefits are compared properly to avoid any bias. For instance, transmission gear ratio will be designed and shift parameters calibrated using optimization algorithms for each advanced engine to ascertain the maximum potential benefits of each technology. Engine-out emissions, as well as thermal impact, will also be assessed with engine dynamometer testing and Engine-in-the-Loop techniques. It is critical to evaluate component technologies, such as engines, within the proper vehicle context so that their fuel consumption benefits may be properly predicted.

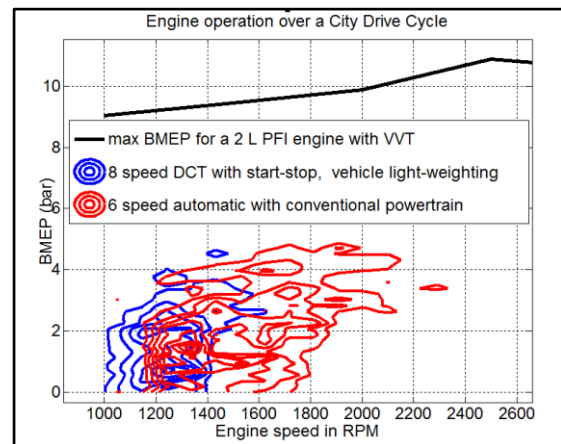


Figure 1. Comparison of engine operation with a 6-speed automatic and an 8-speed dual-clutch transmission (DCT) with start-stop and vehicle light-weighting (future drivetrain technology).

EETT/VSATT 2014 Vehicle Benchmarking Collaboration

The Electrical and Electronics Technical Team and Vehicle Systems Analysis Technical Team are coordinating extensive vehicle and component level benchmarking efforts to enhance understanding of advanced powertrain systems.

Argonne National Laboratory and Oak Ridge National Laboratory

The Electrical and Electronics Technical Team (EETT)/Vehicle Systems Analysis Technical Team (VSATT) benchmarking collaboration builds upon the partnership and expertise of Argonne National Laboratory's (ANL) in-situ vehicle testing and Oak Ridge National Laboratory's (ORNL) component testing and design analysis. The laboratory at ANL, shown on the left in Figure 1, includes a temperature controlled 4WD chassis dynamometer with a range of advanced data acquisition capabilities, including the capability to monitor and log in-vehicle CAN communications as well as more traditional signals, such as temperatures, fuel flow, electrical power, and coolant flows. To illustrate the collaboration, which better facilitates benchmarking and data collection relevant to both EETT and VSATT, the team focuses on the 3-phase electrical system of a 2014 Honda Accord plug-in hybrid electric vehicle.

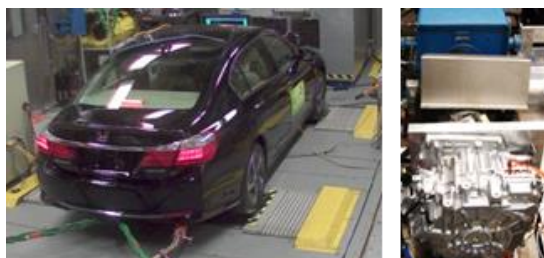


Figure 1. Chassis roll dynamometer for vehicle testing at ANL (left). Motor dynamometer for component testing at ORNL (right).

ORNL benchmarking efforts include component testing on a dynamometer, shown on the right in Figure 1, as well as component teardown and analysis illustrated in Figure 2. During testing of component performance and efficiency mapping, ORNL implements custom control algorithms while using the original equipment manufacturer (OEM) driver board and inverter. ANL provides detailed information about important vehicle-level

parameters such as battery voltage, component temperatures, and hybrid coolant temperatures throughout drive cycle operation – information that is critical for properly testing power electronics and electric machine components. Additionally, ORNL researchers visit ANL to assist with the analysis of component characteristics such as boost converter and inverter drive waveforms.

Figure 3 illustrates inverter voltage and current waveforms collected by ANL/ORNL under various conditions, demonstrating a common inverter switching frequency of 5 kHz and boosted voltage levels of up to 700 volt. Higher switching frequencies are used at low speeds to mitigate noise and vibration. Operational details such as these are not only important for emulating OEM operation during component testing, but they also reveal important system and component design and specifications. Knowledge gained from this collaboration enhances both vehicle and component level benchmarking efforts, helping to define current state-of-the-art technologies and define future research opportunities.

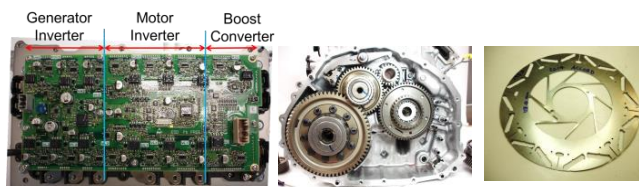


Figure 2. 2014 Honda Accord component teardowns: power electronics (left) and transmission/electric machines (right).

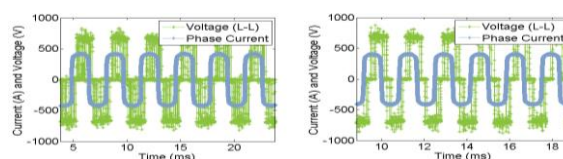


Figure 3. Inverter/motor waveforms taken by ANL/ORNL during peak operation at 40 (left) and 80 miles per hour (right).

Auxiliary Load: On-Road Evaluation & Characterization

On-road auxiliary loads are benchmarked to support U.S. automotive manufacturers in an effort to quantify the real-world energy consumption benefits of advanced technologies used to reduce these loads.

Idaho National Laboratory and Intertek CECET

As part of its testing and data collection support to the U.S. Department of Energy (DOE), the Idaho National Laboratory (INL) and Intertek CECET test advanced technology vehicles in on-road fleets, on test tracks, and in laboratory settings to determine the real-world petroleum reduction potential of various advanced technologies.

Vehicle auxiliary load data collection, analysis, and characterization are conducted on several non-electrified vehicles as part of DOE’s Advanced Vehicle Testing Activity on-road vehicle evaluations. This auxiliary load characterization supports U.S. automotive manufacturer efforts to quantify the real-world energy consumption benefits of advanced technologies used to reduce these loads. Examples of these technologies include advanced alternators, lighting, and heating/ventilation/air conditioning systems. The data collection and analysis details the auxiliary load during the on-road operation of 126,000 miles of eight (four Honda Civic CNG and four Volkswagen Jetta TDI) vehicles as shown in Figure 1. The analysis also details the impacts of real-world driving and ambient conditions on auxiliary load.



Figure 1. Photo of the two vehicle models tested on-road.

Table 1 summarizes the on-road auxiliary loads results, which range from 200 to 1300 watts. The wide range of auxiliary load, illustrated in Figure 2, is caused by widely varying ambient conditions and the driver’s choice for accessory use (air conditioner [A/C], heater, lights, radio, etc.). Investigators

observed an average impact of eight watts of increased load per degree Fahrenheit rise in ambient temperature. This load increase is due primarily to increased A/C operation, which uses the vehicle’s interior fan and the A/C condenser fans. Additionally, nighttime driving results in a typical auxiliary load increase of 150 watts due to exterior lighting.

	Base Load (watts)	On-Road Average Load (watts)
VW Jetta TDI	300	760
Honda Civic CNG	200	330

Table 1. On-Road base and average auxiliary loads.

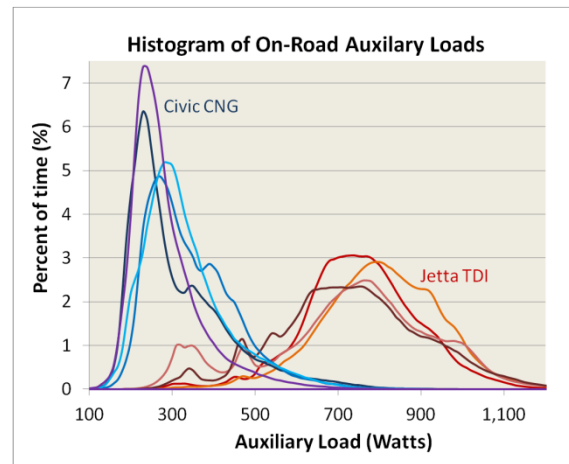


Figure 2. Histogram of on-road auxiliary loads.

The data collection, analysis, and characterization efforts benchmark the real-world auxiliary load from a small sample of non-electric-drive vehicles. and support industry efforts to quantify the real-world energy consumption benefits of advanced technologies used to reduce auxiliary loads.

Leveraging Big Data to Estimate On-Road Fuel Economy

National laboratories collaboratively developed an innovative real-world fuel economy prediction procedure, using a fusion of standardized testing and large datasets of in-use driving behavior and ambient conditions.

National Renewable Energy Laboratory and Argonne National Laboratory

Vehicle efficiency is known to vary significantly with driving style and climate. Existing standardized test procedures aim to estimate average fuel economy under representative conditions using a series of chassis dynamometer tests (basically, a treadmill for cars). Despite the best efforts of regulators, disagreements over certified fuel economy inevitably arise as driver behavior and vehicle technology evolve over time and as dynamometer testing cannot adequately capture the real-world behavior of every technology. Inconsistencies between real-world fuel economy and standardized estimates are problematic for consumers and can be for automakers as well, if underestimates of real-world efficiency benefits hinder internal investments in certain fuel saving technologies.

The National Renewable Energy Laboratory (NREL) and Argonne National Laboratory (ANL) have worked collaboratively to address one such challenging real-world fuel economy contributor: “cold-start” fuel penalties (i.e., from starting a vehicle after it has been sitting for many hours). The approach can be applied to other real-world assessment challenges, and plans are underway to do so with a broader working group of labs and automakers in 2015. The process included collecting laboratory-grade experimental data at ANL over a wide range of temperatures and powertrain loads, which were then used to calibrate a simplified set of models for predicting mechanical, electrical, and thermal responses of key vehicle components. After demonstrating the model’s ability to predict fuel economy within the bounds of test repeatability, NREL conducted numerical simulations in a high performance computing environment over real-world driving histories from the Transportation Secure Data Center, representing an array of traffic conditions

and regional climates (see Figure 1). Post-processing and weighting simulation results can then yield fuel economy estimates representative of U.S. demographics.

The project found that cold-start effects could account for 8% of real-world fuel use, and that standardized testing may indeed under-predict the potential benefit of mitigation technologies, underscoring the importance of this approach. Given the widespread use of combustion engine vehicles, an efficiency gain of just 1% would equate to taking 2.5 million vehicles off the road.

Project Resources
ANL Advanced Powertrain Research Facility
<http://www.transportation.anl.gov/facilities/aprf.html>
NREL Transportation Secure Data Center & Computing
<http://www.nrel.gov/tsdc> & <http://hpc.nrel.gov/>
NREL/ANL SAE Presentation (September 2014)
<http://www.nrel.gov/docs/fy15osti/62443.pdf>

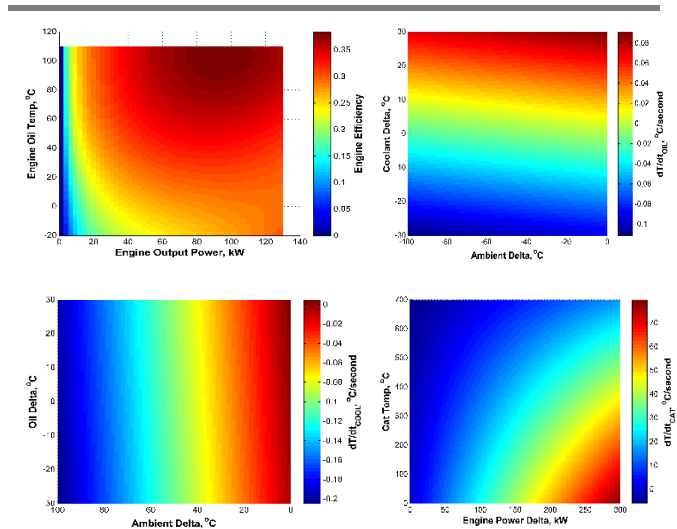


Figure 1. Detailed thermal/powertrain models integrated with real-world driving/temperature data to simulate nearly 40 million miles of driving.

CROSSCUTTING

Codes and Standards



Bridging the Gap between Hydrogen Component Safety and Performance Testing Capability

Hydrogen component testing using the new Energy Systems Integration Facility will improve reliability and standardization of robust designs.

National Renewable Energy Laboratory

To meet the need for near-term commercialization of hydrogen infrastructure, researchers at the National Renewable Energy Laboratory's Energy Systems Integration Facility (NREL's ESIF) have established component testing capability. The capability includes extreme testing environments that range from -40°C to 85°C and pressures up to 100 megapascal. Testing activities are underway to help identify underlying causes of performance degradation in critical components such as compressors, electrolyzers, flow meters, fueling hoses and nozzles, sensors, and pressure relief devices (PRDs). Facility resources support and are accessible industry for hydrogen fueling system components, and the generated data will ultimately lead to safer, more robust components and systems used in hydrogen service.

ESIF opened in 2013 to support common system challenges to deploying cleaner, energy efficient technologies. It has developed a core mission in support of hydrogen technologies: to empirically verify the compatibility of both individual components and integrated systems that range from hydrogen production to fueling systems. High-pressure hydrogen component and system testing capability is key to the understanding of failure modes and supports harmonization of test methods (see Figure 1). Examples of current hydrogen support within ESIF include the qualification of sensors for safe practice in applications including hydrogen vehicle repair facilities and temperature exposure life-cycle testing for PRDs to investigate failure modes.

Results of these much-needed activities cover a variety of component aspects:

- Constructed a mobile test device to evaluate hydrogen metrology methods through a Work For Others with the California Department of Food and Agriculture.
- Performed highly accelerated life cycle testing on compressors to reproduce failures.
- Initiated PRD testing to develop relevant best practices and information to prevent future failures in field operation.

This cross-cutting effort is supported by multiple programs within the DOE Fuel Cell Technologies Office, including Safety, Codes and Standards, Hydrogen Delivery, and Technology Validation.

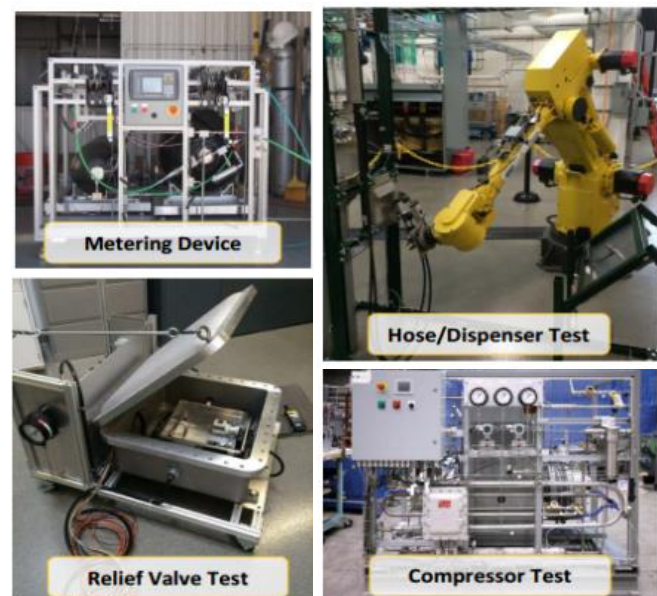


Figure 1. Examples of hydrogen component testing at NREL's Energy Systems High Pressure Test Laboratory within ESIF.

Hydrogen Storage



Optimizing Hydrogen Storage Materials by Defining Requirements via Adsorption System Modeling

Engineering analyses establish precise guidelines for developing viable hydrogen adsorbents.

Hydrogen Storage Engineering Center of Excellence

The Hydrogen Storage Engineering Center of Excellence¹ (HSECoE) has developed integrated system models that provide the hydrogen storage adsorbent material properties necessary to meet the U.S. Department of Energy’s (DOE) 2017 hydrogen storage system targets, thereby accelerating the search for optimal compounds. DOE’s storage targets refer to the complete storage system. Most R&D efforts focus on the development of new storage materials, however, and not systems. Linking the system targets to specific performance metrics at the materials level has remained a knowledge gap that has slowed the development of viable storage systems.

The HSECoE approach combines a detailed adsorption-based hydrogen storage system model with a vehicle model. This combination allowed the team to specify all storage components (e.g., heat exchangers, tanks, valves, etc.) necessary for a fully functional hydrogen storage system to meet realistic drive cycles. The material properties needed to meet DOE’s 2017 hydrogen storage system targets (e.g., volumetric and gravimetric hydrogen capacities as well as the necessary thermodynamics of hydrogen adsorption), were then calculated as a function of system mass and volume.

This approach offers a high fidelity pathway to identify specific material properties necessary for newly developed materials. It also provides an “acceptability envelope” for use by material developers to quickly evaluate candidate storage material for their potential to meet the DOE system targets.

For example, current hydrogen storage adsorbents typically operate at cryogenic conditions in order to achieve significant hydrogen uptake. As illustrated in Figure 1, modeling shows that a viable candidate adsorbent must exhibit a minimum of ~15% improvement in the total hydrogen weight percent (materials basis) over current baseline hydrogen adsorbent (MOF-5) to meet 2017 DOE system gravimetric capacity target.

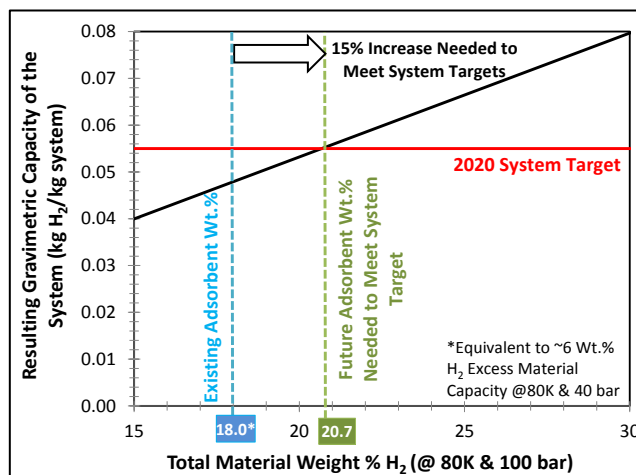


Figure 1. Relationship between system level gravimetric hydrogen capacity (red line) and the material level gravimetric capacity (black line).

¹ HSECoE is led by Savannah River National Laboratory with 10 industry, university, and national lab partners.

Neutron Diagnostic Methods Accelerate Hydrogen Storage Materials Development

Neutron beam material characterization can help design better hydrogen storage materials.

National Institute of Standards and Technology Center for Neutron Research

Neutron-based material characterization methods provide unique insight that accelerates hydrogen storage materials development to meet the 2020 U.S. DRIVE hydrogen storage targets. Researchers at the National Institute of Standards and Technology (NIST) use highly specialized neutron-based characterization techniques to better understand the interaction of hydrogen with storage materials at an atomic level, thereby providing molecular level guidance on how to design better hydrogen storage materials.

The NIST Center for Neutron Research (NCNR) uses neutron beams to understand how hydrogen interacts with, is stored in, and then released from hydrogen storage materials. Working with numerous U.S. Department of Energy-funded research groups, NIST uses instruments that help determine where the atoms and molecules are located in materials, revealing their atomic structure and providing key information to improve material properties necessary for hydrogen storage. In addition, information about the hydrogen release process (e.g., the diffusion of the hydrogen gas through a storage material) as well as properties of the dehydrogenated species can be obtained.

Measurements can be performed on all classes of hydrogen storage materials (i.e., metal-hydrides, sorbents, and chemical hydrogen storage materials). These characterization tools have been particularly useful for metal-organic framework (MOF) sorbents, which operate like molecular sponges for hydrogen. To overcome the high pressures and low temperatures typically required for adequate hydrogen storage capacities in MOFs, interactions and bond strengths between the

hydrogen and the MOF framework must be increased.

As illustrated in Figure 1, work performed at NCNR with collaborators from the University of California, Berkeley, shows direct binding of hydrogen to unsaturated metal centers within a new series of MOFs. This MOF series, which utilizes a new, low cost organic linker, allows for more accessible sites and stronger bonding between the MOF's metal centers and hydrogen gas. This increases the attraction for hydrogen stored in the nanoscopic pores, is an important advancement enabling increased hydrogen storage at lower pressure and near room temperature, and provides researchers additional insight into the key material structural properties necessary for increasing the capacity of hydrogen storage materials.

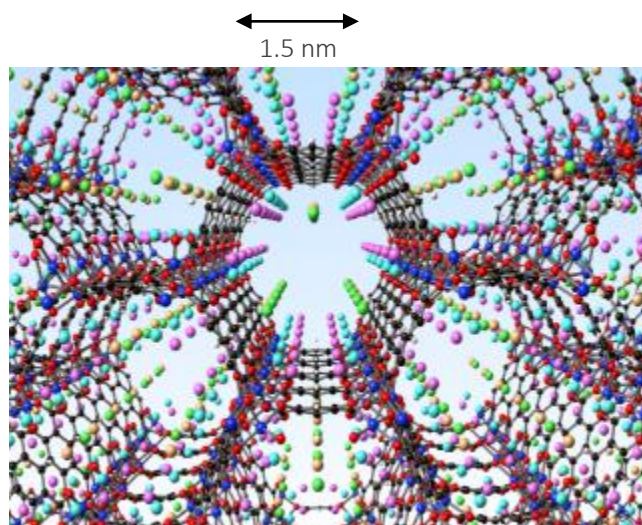


Figure 1. A newly developed MOF structure determined by neutron diffraction showing the preferred binding sites for hydrogen (cyan, pink and green) with the cyan and pink sites being the most favorable sites responsible for the increased interaction strength.

Lower-Cost, High-Performance Carbon Fiber

Development of a low-cost, high volume carbon fiber precursor offers high-performance carbon fiber and lower-cost hydrogen storage systems.

Oak Ridge National Laboratory and Fisipe Fibras Sinteticas de Portugal SA

Oak Ridge National Laboratory (ORNL) and its partner Fisipe Fibras Sinteticas de Portugal SA (FISIPE) have developed a low-cost carbon fiber (CF) precursor based on high-volume textile fiber processes, which is estimated to result in a 25% reduction in CF cost, assuming a \$15/lb. baseline. This equates to roughly a 10% reduction of the overall 700 bar storage system cost based on the U.S. Department of Energy’s 2013 baseline of \$17/kWh. The high cost of aerospace-grade CF is a barrier to widespread commercialization of lightweight, high-pressure hydrogen and natural gas storage tanks. The CF composite overwrap (i.e., CF and resin matrix) accounts for over half of the total cost of high pressure tanks, when manufactured at high production volumes.

To address the high costs of hydrogen storage tanks, the project team developed a new low-cost polyacrylonitrile precursor produced in a textile mill, which formerly made knitting yarn. The team altered the fiber polymer chemistry at a small additional cost over common textile fiber. This development preserved most of the cost benefits associated with high-volume production, thus resulting in a low-cost precursor fiber.

While the first obstacle was to develop a low-cost precursor that could be turned into CF, the more difficult second obstacle was converting these low-cost precursors into high-strength CF suitable for high-pressure hydrogen storage tanks. Properties were optimized by increased quality control standards during precursor spinning and by determining the correct balance between residence time, fiber tension, and exposure temperature during the conversion process.

The finished carbon fiber samples were tested using the ASTM 4018 protocol at the ORNL Carbon Fiber

Test Facility. The project goals were to reach >650 KSI (thousand pounds per square inch) strength fibers with a modulus of 35 MSI (million pounds per square inch) or greater. As shown in Figure 1, the fibers produced to date achieved the project goals and are expected to match the T700 baseline properties at the lower production cost in a commercial line. The results are summarized in Table 1.

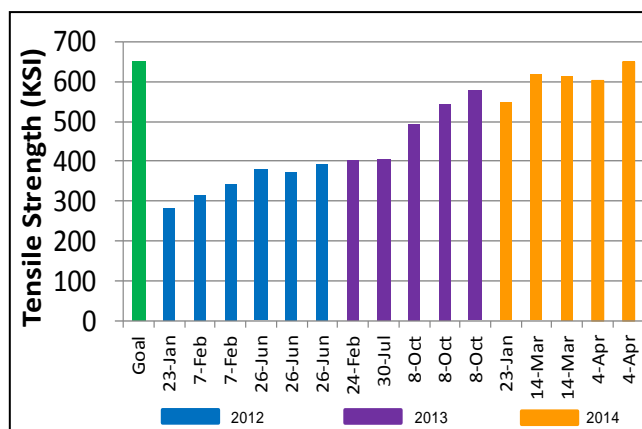


Figure 1. The measured tensile strengths of the carbon fibers developed using low-cost textile grade precursors showing steady improvement over the project’s lifetime.

	Strength (KSI)	Modulus (MSI)	Production Cost (\$/lb.)
T700 Baseline	700	35–38	\$13–15
Project Target	650	35–38	\$11–12
Project Status	653	38	\$11

Table 1. Summary of results for CF produced from a low-cost precursor.

Grid Interaction



Developing the SAE J2953 Interoperability Standard Test Procedures and Tools

Completing the standards and test equipment will enable verification of compatibility of electric vehicles with electric vehicle supply equipment for alternating current charging.

Argonne National Laboratory

The SAE J2953 Interoperability Committee was established to develop a recommended standard practice for connecting plug-in electric vehicles (PEVs) and electric vehicle supply equipment (EVSE, or charging equipment). Argonne National Laboratory (ANL) contributed to this effort by chairing the committee, leading the drafting and consensus process, defining the associated test procedures, and developing custom test equipment.

The standard includes two parts: J2953/1 is a series of charge system requirements based on the SAE J1772 standard that defines how a PEV and EVSE must interact at the coupler interface; and J2953/2 contains the guidelines and procedures for interoperability testing. SAE J2953/1 also defines three degrees of interoperability for alternating current (AC) electric vehicle (EV) charging. A tiered system approach is used to test for fatal EV charging flaws as well as minor nuisances that reduce functionality of unique PEV or EVSE features. Tier 1 testing ensures the most essential functionality, i.e., mechanical interoperability, charge functions, and safety features. Tier 2 gauges the robustness of a charge system under non-ideal conditions, including indefinite and dynamic grid events. Tier 3 tests non-standard feature functionality, including ampacity control, scheduled charge, staggered scheduled charge, and charge interrupt/resume.

A non-invasive breakout fixture (or “man-in-the-middle” test device) was designed to use existing connectors of the PEV and EVSE and operate in tandem with data acquisition and data logging systems, as shown in the generic interoperability test setup along with the hardware developed by

ANL in Figure 1. The test equipment was transferred to Intertek (Plymouth, Michigan) to test 14 PEVs and 11 examples of production EVSE in support of a U.S. Department of Energy-sponsored program.

Learnings from the interoperability testing will guide PEV and EVSE manufacturers and lead to a more precise and refined SAE J1772 charging standard. Both will benefit the industry as well as PEV drivers, who require a safe and reliable charging infrastructure.

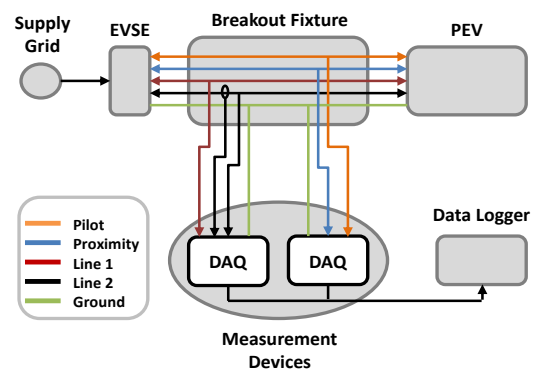


Figure 1. ANL's “man-in-the-middle” test equipment developed to test for compliance with SAE J2953 interoperability standards.

Plug-in Electric Vehicle Charging Technology and Standards

Removing technical barriers to universal charging and market acceptance of plug-in electric vehicles.

Argonne National Laboratory

A standard charging interface and associated technologies/communication protocols across the industry are key enablers for plug-in electric vehicle (PEV) market penetration. Cooperation between industry and U.S. Department of Energy national laboratories has become an effective mechanism to enable and strengthen standardization. Collaboration is accomplished through technical standardization committees, with input and oversight from not only automakers but also charging equipment manufacturers, communication technology suppliers, U.S. utilities, and academia. Specific accomplishments from this effort are highlighted below.

Provided critical data for standards definition: Standardized communication between PEVs and electric vehicle supply equipment (EVSE) is required to ensure interoperability, i.e., universal charging capability. In support of the SAE J2953 (interoperability) committee's assessment of candidate technologies and messaging protocols, Argonne National Laboratory (ANL) provided independent laboratory test data characterizing capabilities and limitations prior to consensus on the standard.

Developed communication control modules: Standardized communication requires electronic components to send and receive messages using the specified protocols. Because no components of this type were available, ANL developed the Smart Grid EV Communication Control (or SpEC) module to aid development/verification of standard messaging protocols. The module has since been licensed for use as a digital communication controller for direct current (DC) fast-charging (see Figure 1) as well as a communication controller for

a high-power DC PEV\EVSE emulator for development purposes.

Developed SAE J1772 PEV compliance tool: ANL has worked with the SAE J2953 committee since its inception to develop alternating current (AC) interoperability requirements and verification procedures. A prerequisite for compliance with the interoperability standard is that PEVs with the SAE J1772 AC connector or AC/DC combo coupler comply with the SAE J1772 connectivity standard. However, test procedures and tools were not developed at that time to demonstrate compliance with the standard, so ANL used the SpEC module to develop a unique test tool that fulfills this need.

The PEV compliance specifications, along with those of the AC interoperability test fixture, have directly contributed to the joint efforts by U.S. and European automakers as well as Europe's Joint Research Centre to develop a global specification and prototype PEV interoperability tool by mid-2015.



Figure 1. SpEC communication control module provides standard EVSE-PEV messaging to enable DC fast charging.

Comprehensive Data Set Informs Future Plug-in Electric Vehicle Infrastructure Planning

Data from largest plug-in electric vehicle and charging station demonstration to date provides valuable insight and lessons learned for future infrastructure planning.

Idaho National Laboratory

In a competitively-awarded, cost-shared effort with industry partners, the U.S. Department of Energy supported the largest-ever demonstration of plug-in electric vehicles (PEV) and electric charging infrastructure. This demonstration – specifically, the corresponding data collection and analysis led by Idaho National Laboratory (INL) – is providing valuable insights to inform future deployment. Using 124 million miles of data from 8,300 PEVs and 12,500 charging stations, INL has identified how drivers use PEVs, as well as preferences for how, where, and when they charge and at what power levels they prefer to charge. Infrastructure utilization and costs have also been reported, providing the most comprehensive view of PEV and charging usage to date.

The size of the dataset has allowed INL to perform numerous analyses that offer important insight on PEV use. For example, one of these studies benchmarked electrified vehicle miles-traveled by different PEV technologies. Initial analysis results prompted automakers outside of the DOE project to contribute similar data. The study found that unlike pure battery electric vehicles (BEVs), plug-in hybrid electric vehicles and extended range electric vehicles are driven as much as conventional gasoline vehicles. The electrified vehicle miles traveled increased roughly in proportion to battery capacity. In fact, 35 miles of electric range was sufficient to electrify nearly as much travel as a BEV without compromising travel needs.

Results such as these are providing critical insights to automotive industry regulators relative to Zero Emission Vehicle regulations as well as states and local communities planning infrastructure development. Another INL study of the data

identified charging location preferences of PEV drivers who had access to charging equipment at home, work, and other locations and found that these drivers strongly prefer to charge at home and work (see Figure 1). Other studies have demonstrated driver response to price signals, such as time-of-use electricity rates and fees for charging services, and documented costs to install alternating current Level 2 and direct current fast-charging electric vehicle supply equipment (EVSE) at residences and public locations.

In total, the INL data analysis has been disseminated in over 100 fact sheets, white papers, technical reports, and presentations. Results are being used by key regulatory agencies, universities, automakers, electric utilities, EVSE suppliers, EVSE deployment planners, other DOE national laboratories, independent research groups, and other industry stakeholders to guide public and workplace charging infrastructure deployment decisions. Results can be found at avt.inl.gov/evproject.shtml.

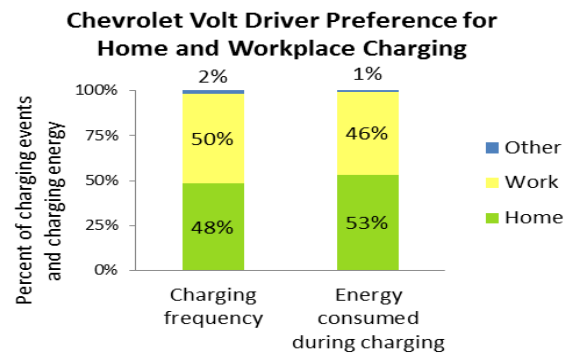


Figure 1. Analysis of charging preferences of Chevrolet Volt drivers who had access to workplace charging in the EV Project demonstrated the importance of workplace charging infrastructure.

FUELS

Fuel Pathway Integration

A decorative graphic consisting of two curved, overlapping lines. The upper line is a darker shade of green and curves from the left side towards the right. The lower line is a lighter shade of green and also curves from the left side towards the right, positioned below the first line.

Hydrogen Dispensing Pressure Analysis

Updated assessment of 350 bar, 500 bar, and 700 bar hydrogen refueling identifies important considerations for hydrogen fueling infrastructure development.

Fuel Pathway Integration Technical Team

Vehicle manufacturers are adopting 700 bar compressed hydrogen storage tank technology to achieve greater than 300 mile range in a fuel cell electric vehicle (FCEV). However, the U.S. Department of Energy is assessing long-term options, such as materials that could store hydrogen (H₂) at pressures lower than 700 bar. Dispensing H₂ at 700 bar requires higher station compression, storage, cooling, and operations and maintenance costs compared to lower dispensing pressures, which increases the fuel cost to the consumer. Using a methodology developed in 2013 to evaluate the tradeoffs between consumer refueling convenience (i.e., fewer trips to the station) and increased H₂ cost (i.e., higher dispensing pressure), the team conducted a tradeoff analysis using the most recent H₂ refueling station cost figures based on the current state of knowledge of refueling technologies.¹

H₂ refueling costs were estimated for H₂ refueling station dispensing pressures of 350, 500, and 700 bar. While higher H₂ dispensing pressures result in longer vehicle ranges and thus improved customer experience, they also result in higher fueling cost due to increased cost of compression, storage, and cooling requirements at the station for fast fills. An intermediate fueling pressure, such as 500 bar, could simultaneously satisfy the criteria of acceptable drive range while reducing cost.

The updated analysis resulted in the following side-by-side comparisons of the three fueling pressures (also illustrated in Figure 1):

¹ Reddi K, Elgowainy A, Sutherland E, "Hydrogen refueling station compression and storage optimization with tube-trailer deliveries," International Journal of Hydrogen Energy, Volume 39, Issue 33, 11 November 2014, Pages 19169–19181. <http://dx.doi.org/10.1016/j.ijhydene.2014.09.099>.

- (1) 700 versus 350: A 700 bar dispensing pressure is more valuable than 350 bar to consumers with trip times (to a station) exceeding 10 minutes and when consumers value their time at greater than \$40/hour;
- (2) 350 versus 500: Total cost of refueling at 350 bar is higher than total cost of refueling at 500 bar for consumers that value time (i.e., consider the cost of the station trip time);
- (3) 500 versus 700: A 500 bar dispensing pressure is favorable to 700 bar when trip times to the station are less than 5 minutes and consumers value their time at less than \$70/hour.

Future analysis will include the impact of vehicle tank cost as a function of maximum on-board storage pressure, to better define consumer total cost of ownership for the trade-off of storage pressure and FCEV range. The cost impact of various refueling pressures on the levelized cost of driving will also be an extension to this work.

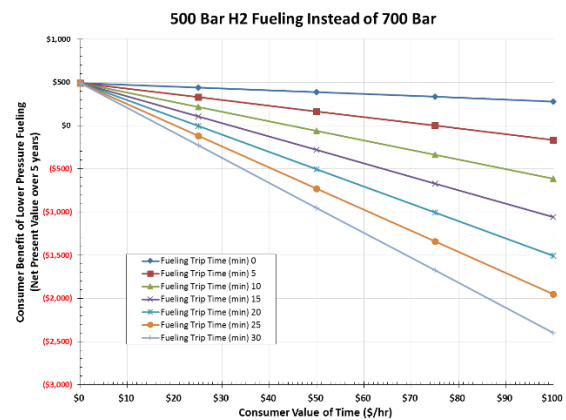


Figure 1. Updated analysis suggests that 700 bar fueling is favored over 500 bar fueling when time to the station exceeds 5 minutes and the consumers value their time greater than \$70 per hour.

Marginal Abatement Cost of Carbon

Analyzing the marginal abatement cost of carbon for various vehicle/fuel pathways represents the relationship between the cost-effectiveness of different abatement options and the total amount of greenhouse gas emissions abated.

Fuel Pathway Integration Technical Team

The Fuel Pathway Integration Technical Team (FPITT) developed a methodology to compare the cost and magnitude of greenhouse gas (GHG) reductions for different vehicle technologies and fuel pathways, compared to a baseline vehicle/fuel. Given the wide range of vehicle technologies and fuel pathways, it is not immediately apparent which options deliver the most economically efficient reductions in GHGs within the transportation sector.

The team’s methodology calculates the marginal abatement cost of carbon for various vehicle technologies and fuel pathways. The method has been developed into a spreadsheet that shows the relationship between the cost-effectiveness of different abatement options and the total amount of GHGs abated, compared to a baseline vehicle/fuel.

The vehicle technologies selected include battery electric, plug-in hybrid, compressed natural gas, fuel cell, diesel, and gasoline. These technology choices and assumptions align with the pathways analyzed by U.S. DRIVE’s Cradle-to-Grave (C2G) working group. The analysis includes short- and long-term technology perspectives to assess changes once newer technologies are produced “at scale.”

The team incorporated a stochastic analysis to the model to assess uncertainty ranges. Figure 1 provides a sample illustration of how the results will be presented; the horizontal axis indicates tonnes of equivalent carbon dioxide (CO₂e) saved during the lifetime of the vehicle compared to a baseline technology and the vertical axis shows additional cost paid per tonne of avoided CO₂e compared to the same baseline. Stochastic error distributions for the cost and GHG emissions will be incorporated using Monte Carlo analysis.

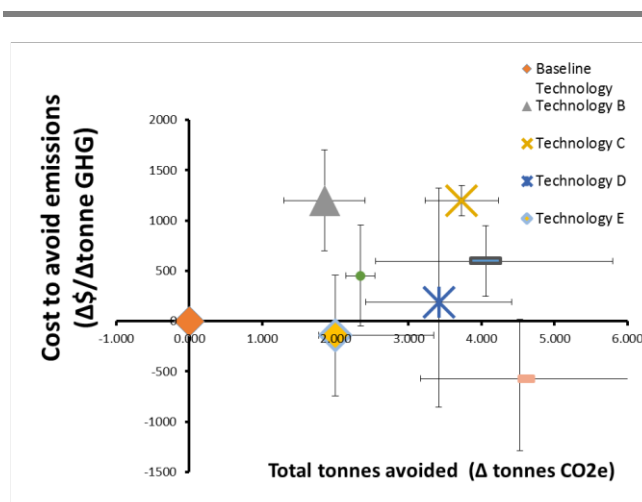


Figure 1. Graphical representation of results with uncertainty ranges. Note: For illustrative purposes only.

The following equations present the calculations of the horizontal and vertical variables that are plotted in Figure 1.

Cost to avoid emissions (Δ\$/ Δ tonne GHG):

$$\frac{\text{Cost of Ownership Vehicle X} - \text{Cost of Ownership Gasoline ICEV}}{\text{GHG Gasoline ICEV} - \text{GHG Vehicle X}}$$

Total tonnes avoided (tonnes GHG):

$$\text{GHG Gasoline ICEV} - \text{GHG Vehicle X}$$

The team presented the methodology to vehicle manufacturers and revised the analysis approach based on their input. FPITT will collaborate with the C2G working group to ensure harmonization of data and assumptions. In 2015, FPITT will vet the probability distribution functions with subject matter experts and prepare a figure similar to Figure 1 with preliminary analytical results.

Hydrogen Delivery



14% Reduction in Hydrogen Delivery Cost using Tube Trailer Consolidation

Model optimizes station operation to minimize cost.

Argonne National Laboratory

Researchers at Argonne National Laboratory (ANL) reduced by 14% the projected cost of hydrogen delivery via 350 bar tube trailers for 700 bar dispensing into fuel cell electric vehicles. This was achieved through the use of a newly-developed tube trailer consolidation operation mode designed by ANL researchers (see Figure 1).

The projected cost reduction was estimated using the Hydrogen Station Cost Optimization and Performance Evaluation (H2SCOPE) model that ANL developed. The H2SCOPE model solves the physical laws of mass, momentum, and energy conservation. It tracks the mass, pressure, and temperature over time throughout the refueling system – including the onboard vehicle tank – to provide a science-based approach for optimizing station operation to reduce cost. Results are published in the International Journal of Hydrogen Energy 39 (2014) 20197-20206.

The purpose of consolidation is to ensure that the compressor has high pressure hydrogen available at the inlet at all times. By consolidating the remaining hydrogen in the tube trailer during off-peak hours, a 750 kg/day station can be served by a 15 kg/hour compressor (rated at 20 bar inlet).¹ Figure 1 details a tube trailer consolidation schematic. The compressor operates in two modes. First, peak demand: Compressor compresses hydrogen from the tube trailer into vehicle or buffer storage. Second, off peak: Compressor consolidates tube trailer hydrogen from the tube trailer’s lower pressure vessels into the tube trailer’s higher pressure vessels.

¹ The energy content of 1 kg of hydrogen is approximately equal to 1 gge.

This reduces the required compressor capacity, and thus the compressor capital cost by approximately 50%, while using 86% of the tube trailer payload and simultaneously reducing the buffer storage (cascade) requirement. Table 1 shows actions suggested by the simulation.

As a result, the projected high-volume cost to deliver and dispense hydrogen via tube trailer was reduced from \$3.30/gas gallon equivalent (gge) to \$2.85/gge for 700 bar hydrogen dispensing. The cost estimate assumes an individual station capacity of 750 kg/day and a regional market demand for hydrogen of 80 metric tons per day (~10% of vehicles in a U.S. city with a population of 1.2 million).

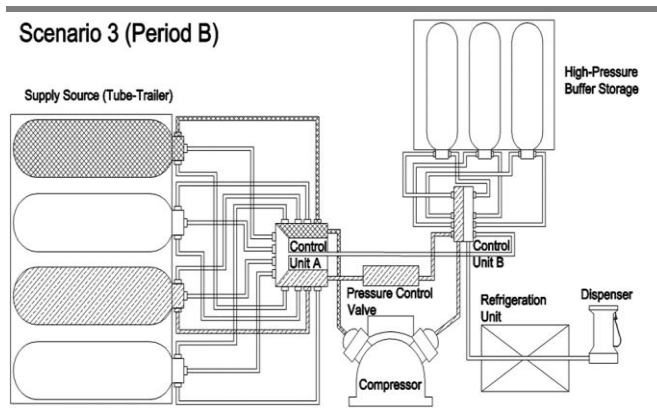


Figure 1. Tube trailer consolidation schematic.

Original	Optimized
Nine cascade pressure vessels (15 kg each)	Six cascade pressure vessels (15 kg each)
73 kg/hour compressor	15 kg/hour compressor
93% trailer payload utilization	86% trailer payload utilization

Table 1. Actions suggested by the simulation.

Hydrogen Production



Advanced Oxygen Evolution Catalysts for Proton Exchange Membrane Water Electrolysis

Giner Inc. demonstrated an order of magnitude reduction in precious group metal loading at the anode while maintaining equivalent electrolyzer performance.

Giner, Inc.

Giner, Inc. (Giner), in partnership with 3M and the National Renewable Energy Laboratory, has developed advanced iridium (Ir) catalysts with enhanced catalytic activity, allowing for significantly lower Ir loading while maintaining equivalent electrolyzer performance. These catalysts will help to lower the polymer electrolyte membrane (PEM) electrolyzer capital cost, making PEM water electrolysis more viable for a variety of applications. It is estimated that decreasing the anode precious group metal (PGM) loading by an order of magnitude, as demonstrated here, will decrease the electrolyzer stack capital costs by up to 15%.

Two approaches to incorporate the Ir catalysts into PEM electrolyzer anodes were developed and evaluated: (1) Giner's Ir nanoparticles dispersed on an oxidation-resistant tungsten-doped titanium oxide support (Ir/W-TiO₂); and (2) 3M's Ir nanostructured thin film (IrNSTF) catalyst approach, which is roll-to-roll fabrication compatible.

Although water electrolysis for hydrogen production is attractive due to its potential for positive environmental impacts, the technology is still expensive because of high materials cost for the membranes, bipolar plates, and catalysts. In most commercial processes, an iridium-black (Ir-Black) PGM catalyst is used for the oxygen evolution reaction at the anode. Significant anode activation losses caused by this reaction's sluggish kinetics have required high PGM loadings (>4 mg/cm²).

The low PGM loaded catalysts developed in this project perform as well as conventional, heavier loaded catalysts. As shown in Figure 1, both Ir/W-

TiO₂ (0.4 mg PGM/cm²) and IrNSTF (0.25 mg PGM/cm²) based anodes nearly match the performance of Giner's standard anode with a 4 mg PGM/cm² catalyst loading.

These new reduced-PGM catalysts also have superior performance over commercial Ir-black catalysts of similar loading, as indicated in Figure 1 by the 40-50 millivolt (mV) lower potentials at a given current density. This voltage differential (40-50 mV) is equivalent to approximately a three-percentage point increase in efficiency. Even with the extremely low PGM loading, high electrolyzer performance is achieved with the new catalysts due to enhanced catalyst mass activity or specific activity. In addition to the increased activity, these new catalysts have demonstrated good durability in a nearly 1,000-hour endurance test at 80°C.

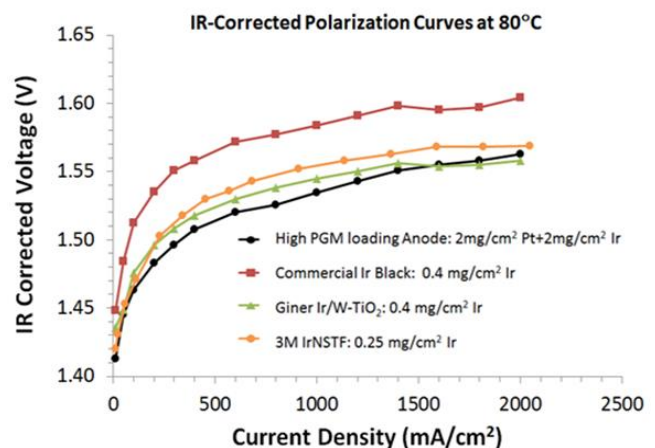


Figure 1. PEM electrolyzer performance of two advanced oxygen evolution catalysts, Ir/W-TiO₂ and IrNSTF, in a comparison with high PGM loading anode and commercial Ir-black anode.

Low Precious Group Metal Loaded Catalysts/Electrodes for Hydrogen Production by Water Electrolysis

Proton OnSite successfully demonstrated the reduction of the precious metal group metal content of its electrolyzer-cathodes by an order of magnitude without sacrificing electrochemical performance.

Proton On Site

Proton OnSite, working with Brookhaven National Laboratory (BNL), has reduced the precious group metal (PGM) catalyst loadings in polymer electrolyte membrane (PEM) electrolyzer electrodes by an order of magnitude to levels comparable to state-of-the-art PEM fuel cells. This achievement, leveraging an electrocatalysis approach originally investigated for lowering PGM loading in PEM fuel cell cathodes, combines an adaptation of BNL's core shell catalyst technology for electrolyzer use with Proton's scalable manufacturing process for effectively synthesizing and depositing the nanoparticle catalysts. It is estimated that decreasing the electrolyzer cathode PGM loading by an order of magnitude, in combination with manufacturing developments, will decrease the electrolyzer stack capital costs by approximately 18%.

PEM electrolyzers have been slow to adopt many of the advancements made in their PEM fuel cell counterparts. For example, the electrode catalyst loadings in today's PEM electrolyzers are typically higher than those in PEM fuel cells by at least a factor of five. One historical reason for this lag is that electrolyzers were originally developed for life support applications in space and on submarines, requiring ultimate dependability achieved through over-engineered stack designs, including high catalyst loadings. Also, achieving uniform catalyst distribution across the electrodes using the legacy deposition processes inherently requires substantial catalyst loadings.

Proton and BNL targeted the cathode, or hydrogen electrode for the electrolysis cell, for initial demonstration. Researchers used an environmentally-friendly ethanol-based process developed at BNL to synthesize atomically well-

designed core-shell nanocatalysts, which consist of a less expensive core metal covered by a more expensive, catalytically active shell material. These nanocatalyst particles were integrated with carbon supports and deposited on a microporous layer in a test cathode at PGM loadings of $<0.15 \text{ mg/cm}^2$. Performance tracked very well with Proton's baseline electrode, which had an order of magnitude higher PGM loading (see Figure 1). The new catalyst demonstrated stable performance in a 500 hour test showing that even though significantly less catalyst is used, good performance life is still achievable.

Proton successfully transferred manufacturing of the core shell catalysts to its facilities at a scale practical for Proton's current fabrication processes. The catalyst deposition method was transitioned from a manual process to an automated ultrasonic printing process, which has proven effective for uniformly dispersing the core shell catalysts at low loadings.

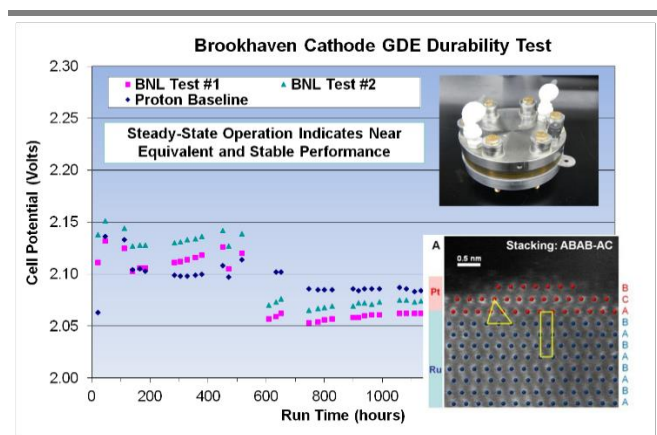


Figure 1. Core shell catalyst structure and performance data.

This page left intentionally blank.